UNIVERSITÀ DEGLI STUDI DI CAGLIARI

DOTTORATO DI RICERCA

Scienze della Vita, dell'Ambiente e del Farmaco

CICLO XXXI

Evasion of IFN Signaling by Ebola Virus and Zika Virus: Characterization and Exploitation of Viral Proteins as Drug Targets

Settore scientifico disciplinare di afferenza

Microbiologia BIO/19

Relatore: Presentata da:

Prof. Enzo Tramontano   **Elisa Fanunza**

Coordinatore Dottorato:

Prof. Enzo Tramontano

Esame finale anno accademico 2017 – 2018
Tesi discussa nella sessione d'esame Gennaio-Febbraio 2019

Abstract

Emerging and re-emerging RNA viruses have been the cause of epidemics within the past few years, raising public health concerns throughout the world. The 2014-2016 outbreak of Ebola Virus (EBOV) resulted in over 28000 infections with more than 11000 deaths. In 2015, a widespread epidemic of an emerging mosquito-borne flavivirus, Zika Virus (ZIKV), was associated with the increased incidence of neurological complications in South and Central America.

As an early response to viral infection, type I interferon (IFN-α/β) produced by mammalian cells exerts antiviral activity. The RIG-I-like receptors are critical sensors for RNA viruses, including EBOV and ZIKV. The IFN response begins with recognition of pathogen-associated molecular pattern by pattern recognition receptors, whose activation leads to a signaling cascade resulting in the production of IFN-α/β. Once secreted, type I IFN binds to the specific receptor activating the IFN signaling cascade leading to the induction of hundreds of IFN-stimulated genes (ISGs), which establish the antiviral state of the cells, targeting specific aspects of the viral life cycle. The majority of viruses have evolved strategies to disarm the IFN-I response: (i) blocking IFN-I production, (ii) IFN-I signaling, (iii) ISGs action. The antagonism of the IFN system has significant implications in both EBOV and ZIKV immune pathogenesis and virulence. EBOV multifunctional protein VP24 is one of the main determinants of EBOV virulence by virtue of its inhibition of the IFN signaling cascade. ZIKV antagonism of IFN response is also correlated to virulence, in particular mutations in residues of NS1 and NS4B have been associated with increased viral replication and neurovirulence in mice.

Today no approved drugs are available to treat EBOV and ZIKV infections. Therefore, the knowledge gained by characterizing the mechanisms through which both viruses evade the IFN response is at the base for the attenuation of the pathogenesis, contributing to the development of countermeasures directed against novel potential pharmacological targets.

This PhD thesis, on one hand, focuses on the study of EBOV VP24 protein and its inhibition of the IFN signaling cascade. Being a key factor for EBOV virulence, with the aim of identifying novel therapeutic agents against VP24, a new cellular drug screening assay has been developed. The assay is based on the transfection of cells with a luciferase reporter under the control of the promoter of ISGs (pISRE-luc) and an expression plasmid for VP24 that results in the inhibition of the IFN-mediated ISRE transcription. Addition of compounds leads to the partial restoration of the IFN signaling cascade. We optimized the assay to achieve excellent signal, robust performance and high reproducibility.

Among plants components, flavonoids have been reported to be active against many viruses, including EBOV, and to potentially bind VP24 *in silico* studies. Hence, using our drug screening assay, we screened a number of flavonoids among which Quercetin was identified to be the most active derivative against VP24, allowing to restore the IFN response with an IC_{50} value of 7.4 µM. Quercetin is the first compound reported to target specifically the EBOV VP24 IFN inhibitory function, thus, being potentially able to block EBOV infection at the early steps.

On the other hand, driven by the need for a comprehensive understanding of the molecular pathogenesis of the newly emergent ZIKV, the present PhD thesis aims to identify the ZIKV proteins with IFN signaling inhibitory functions. For the first time, we describe new functions for ZIKV NS2A and NS4B as IFN

signaling inhibitors, being able to block ISRE expression and ISGs transcripts through the suppression of STAT1/STAT2 phosphorylation. Given their impact on IFN response, they may represent novel and attractive targets for the further development of antiviral therapies against ZIKV.

Acknowledgments

During my PhD studies in the laboratory I realized that it is just like a family where everyone collaborates making his best efforts for fetching best results. A good support system is essential to work with enthusiasm and optimism. I was lucky to be a part of the magic 'Tramy Lab' family and it was a privilege to work with its fantastic members. There are so many people to thank who have guided, supported and shared many experiences with me during this journey.

First of all, I would like to express my deep gratitude to the father of the laboratory: prof. Enzo Tramontano. I recognize and thank him for his support during these years. His dedication has been inspiring for me. His advice taught me to constructively and critically think about a variety of very challenging scientific questions. His powerful guidance allowed me to formulate appropriate experiments and ideas for the success of my project. He is my best model for a scientist, mentor, and teacher.

Thank you to my lab's mum Francesca Esposito for her professional and personal support. Thanks to her positive outlook and her ability to make me smiling even after a hard work day.

It has been an absolute pleasure to share the study with a wonderful mate, Angela Corona. She frequently helped me to organize my ideas and generate new ones. She is a perfect cocktail of knowledge and craziness.

A special thanks to Nicole Grandi and Maria Paola Pisano. I am grateful for their continued encouragement and their kind help in questions of bioinformatics, such the alignments and the phylogenetic trees of this thesis. We spent together lots of moments, from the breakfast in the morning to the runs in the evening. I am really thankful for the stimulating discussions, for their friendship and for all the fun we have together.

Finally, a special and sincere thanks to my fantastic parents and my adorable sisters, Sofia and Gloria, for all their sacrifices, unconditional love, constant support, inspiring me to always follow my dreams. Words would never say how grateful I am to you. Thank you.

I dedicated this thesis

to whom has been a true and great supporter

and has unconditionally loved me during my good and bad times.

I love you dearly.

Table of Contents

List of Tables

List of Figures

List of Publications

Data presented in this Ph.D. thesis have been published in the following publications:

1. Fanunza, E., Frau, A.,Sgarbanti, M., Orsatti, R., Corona, A., Tramontano, E., Development and Validation of a Novel Dual Luciferase Reporter Gene Assay to Quantify Ebola Virus VP24 Inhibition of IFN Signaling, Viruses 2018, 10(2):98 doi: 10.3390/v10020098.

2. Fanunza, E., Frau, A., Corona, A., Tramontano, E., Antiviral Agents Against Ebola Virus Infection: Repositioning Old Drugs and Finding Novel Small Molecules, Annual Reports in Medicinal Chemistry 2018, 51:135-173 doi: 10.1016/bs.armc.2018.08.004.

3. Fanunza, E., Frau, A., Corona, A., Tramontano, E. Insights into Ebola Virus VP35 and VP24 Interferon inhibitory functions and their initial exploitation as drug targets, Infectious Disorders - Drug Targets 2018, doi: 10.2174/1871526519666181123145540.

4. Fanunza, E., Distinto, S., A., Quartu, M., Corona, A., Maccioni, E., Tramontano, E. Flavonoid derivatives restore Interferon signaling pathway inhibited by Ebola virus VP24. *Under preparation*.

5. Fanunza, E., Caglioti, C., Grandi, N., Quartu, M., Capobianchi M. R., Ippolito, G., Tramontano, E. Zika Virus NS2A and NS4B inhibit Interferon signaling and are potential targets to restore the host immune response. *Under preparation*.

Chapter 1

Introduction

1.1.   The Innate Immune Response

The cellular defense mechanisms against invading pathogens involve both innate and adaptive immunity (Figure 1). The connection between the two responses is fundamental in controlling the infection. In fact, the magnitude and efficiency of the adaptive immunity depend on signals derived from the first response, the innate immunity.
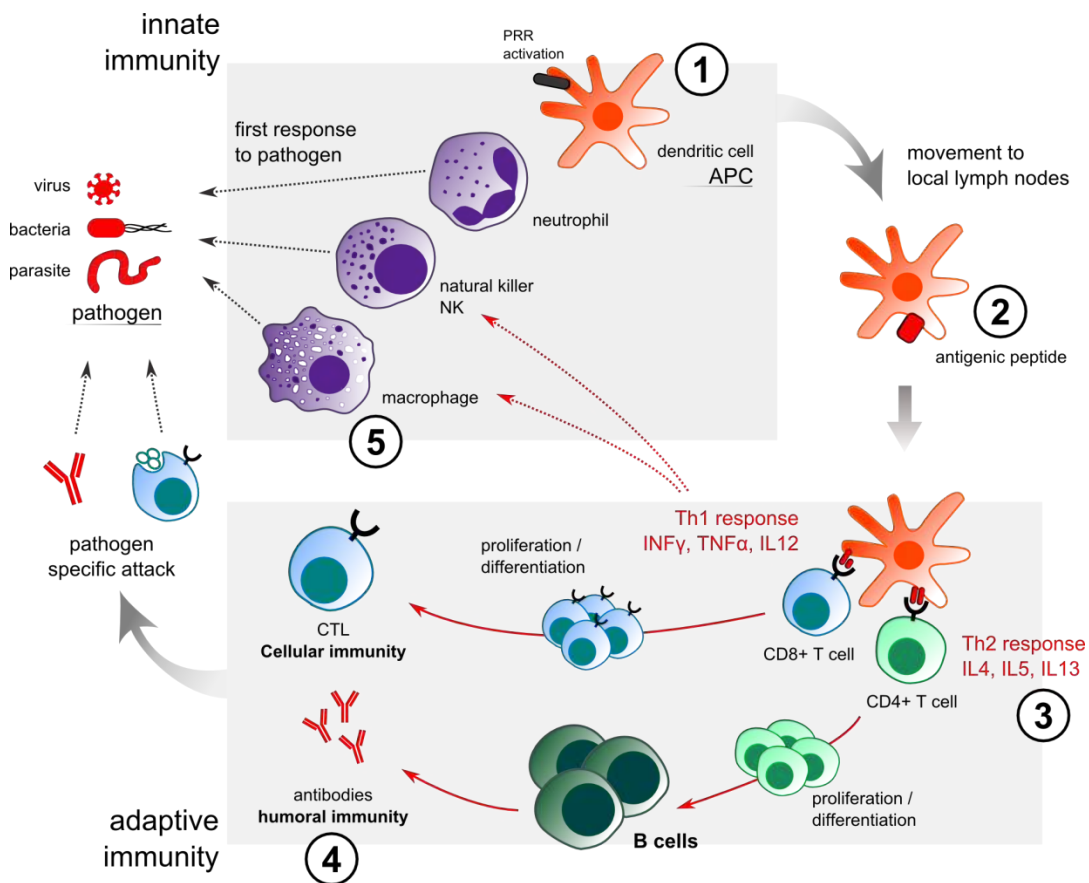
Figure 1. The immune response (Ozbiosciences)

Several important innate immune functions have been reported: (i) activation of the antiviral state of infected cells by producing type I interferons, (ii) reduction of the number of infected cells by promoting natural killer (NK) cell-mediate killing, and (iii) promotion of the maturation and site recruitment of the adaptive components through production of pro-inflammatory cytokines and chemokines (Akira et al., 2006).

The innate system is an evolutionarily ancient component, characteristic of all multicellular organisms. This host protection is performed by hematopoietic cells, including macrophages, dendritic cells, mast cells, neutrophils, eosinophils, NK and NK T cells, and non-hematopoietic cells, such as epithelial cells of the respiratory, gastrointestinal, and genitourinary tracts and the skin (Turvey and Broide, 2010). Since it is able to recognize molecules expressed broadly on a large number of cells, the innate immune system is poised to act rapidly in case of a viral infection, in contrast to the adaptive cells (T and B lymphocytes) that must proliferate after the antigen recognition to reach a sufficient number to mount an effective response. This implicates that within minutes of pathogen exposure, the protective inflammatory response is activated, while a time delay is requested to generate a protective adaptive immune response (Chaplin, 2010).

The activation of the innate immunity relies on the recognition of three different type of invading agents: (i) damage-associated molecular patterns, molecules released as a consequence of infection and inflammation, indicative of tissue damage, (ii) missing self, molecules normally expressed by healthy cells whose recognition functions as inhibitory signal to prevent activation of the immune response against host tissues, and (iii) pathogen associated molecular patterns (PAMPs), molecular signatures of the presence of non self organisms into the cells (Turvey and Broide, 2010).

1.2. Host Recognition of Viral PAMPs

The term 'pathogen associate molecular pattern (PAMP)' was coined about 20 years ago by Charles Janeway to define the molecular determinants encoded by different classes of pathogens that could interact with pattern recognition receptors (PRRs) of innate cells that, as a consequence of this recognition, are activated for the initiation of immune functions (Kawai and Akira, 2006). Since then, several PRRs have been discovered and demonstrated to target a wide range of PAMPs, including lipopolysaccharide, flagellin, peptidoglycan and microbial nucleic acids.

Several classes of PRRs are involved in the recognition of virus-specific molecules in innate immune cells, including Toll-like receptors (TLRs), retinoic acid-inducible gene I (RIG-I)-like receptors (RLRs), DExD/H-box proteins and other cytosolic DNA receptors. The host PRRs recognize as PAMPs viral genomic DNA, single-stranded RNA (ssRNA), double-stranded RNA (dsRNA), RNA with 5'-triphosphate (5'-ppp) ends and viral proteins (Figure 2).
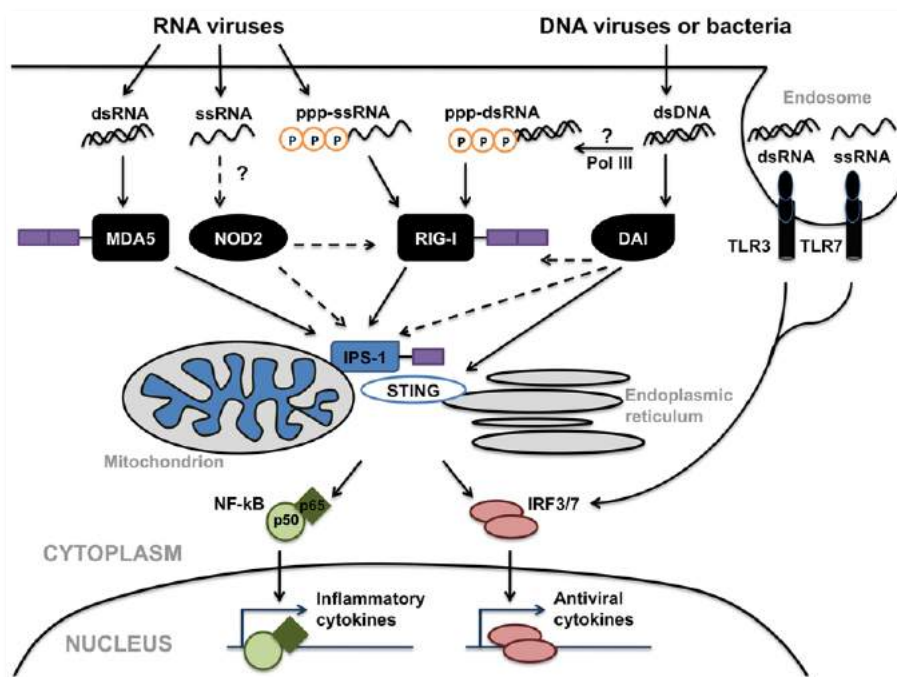
Figure 2. PRRs sensing of viruses (Furr and Marriott, 2012)

Extracellular viral DNA, ssRNA and dsRNA are recognized by TLR9, TLR7 and TLR3 receptors, respectively., TLR9 and TLR7 are localized only in the endosome membrane, thus being able to detect viral nucleic acids produced during virus uncoating or by degradation of entering viral particles, while TLR3, is localized in endosomes but also in the cell surface, thus targeting also dsRNA present in the extracellular environment. The viral DNA is recognized by TLR9 as non self because it is usually unmethylated (CpG), differently from the host genomic DNA, while the recognition between TLR7 and the ssRNA is not sequence-specific but multiple uridines are required in close proximity (Randall et al., 2015).

As intermediates and byproducts of the viral replication and transcription, intracellular double-stranded RNA (dsRNA), especially with the atypically-featured 5'-ppp termini, have no homologues in the cytoplasm and therefore is the most efficient targets for PRRs activation. They are recognized by the family of RLRs that includes RIG-I (Figure 2), the melanoma differentiation associated factor-5 (MDA5) and the laboratory of genetics and physiology-2 (LGP2) proteins (Yoneyama et al., 2004; Zinzula and Tramontano, 2013a). RIG-I and MDA5 preferentially sense distinct types of dsRNA, based on their length, bluntness and end overhangs. RIG-I optimal ligands are 5'-ppp dsRNAs shorter than 20 bp in length, but it can also bind 5'-hydroxyl (OH) blunt-ended dsRNAs, however the presence of the 5'-ppp group is critical for its proper activation. MDA5 optimal ligands were initially shown to be blunt-ended dsRNA moieties longer than 1 kbp in length while a subsequent study showed that this helicase is activated by an RNA aggregate formed by branched dsRNA stretches. Less is known about LGP2 which was shown to bind ATP hydrolysis-dependently blunt-ended dsRNA (Zinzula and Tramontano, 2013b).

Cytosolic DNA sensors are the less characterized among PRRs but several have been identified to date (Goubau et al., 2013). Among them, the DNA-dependent activator of IFN-regulatory factors (DAI) was the first to be described (Takaoka et al., 2007). Other cytosolic DNA sensors are cGAS and the stimulator of interferon genes (STING) (Cavlar et al., 2012; Ishikawa et al., 2009; X. D. Li et al., 2013). Specifically, the binding with the viral DNA activates cGAS that generates a dinucleotide, cGAMP, that serves as a second messenger, which binds and activates (STING). The ER-localized protein STING can also function as a direct cytosolic DNA sensor being able to directly bind DNA. STING is hence the key for activation of downstream signaling pathways. In addition, members of the DEAD/H-box helicases family, such as DHX9, DHX36 and DDX41 are implicated in the recognition of cytoplasmic DNA. Differently from TLRs and RLRs, DExD/H-box proteins involved in DNA sensing do not possess clearly defined signaling domains. Thus, the mechanisms by which they are able to recruit signaling adapters have to be further investigate (Dempsey and Bowie, 2015). Finally, AT-rich DNA can be transcribed in the cytosol by RNA polymerase (pol) III into uncapped 5'-ppp-RNA, which then activates the RLRs pathway (Ablasser et al., 2009; Chiu et al., 2009).

1.3.   The Interferon System

Recognition of viral PAMPs by host PRRs is the first step to activate the Interferon pathway which ultimately induces the expression of hundreds of Interferon Stimulated Genes (ISGs), whose encoded proteins are involved in the inhibition of viral replication, transcription and translation as well as the degradation of viral nucleic acids and the alteration of the host cells lipidic metabolism (Kühl and Pöhlmann, 2012; Ma and Suthar, 2015; Schneider et al., 2014).

1.3.1. An Historical Perspective: Discovery of Interferon

The notion of Interferon is strictly related to the concept of viral interference, which implies that some cells, after infection with a virus, displays reduced susceptibility to re-infection. The phenomenon of viral interference was firstly described in 1935 by Magrassi who observed that the inoculation of a non-encephalitogenic strain of Herpes Virus into the cornea of eyes of rabbits, previously infected with an encephalitogenic strain, prevented the development of encephalitis, and by Hoskins who noted a protective action of a neurotropic strain of Yellow Fever Virus against infection with the viscerotropic strain of the same virus in *Macacus rhesus* (Hoskins, 1935; Magrassi, 1935). Two years later, in 1937, Findlay and MacCallum found that Rift Valley Fever Virus protected monkeys from infection with the immunologically unrelated Yellow Fever Virus (Findlay et al., 1937). Only twenty years later, in 1957, Isaacs and Lindenmann (Figure 3) discovered the protein mediator of interference (Isaacs et al., 1957). The experiment that they performed was simple but original at that time. They incubated chicken egg chorioallantoic membranes with heat-inactivated Influenza Virus. Then, the not adsorbed virus was removed and membranes incubated for several hours. Membrane fragments were removed and replace with fresh membranes. After 18-24 hours live Influenza Virus was added but its replication was inhibited. They observed that the tissue exposed to the inactivated virus released a factor that transferred interference, or virus resistance, and they called it Interferon (IFN) (Isaacs et al., 1957).

Figure 3. The fathers of Interferon: Isaacs and Lindenmann (Reuben, 2005)

1.3.2. The IFN Family

The IFNs are a family of cytokines grouped into three classes: type I, II and III IFNs, that differ for their amino acid sequence. Type I IFNs, the first cytokines discovered by Isaacs and Lindenmann, include a large group of molecules secreted by mammalian cells: IFN-α, IFN-β, IFN-ω, IFN-ε, IFN-κ, IFN-ζ, IFN-δ and IFN-τ. In humans there are 13 IFN-α genes and only one functional gene for IFN-β, IFN-ω, IFN-ε and IFN-κ. IFN-ζ is only found in mice, while a structural homolog, IFN-δ, is found in non-primate and non-rodent placental mammals. IFN-τ is expressed in ungulates where it is required for implantation of the ovum. The IFN-α and-β genes are expressed in response to viral infection, whereas IFN-ω, -ε, -κ play roles in regulation of reproductive function in placental mammals (Randall et al., 2015). Type II IFN has a single member, IFN-γ, secreted by activated T cells and natural killer (NK) after stimulation with specific antigens or mitogens, rather than in direct response to viral infections. Type III IFNs have been described more recently and comprise IFNλ1, IFN-λ2 and IFN-λ3, also named IL-29, IL-28A and IL-28B, respectively (Ank et al., 2006). These cytokines are also induced in direct response to viral infection and use the same cascade as the IFN-α/β genes to target viral infection, but, unlike IFN-α/β, the type III IFNs receptor displays a limited tissue distribution (Pestka et al., 2004; Randall et al., 2015).

1.3.3. The IFN Production Cascade

The mechanisms of induction of IFN follow a distinct profile for the different PRRs (Randall et al., 2015) (Figure 4). In response to TLR7 and TLR9 sensing, the canonical IkB kinase (IKK) pathway is activated. Upon sensing of viral ssRNA (Diebold et al., 2004) or DNA (Ashkar and Rosenthal, 2002) the adaptor myeloid differentiation factor 88 (MyD88) is recruited and, in turn, engages a

complex containing the kinases interleukin-1 receptor-associated kinase 4 (IRAK-4), IRAK-1 and tumor necrosis factor (TNF) receptor-associated factor 6 (TRAF6) (Deguine and Barton, 2014). This complex binds directly to the IFN-regulatory factor 7 (IRF7) which is polyubiquitinated by the ubiquitin E3 ligase function of TRAF6. Recruited IRF7 is phosphorylated by IRAK1 and translocates into the nucleus still in association with MyD88, TRAF6 and IRAK1 (Honda et al., 2004; Kawai et al., 2004). Into the nucleus, it binds to cellular DNA and stimulates transcription of IFN-α/β promoter (Randall et al., 2015) (Figure 4).
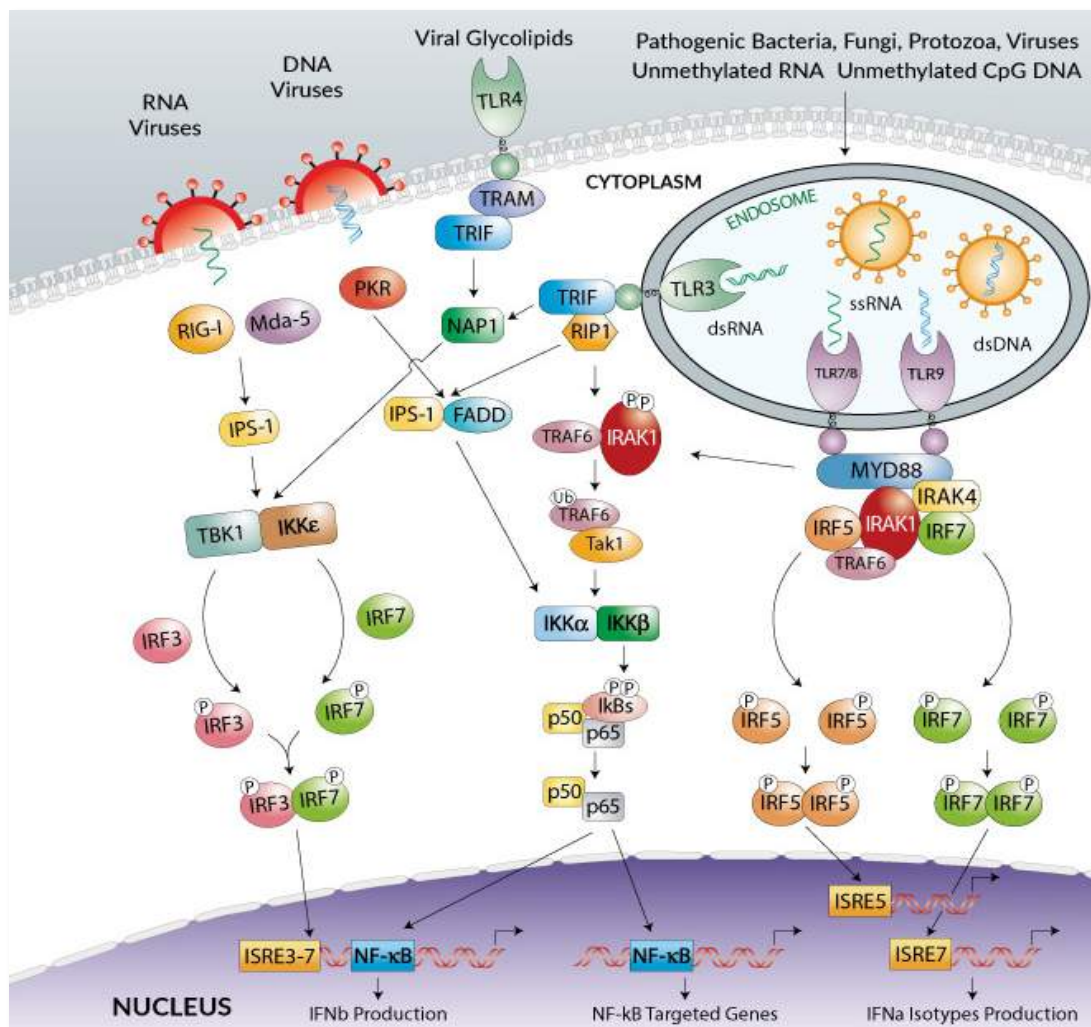
Figure 4. IFN production cascade (Invivogen, 2005)

The signal transduction at the base of the recruitment of dsRNA by TLR3 starts with the dimerization and phosphorylation of TLR3 (Sarkar et al., 2004) and the engagement of the adaptor Toll–interleukin (IL)-1-resistance (TIR) domain-containing adaptor inducing IFN-β (TRIF) which leads to the activation of IRF3 through its phosphorylation mediated by the TRAF family member-associated nuclear factor-kB (NF-kB) activator (TANK)-binding kinase 1 (TBK1) and the inducible IKK-ε (Fitzgerald et al., 2003; Sharma et al., 2003; Yamamoto et al., 2003). The activated IRF3 migrates to the nucleus and assemble on the IFN-β promoter leading to the stimulation of IFN-I transcription (Figure 4).

The recognition of viral nucleic acids by cytosolic RLRs promotes the recruitment and activation of a mitochondrion-associated adaptor, the IFN-β promoter stimulator protein 1 (IPS1), also named mitochondrial antiviral signaling protein (MAVS) (Johnson and Gale, 2006; Kawai et al., 2005; Meylan et al., 2005; Seth et al., 2005; Xu et al., 2005). The engagement of RIG-I from the cytosol to mitochondrial membranes is mediated by the tripartite motif 25 alpha (TRIM25a) E3 ligase which is important for the interaction with IPS1 (Gack et al., 2007; Liu et al., 2012). The prosecution of the cascade is characterized by IPS1 prion-like polymerization (Hou et al., 2011) and the recruitment of two adaptors, TRAF3 and NF-kB essential modifier (NEMO), which connect and regulate signaling between IPS1 and the complex formed by TBK1 and IKK-ε and other scaffold proteins TANK, NAP1 (NAK-associated protein 1) or SINTBAD (Belgnaoui et al., 2012; Fitzgerald et al., 2003; Oganesyan et al., 2005; Wang et al., 2012; Zhao et al., 2007). The formation of the complex TBK1-IKK-ε-IPS1 is essential for IRF phosphorylation and is strongly enhanced by STING, (Ishikawa and Barber, 2008; Sun et al., 2009; Zhong et al., 2008). Once phosphorylated IRF3 and IRF7 homo- or heterodimerize and associate with other transcription factors, driving the transcription of IFN-α/β promoter (Figure 4) (Panne et al., 2007).

1.3.4. The IFN Signaling Cascade

The signaling pathway activated in response to IFN-α/β has been deeply characterized (Platanias, 2005; Stark et al., 1998; van Boxel-Dezaire et al., 2006). IFN-α and IFN-β bind a heterodimeric receptor named IFN-α receptor (IFNAR), composed of two subunits, IFNAR1 and IFNAR2 (Figure 5).
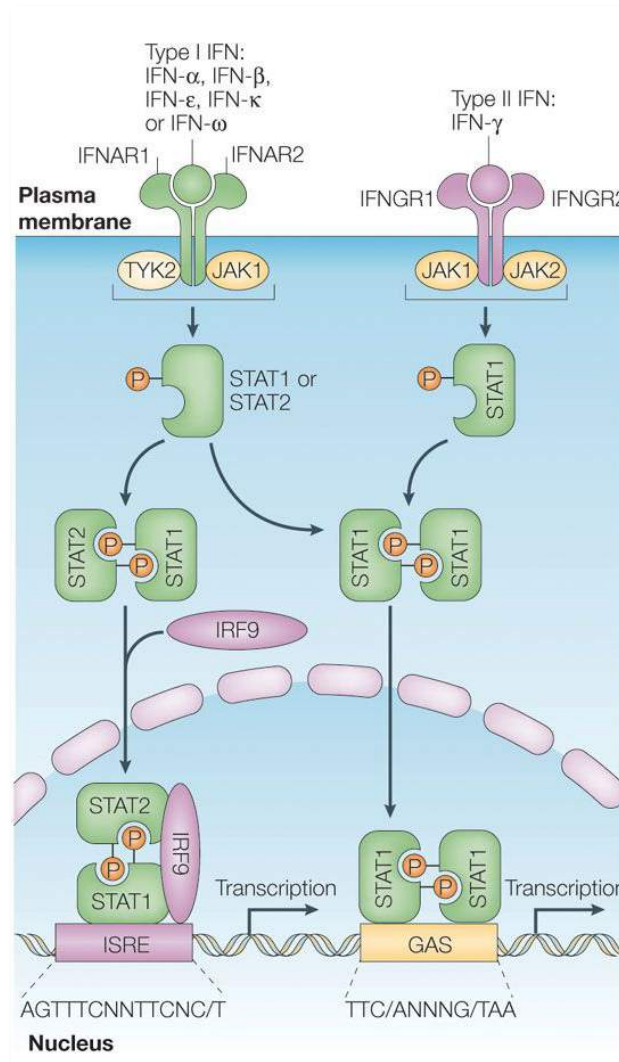
Figure 5. IFN signaling cascade (Platanias, 2005)

Prior to activation, IFNAR1 is associated with tyrosine kinase 2 (Tyk2) and the IFNAR2 subunit with the tyrosine kinase JAK1. IFNAR2 is also bound to the signal transducer and activator of transcription 2 (STAT2) and is associated weakly with STAT1. The IFNAR receptor conformational change caused by the

ligand-induced dimerization results in the phosphorylation of the tyrosine 466 on IFNAR1 by Tyk2, creating a strong binding site for STAT2. Then, Tyk2 also phosphorylates STAT2 on tyrosine 690, while JAK1 phosphorylates STAT1 on tyrosine 701 (Stancato et al., 1996; Tang et al., 2007; Yan et al., 1996). Phosphorylated STAT1 (P-STAT1) homo-dimerizes or hetero-dimerizes with phosphorylated STAT2 (P-STAT2) and then binds the IFN-regulatory factor 9 (IRF9) to form a heterotrimeric complex, termed IFN-stimulated gene factor 3 (ISGF3) (Fu et al., 1990; Stancato et al., 1996; Tang et al., 2007). The translocation of the complexes STAT1:STAT1 and ISGF3 to the nucleus is dependent on the tyrosine phosphorylation of STAT1 which is at the base of the conformational change resulting in the recognition by a subset of the karyopherin-α (KPNα) family of nuclear transport factors (Chen et al., 1998; McBride et al., 2002). The binding of P-STAT1 with a non-classical nuclear localization signal (ncNLS) motif of KPNα results in the nuclear transport of the complex (Xu et al., 2015). In the nucleus, STAT1:STAT1 and ISGF3 recognize the IFN-stimulated response elements (ISRE), promoter of the ISGs (Fink and Grandvaux, 2013; Fu et al., 1990; Kessler et al., 1988). Signaling in response to type III IFN is similar to that in response to type I IFN.

The cascade in response to type II IFN differs for some aspects from these pathways (Figure 5). The IFN-γ receptor is also a heterodimeric protein, formed by two major subunit, IFNGR1 and IFNGR2, that pre-associate weakly in not stimulated cells. The cytoplasmic tails of the IFNGR1 and IFNGR2 receptor subunits are associated with JAK1 and JAK2, respectively. The binding between IFN-γ and the receptor subunits triggers the receptor dimerization. This recruits JAK1 and JAK2 and results in the activation of JAK2 which phosphorylates JAK1 activating it. Subsequently, the activated JAKs phosphorylate a region between tyrosine 440 and tyrosine 444 of IFNGR1, creating a binding sites for STAT1. Two STAT1 molecules then interact with IFNGR1 and are

phosphorylated at tyrosine 701, resulting in their activation and dissociation from the receptor. P-STAT1 dimerizes forming a STAT1–STAT1 homodimer, that translocates into the nucleus and binds to the gamma-activation sequence (GAS), stimulating transcription of ISGs. The JAK/STAT cascade is essential for mounting a massive host response against viral infections. Accordingly, mice deficient in IFN signaling proteins, such as IFNAR, showed an increased susceptibility to several viruses but maintain resistance to other microbial pathogens. Similarly, humans with genetic defects in components of IFN-I signaling (STAT1, TYK2) died for viral diseases.

1.3.5. The IFN-Induced Antiviral State

As part of the innate immune response, the IFN system serves as first-line protection against virus infections, inducing antiviral states in infected cells limiting early viral replication and spread (Haller et al., 2006; Kühl and Pöhlmann, 2012). After binding of IFN-I to IFNAR, more than 300 ISGs are expressed (Der et al., 1998). Only some of them exert a direct antiviral function while the majority encode for PRRs that detect viral molecules and modulate signaling pathways, or transcription factors leading to an amplification of the IFN production and protection from viral spread to limit infection (Sadler and Williams, 2009). ISGs products with direct antiviral activity include proteins that catalyze cytoskeletal reorganization, that induce apoptosis and that drive post-transcriptional events, such as mRNA editing, splicing, RNA degradation, protein translation and post-translational modifications. Different studies of gene knockout mice validated ISGs encoded proteins, such as ISG15, Mx1, 2′, 5′-oligoadenylate synthetase 1/ribonuclease L (RNaseL) and protein kinase R (PKR), as direct antiviral effectors. In fact, increased susceptibility to virus infection was observed in mice with mutations or deficiency in residues

involved in the cascades triggered by these proteins (Sadler and Williams, 2009).

ISG15 is an IFN-regulated ubiquitin-like protein (Loeb and Haas, 1992) that can be covalently attached to both host and viral proteins. Conjugation of ISG15, commonly referred to as ISGylation, results in viral inhibition through still not well-known mechanisms. ISG15 prevents the virus-mediated degradation of IRF3, thereby enhancing the induction of IFNβ transcription. Other ISG15 targets include the PRRs, such as RIG‑I, the signaling components, JAK1 and STAT1, and also other the antiviral effector proteins, such as MxA, PKR, and RNaseL (Sadler and Williams, 2009). Mice deficient in ISG15 have increased susceptibility to infection with different viruses, including the Influenza A and B Viruses (IAV, IBV), Sindbis Virus, Herpes Simplex Virus 1 (HSV‑1) and murine γ‑Herpes Virus (Lenschow et al., 2005; Osiak et al., 2005). It mediates also resistance to Ebola Virus (Malakhova and Zhang, 2008) and Human Immunodeficiency Virus (HIV) (Okumura et al., 2006).

The Mx family GTPases comprise MxA and MxB in humans (Aebi et al., 1989). Only MxA has been reported to have antiviral activity (Chieux et al., 2001; Gordien et al., 2001). The MxA protein accumulates in the cytoplasm on intracellular membranes as oligomers formed by association between the central domain and the leucine zipper domain. During a viral infection, MxA monomers are released and bind viral nucleocapsids or other viral components, to trap and promote their degradation (Sadler and Williams, 2009). Several viruses have been reported to be susceptible to the activities of Mx proteins including orthomyxomaviruses, paramyxomaviruses, rhabdoviruses, togaviruses and bunyaviruses and also Coxsackie Virus, Hepatitis B Virus (HBV) and Hepatitis C Virus (HCV) (Andersson et al., 2004; Chieux et al., 2001; Gordien et al., 2001; Hijikata et al., 2000).

2',5'-oligoadenylate synthetase 1 (OAS1) is expressed at low constitutive levels and is upregulated after IFN-I induction (Zhou et al., 1997). OAS1 accumulates in the cytoplasm as an inactive monomer. Following stimulation by dsRNA, the enzyme oligomerizes to form a tetramer that synthesizes 2',5'-oligoadenylates that, in turn, activate the constitutively expressed but inactive RNaseL. The binding of 2',5'-oligoadenylates to RNaseL promotes the dimerization of enzyme monomers that enables RNaseL to cleave cellular and viral RNAs (Malathi et al., 2007; Rebouillat and Hovanessian, 1999; Sadler and Williams, 2009). RNaseL-deficient mice have been shown to possess an increased susceptibility to RNA viruses from the Paramyxoviridae, Orthomyxoviridae, Flaviviridae Retroviridae, Picornaviridae, Reoviridae and Togaviridae families (Silverman, 2007).

Protein kinase R (PKR) is constitutively expressed and it is also activated by stimulation with IFN-I (García et al., 2007). A kinase conserved sequence (KCS) and IFN-stimulated response element (ISRE) are features of the PKR promoter (Sadler and Williams, 2009; Ward and Samuel, 2002). The kinase accumulates in the nucleus and cytoplasm as an inactive monomer, which is activated directly by viral RNAs, and by several other ligands, such as the protein activator of the IFN-inducible protein kinase (PACT) (García et al., 2007; Sadler and Williams, 2009). Once activated, PKR monomers are phosphorylated and dimerize to form an active form of the enzyme that inhibits translation by phosphorylation of eukaryotic translation initiation factor 2α (EIF2α), which results in the suppression of protein synthesis (Feng et al., 2007). Studies in PKR-deficient mice demonstrated PKR role in protection against several viruses infections, including HCV (Noguchi et al., 2001), Hepatitis D Virus (HDV) (Chen et al., 2002), West Nile Virus (WNV) (Samuel et al., 2006), HIV‑1 (Nagai et al., 1997) and HSV-1 (Al-Khatib et al., 2003).

1.4. Viral Evasion of the IFN system

Viruses need to replicate extensively in the infected organisms in order to ensure transmission and survive. The coevolution of viruses and host led to the emergence of an inverse interference. In fact, viruses have evolved multiple viral strategies to escape the host immune response becoming resistant to the host defense mechanisms. These strategies can be ascribed to four (i) masking of viral PAMPs to PRRs; (ii) inhibition of IFN production pathway, (iii) block of the IFN signaling cascade, and (iv) counteraction with the ISGs antiviral functions (Figure 6).

1.4.1. Masking of Viral PAMPs to PRRs

A mechanism by which many viruses escape the host defense is to assemble replication complexes and drive viral genome synthesis within a virally induced enclosed organelle inside the host cell, called viroplasm-like structures (VLS), that shield the nascent viral genome from the PRRs sensing. This mechanism has been found in various RNA viruses including Corona Virus (CoV) and flaviviruses WNV, Dengue Virus (DENV) and Japanese encephalitis virus (JEV), but also in DNA viruses, such as the Vaccinia Virus (VACV) (Dalrymple et al., 2015; den Boon and Ahlquist, 2010; Hwang et al., 2009). IAV, retroviruses, and most of the DNA viruses are able to directly replicate inside the nucleus of infected cells masking themself from cytosolic RLRs and TLRs (García-Sastre, 2017; Weber et al., 2015). Since activation of RIG-I and MDA5 occurs upon recognizing non-self dsRNAs consisting of unmethylated 5'-ppp or diphosphate ends, different viruses have evolved phosphatases and methyltransferases (MTases) functions that catalyze post-translational modification of nascent mRNAs effectively hiding viral PAMPs by adding 5'-
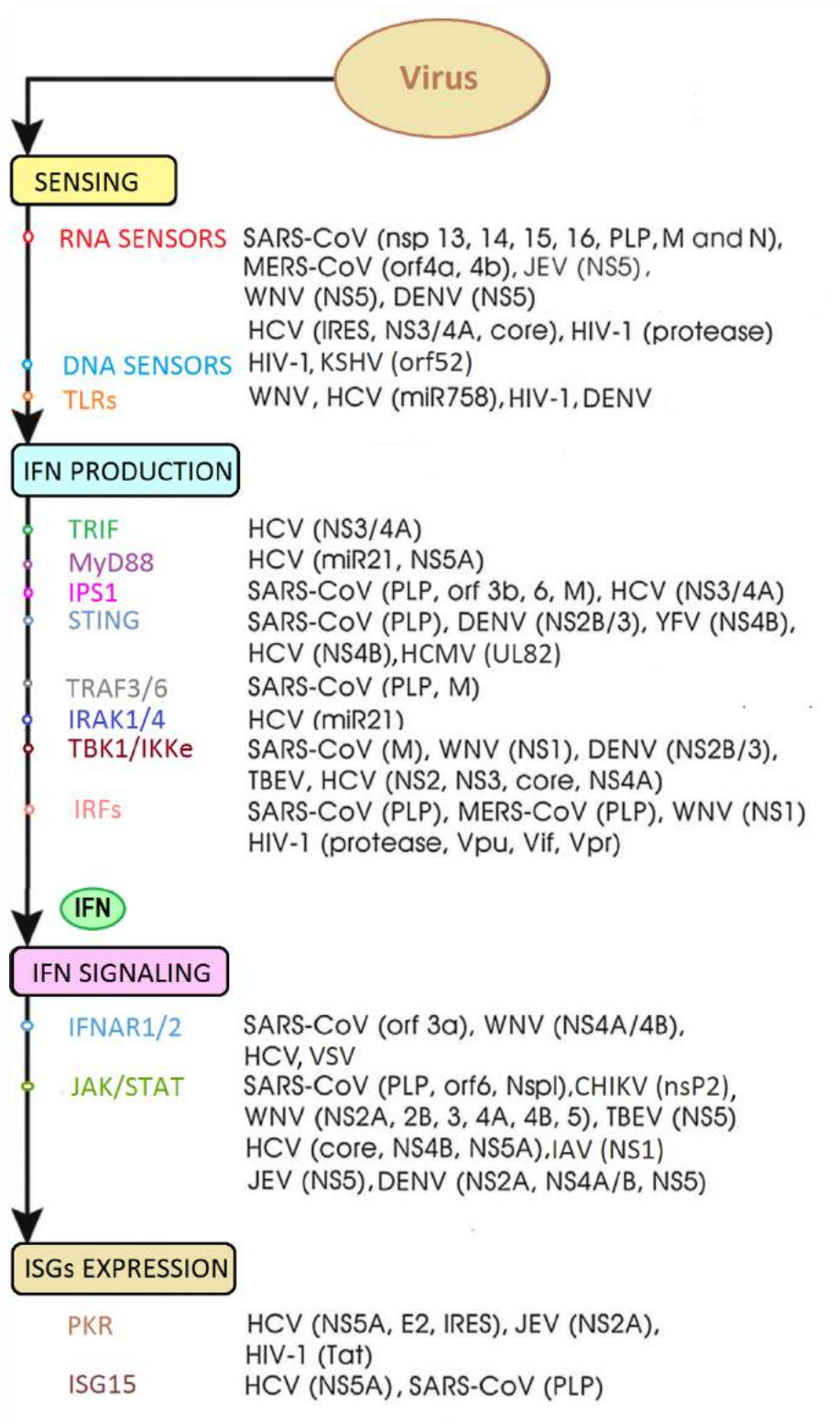
Figure 6. Viral evasion of IFN system

cap structures to viral RNA mimicking eukaryotic RNA structures. Post-translational modification of viral mRNA have been shown also for Severe Acute Respiratory-Corona Virus (SARS-CoV) and JEV, while IAV and bunyaviruses have been shown to use a mechanism of 'cap snatching'. Since they do not possess enzymes to synthetize their own RNA cap, they express viral endonucleases with cap binding activity masking the viral RNA PAMP (Ma and Suthar, 2015).

1.4.2. Inhibition of IFN Production Pathway

Many DNA and RNA viruses encoded a plethora of viral proteins that block IFN production by interacting with cellular proteins at various stages of the IFN response. For example, direct inhibition of the DNA sensor cGAS by the ORF52 protein Kaposi's Sarcoma-Associated Herpes Virus (KSHV) has been described, preventing the synthesis of cGAMP (Wu et al., 2015). Similarly, the binding of the human cytomegalovirus (HCMV) UL82 tegument protein to STING prevents the downstream signaling of IFN-I mRNA synthesis (T. Li et al., 2013). Yellow Fever Virus (YFV) and HCV NS4B were reported to binds STING (Ding et al., 2013; Ishikawa et al., 2009; Nitta et al., 2013), DENV NS2B/NS3 protease complex was shown to degrade STING (Aguirre et al., 2012), while herpesviruses and SARS-CoV have been reported to inhibit STING (Chen et al., 2016; Sun et al., 2012). IAV NS1 is able to interact with both RIG-I and MAVS (Mibayashi et al., 2007). MAVS is also inhibited by the HCV protease NS3 and its cofactor NS4A (Loo et al., 2006; Meylan et al., 2005). IAV NS1 and Thrombocytopenia Syndrome Virus (SFTSV) NSs target TRIM25, preventing RIG-I poly-ubiquitination (Gack et al., 2007; Qu et al., 2012). DENV has been reported to inhibit TBK1 and IKK-ε preventing translocation of transcription factors IRF3 and IRF7 (Dalrymple et al., 2015). N protein of arenaviruses is also

involved in IKKε inhibition (Pythoud et al., 2012). Moreover, the ORF36 protein murine gamma-herpesvirus binds to activated IRF3 in the nucleus blocking its interaction with transcriptional factors to induce IFN expression (Hwang et al., 2009). VACV C6 blocks the scaffold proteins in complex with the kinases TBK1 and IKK-ε thus shutting down the activation of IRF3 and IRF7.

1.4.3. Block of the IFN Signaling Cascade

IFN signaling cascade is also subjected to inhibition at different steps. For example, the IFNAR1 chain of the IFN receptor can be targeted by Vesicular Stomatitis Virus (VSV) and HCV for degradation following phosphorylation on specific serine residues (Liu et al., 2009). NS5 JEV and NS4B WNV inhibit phosphorylation and activation of JAK1 (Guo et al., 2005; Lin et al., 2006). NS4B WNV and LMP1 of Epstein-Barr Virus are able to block the phosphorylation of TYK2 (Geiger and Martin, 2006; Guo et al., 2005). Chikungunya virus (CHIKV) nsP2 (Jia et al., 2010; Uetani et al., 2008), IAV NS1 (Fros et al., 2010) and several non-structural proteins of flaviviruses, such as NS2A, NS4A, NS4B and NS5 (Ma and Suthar, 2015; Munoz-Jordan et al., 2003), inhibit the STAT1/2 phosphorylation and their subsequent nuclear translocation. DENV NS5 has been shown to promote the proteosomal degradation of STAT2 (Morrison et al., 2013). YFV NS5 physically binds STAT2 blocking its function. The binding-dependent inhibition of STAT1 and STAT2 are characteristic of a diverse range of viruses, such as paramyxoviruses, VACV, Rabies Virus (García-Sastre, 2017). SARS-CoV evolved three mechanisms to antagonize STAT1 function: the nsp1-dependent suppression of STAT1 phosphorylation, the ORF6-dependent sequestration of KPNα1 and the papain-like protease (PLP)-dependent induction of E3 ubiquitin ligase E2-25k, which results in the extracellular signal-

regulated kinase 1 (Erk1) degradation and, as a consequence, in the decrease of STAT1 phosphorylation (Ma and Suthar, 2015).

1.4.4. Counteraction with the ISGs Antiviral Functions

Viral countermeasures against the ISGs functions have also been identified. The mouse hepatitis virus (MHV) employs a viral enzyme with 2′,5′-phosphodiesterase activity to degrade the products of 2′,5′-OAS and effectively block the RNaseL antiviral pathway (Zhao et al., 2012). The HCV NS5A and the glycoprotein E2 directly counteract with the antiviral action of PKR. NS5A binds physically to PKR while E2 acts as competitive substrate with EIF2α for PKR binding, resulting in suppression of PKR kinase activity and in increased HCV replication (Arnaud et al., 2010). NS2A protein of JEV also directly interacts with PKR (Tu et al., 2012). During HIV-1 infection of lymphocytes, an IFN-induced RNA editing enzyme that binds to PKR to shut down its activation has been observed (Coccia and Battistini, 2015). SARS-CoV and MERS-CoV encode for a PLP, which possesses deISGylation activity. This viral function permits to modify cellular processes, such as the host protein localization and activity, signal transduction allowing viruses to massively replicate increasing the severity of infection (Clementz et al., 2010).

1.4.5. IFN Impairment and Virulence

The viruses ability to evade the immune response is strictly correlated with the high virulence of many human infections. An example, the inhibition of the IFN-induced phosphorylation of STAT1 and STAT2 is the cause of the high pathogenicity of the WNV lineage 1 Texas-HC2002 strain that widely determines encephalitis and meningitis, whereas WNV lineage 2 Madagascar-AnMg798 strain which lacks the ability to inhibit IFN signaling is typically non-

pathogenic, non-emergent, and geographically confined to Africa and Madagascar (Suthar et al., 2012).

During evolution, many viruses have evolved mutations in residues principally involved in the function of IFN antagonism that are critical for the acquisition of virulence in animal models contributing to the severity of the infection. The introduction of a single mutation (an alanine at position 30 to proline, A30P) in the protein NS2A of Kunjin Virus, a WNV subtype, abrogated the viral ability to suppress the IFN production, leading to the attenuation of viremia in mice (Liu et al., 2006). The Rift Valley Fever Virus (RVFV) NSs mutant C39S/C40S was highly attenuated in mice. The attenuation was due to the loss of the ability to degrade PKR (Monteiro et al., 2018). Among DENV-1 clinical isolates, alanine, methionine and valine at position 116 of NS4B were identified. Mutations with alanine and methionine resulted in enhanced virus growth in human cells in comparison to the clone with the valine. This enhanced viral replication was dependent on the ability of NS4B mutants to prevent host IFN response (Bui et al., 2018). VACV mutants in which the C6L gene is deleted, or mutated so that the C6 protein is not transcribed, were attenuated *in vivo* models of infection compared to wt and revertant controls. The C6 contribution to VACV virulence depends on the protein ability of interfere with the inhibition of IRF3 and IRF7 activation downstream of TBK1 and IKK-ε (Unterholzner et al., 2011).

The correlation between virulence and evasion of the IFN response is particularly evident for well-known viruses such as the deadliest Ebola Virus, for which the IFN escaping mechanisms have been deeply investigated, but also for newly emergent viruses, such as Zika Virus, whose strategies of IFN evasion are still under investigation. Both viruses are able to counteract the IFN system at various levels, using different proteins to completely shut down the host

defense. In the next sections, the biology and pathogenesis of Ebola Virus and Zika Virus will be described in detail focusing on their molecular mechanisms of evading the IFN response and their contribution to virulence.

1.5. Ebola Virus

1.5.1. Epidemiology

In 1976 epidemic of hemorrhagic fever were described in southern Sudan and subsequently in northern Zaire, now known as Democratic Republic of the Congo (DRC) (Cox et al., 1983; Johnson et al., 1978; Team et al., 1978). An unknown causative agent was isolated from patients in both outbreaks and named Ebola Virus after a small river in DRC. These two epidemics were caused by two distinct species of Ebola Virus: Sudan Ebola Virus and Zaire Ebola Virus, respectively. In 1994, the third African Ebola Virus species, Côte d'Ivoire Ebola Virus, was isolated in the Tai Forest reserve in Côte d'Ivoire (Le Guenno et al., 1995). Another Ebola Virus species, Reston Ebola Virus, was found in the Philippines in 1989 (Centers for Disease Control, 1990), while the latest discovery was Bundibugyo Ebola Virus, the fourth African species of human-pathogenic Ebola virus found at 10° north and south of the equator in Africa (Towner et al., 2008).

Ebola hemorrhagic fever is a plague for the African population with an increase in outbreaks and cases since 2000. Almost all human cases are due to the emergence or reemergence of Zaire Ebola Virus, the major public health concern. The most devastating Zaire Ebola Virus West African epidemic occurred in 2014-2016 standing as a landmark in Ebola Virus history, resulting in more than 28000 cases and 10000 deaths (Figure 7) (World Health Organization, 2016a).
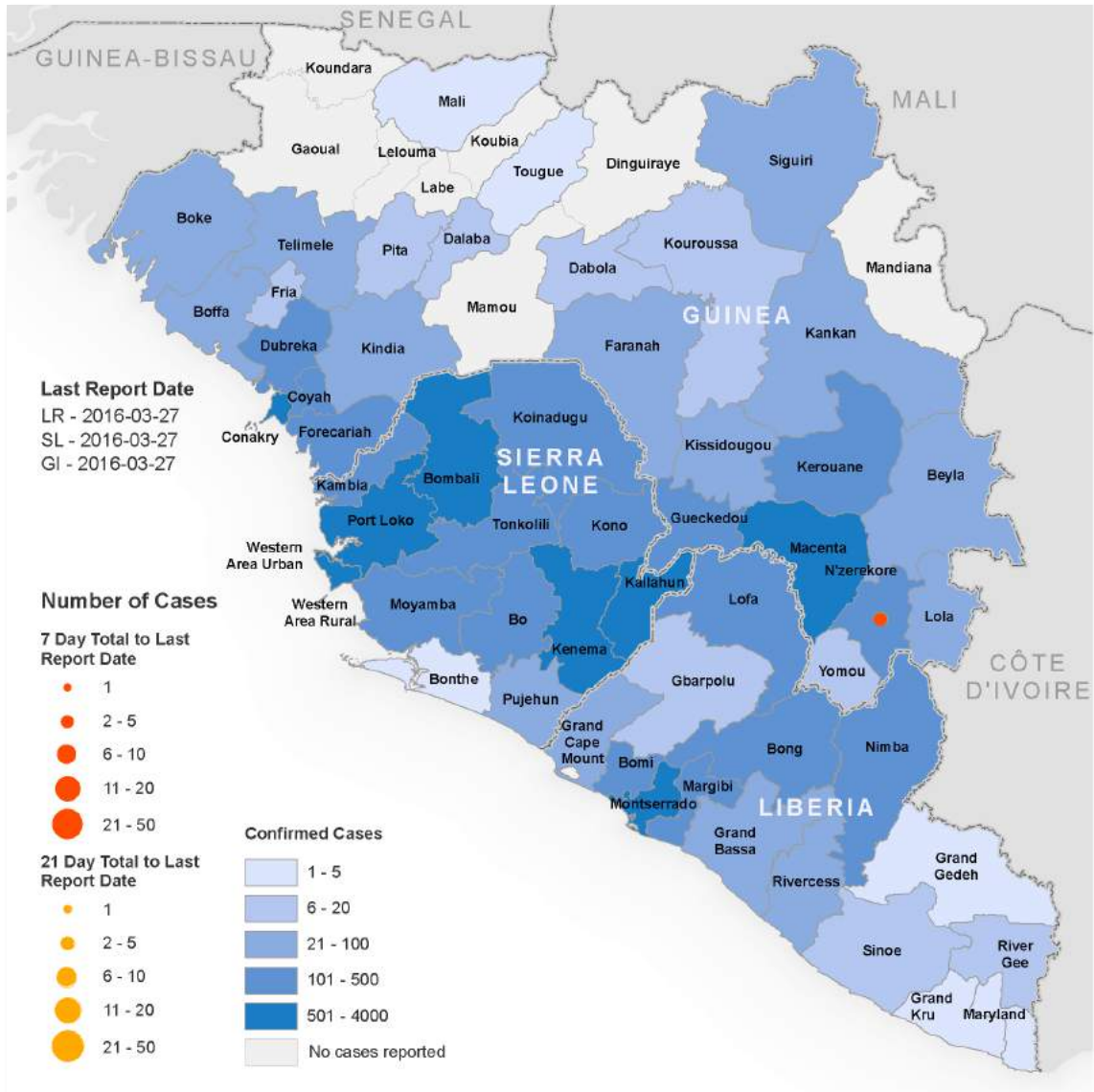
Figure 7. Number of cases during the west African 2014-2016 outbreak (World Health Organization, 2016a)

1.5.2. EBOV Genome and Proteins

Zaire Ebola Virus (EBOV) belongs to the family of *Filoviridae* in the order of Mononegavirales (International Committee on Taxonomy of Viruses, 2012). It is an enveloped virus with a linear, non-segmented, negative, single strand RNA (ssRNA-) of approximately 19 kb in length, organized in seven linear genes which encode for the nucleoprotein (NP), viral protein (VP) 35, VP40, glycoprotein (GP), VP30, VP24 and the Large (L) RNA-dependent RNA polymerase (Figure 8) (Feldmann and Geisbert, 2011; Wan et al., 2017). The ribonucleoprotein (RNP) complex consists of the ssRNA- genome encapsulated by the nucleoprotein NP with VP35, VP30, and the RNA-dependent RNA polymerase to form the functional transcription–replication complex. VP40 is the matrix protein and mediates virion particles formation, while VP24 is a structural protein associated with the membrane. The glycoprotein is the only protein located in the surface membrane forming trimeric spikes consisting of glycoprotein 1 (GP1) and glycoprotein 2 (GP2) (Feldmann and Geisbert, 2011).
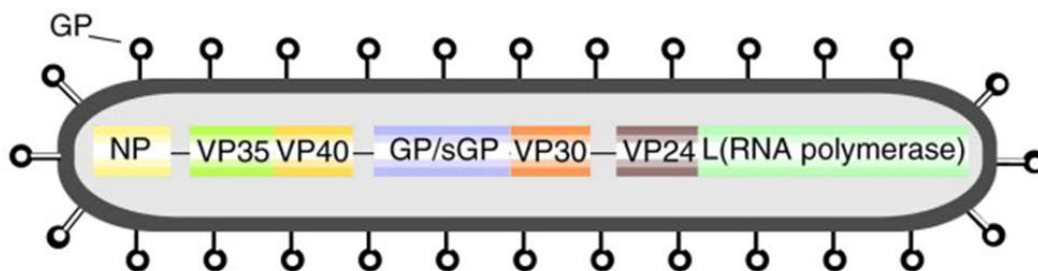
Figure 8. EBOV viral proteins (Takada and Kawaoka, 2001)

1.5.3. EBOV Life Cycle

Viral attachment on target cells occurs through the binding of the fusogenic virus envelope glycoprotein (GP1,2) produced by the cleavage of a precursor (GP0) obtained by the translation of the mRNA of the homonymous fourth gene

on the EBOV genome. EBOV entry mainly occurs through a macropinocytic pathway characterized by actin-dependent membrane ruffling (Figure 9). However, it is believed that also endocytic pathways can take place
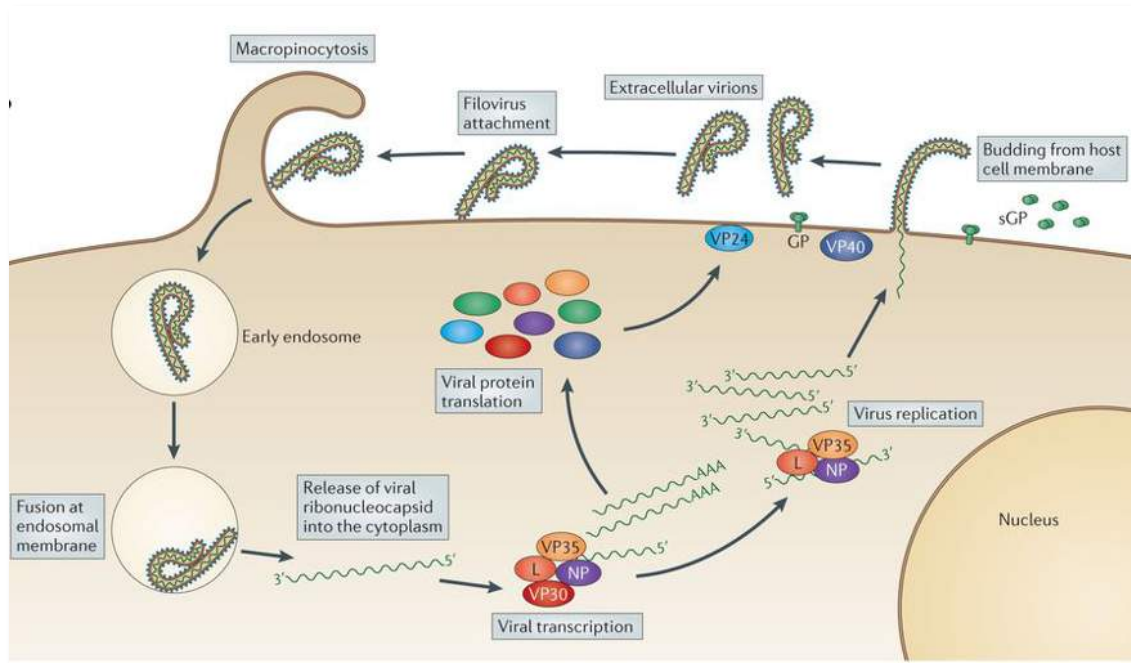
Figure 9. EBOV life cycle (Messaoudi et al., 2015)

(Empig and Goldsmith, 2002; Simmons et al., 2003; Yonezawa et al., 2005). From the early endosome the virus is trafficked to a late endocytic compartment containing the cysteine proteases cathepsin B (CatB) and cathepsin L (CatL) (White and Schornberg, 2012). These proteases digest GP1,2 to a 19 kDa form, which is then triggered to initiate fusion between the viral and endosomal membranes (White and Schornberg, 2012). After entry and membrane fusion, the RNP complex is released into the cytoplasm and serves for transcription and replication of the viral genome. In the RNP, the L protein must interact with VP35 to form a functional replicase and transcriptase complex. Moreover, the binding of VP35 to NP promotes the release of the RNA from the NP-RNA complex allowing RNA to be transcribed. The EBOV mRNA synthesis starts at 6–7 h post infection. The leader region of each ssRNA- is targeted by the EBOV

RNA-dependent RNA polymerase which slides along the RNA template, transcribing genes with a mechanism strongly dependent by VP30. Among the seven genes, NP is the most transcribed. When enough NP is present to encapsidate neosynthetized genomes the replication process starts. During replication, a full-length, positive sense antigenomic RNA is synthetized and serves as a template for production of progeny negative-sense genomes (Wang et al., 2015). Viral particles accumulate in the perinuclear region and are subsequently translocated to the budding sites at the plasma membrane. Virion assembly is mediated by GP, VP24, NP, and VP40 proteins. The matrix protein VP40 allows also the budding of the filamentous virions. The interaction of NP with VP40 is demonstrated to be crucial for NC transport to the cell surface and for its incorporation into virions, leading to the formation of mature virus particles (Yu et al., 2017).

1.5.4. EBOV Transmission

EBOV is a zoonotic pathogen whose reservoir has not been definitively clarified, possibly due to the difficulty to isolate EBOV or viral RNA in animals that are infected at very low titer. Currently, bats are considered to be the most likely reservoir species (Groseth et al., 2007) (Figure 10), while also plants, arthropods and birds are considered possible viral reservoirs.

Figure 10. A bat captured for testing EBOV (Philippe Psaila/Science Photo Library)

Traces of EBOV were found in the carcasses of gorillas and chimpanzees that represent the principal sources of human infections (Pourrut et al., 2005). Humans, in fact, are only occasional hosts. Animal-to-human spread mainly happens when humans come into contact with tissues and bodily fluids of infected animals, while human-to-human transmission occurs after direct contact with the blood or other fluids (saliva, tears, mucus, vomit, sweat, urine, feces, breast milk, and semen) of infected people or indirect contact with environment contaminated with infected body fluids (Rajak et al., 2015).

1.5.5. EBOV Pathogenesis

EBOV causes a highly contagious hemorrhagic fever in humans and non-human primates (NHPs) called Ebola virus disease (EVD). After viral inoculation onto mucosal surfaces or skin's injuries, EBOV targets dendritic cells, monocytes and macrophages, then it reaches the lymphatic system from which it spreads along multiple tissues and organs (Feldmann and Geisbert, 2011; Geisbert et al., 2003a, 2003b).

After an incubation period of generally 2–21 days, the first stages of the infection include an asymptomatic incubation followed by the onset of nonspecific symptoms consisting of fever, chills, fatigue, headache, myalgia and general malaise (Baseler et al., 2017; Feldmann and Geisbert, 2011). EVD subsequent manifestations are characterized by a multisystem involvement with systemic, gastrointestinal, respiratory, vascular and neurological disorders. During the peak of the illness, the hemorrhagic complications (macropapular rash, petechiae, ecchymosis, mucosal hemorrhages) occur followed, in later stages, by shock, convulsions, severe metabolic disturbances, and death typically within about 10 days of symptom for hypovolemic shock and multiorgan failure (Feldmann and Geisbert, 2011).

1.5.6. EBOV Therapeutics

A number of antiviral compounds have shown to be efficacious in both *in vitro* and *in vivo* studies and some of these were administered to EVD patients, or to people undergoing clinical trial evaluation, in particular during the 2014-2016 West African epidemic. Anti-EBOV agents include small molecules, antisense therapies and immunotherapeutics and can be categorized based on their proposed mechanism of action against the specific steps of the viral life cycle (Figure 11) (Fanunza et al., 2018a). Most of the identified EBOV inhibitors target the entry, transcription and replication steps.
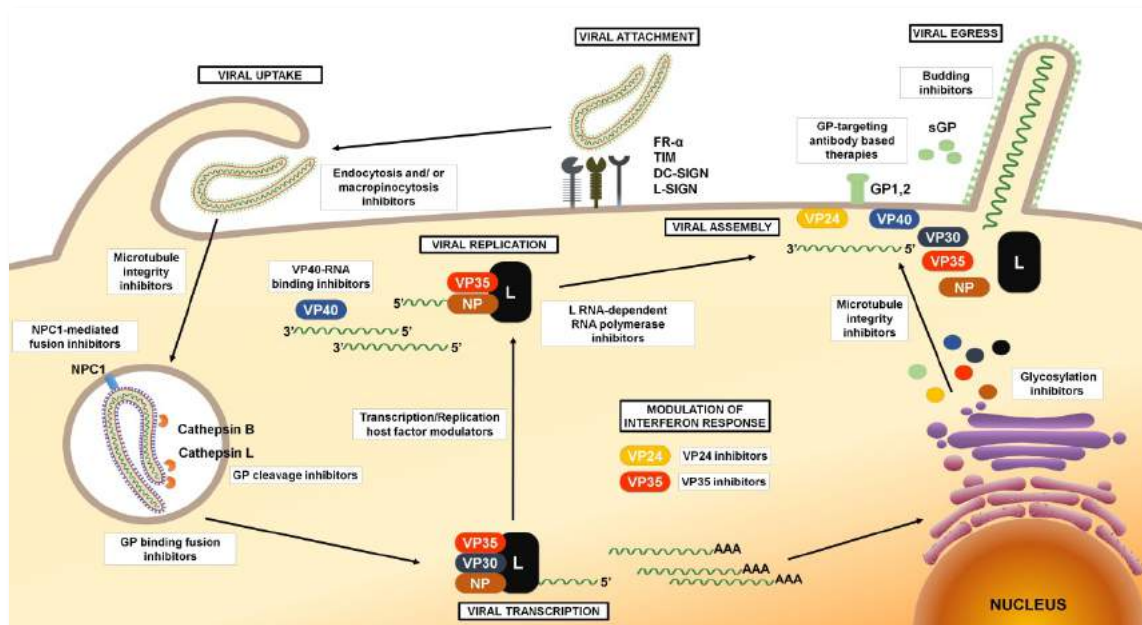
Figure 11. EBOV Inhibitors targeting the viral life cycle (Fanunza et al., 2018a)

Madrid et al. showed that the anti-malarial chloroquine inhibited EBOV entry in both viral pseudotype entry and replication assays with EC_{50} values of 4.7 µM and 16 µM, respectively (Madrid et al., 2013). Treatment of infected mice with 90 mg/kg of chloroquine 4 hours before infection was able to significantly reduce mortality, leading to a 90% survival benefit 13 days post infection. Chloroquine has been shown to directly perturb virus trafficking, partially due to its inhibitory effects on the pH-dependent CatB and CatL, which have been

shown to play a crucial role in EBOV GP1,2 processing events prior to fusion (Madrid et al., 2013).

Among GP antibody therapies, ZMAb (Defyrus/PHAC) and ZMapp have demonstrated in animal models some of the most significant therapeutic potential for treating EVD, showing to be highly effective in post-exposure prophylaxis of NHPs against EBOV. Administration of 25 mg/kg murine mAb cocktail ZMab to NHPs 24 h after EBOV challenge showed 100% effectiveness, while 50 mg/kg ZMapp treatment showed 100% protection when administered 3 days post infection (Qiu et al., 2012). ZMAb and ZMapp cocktails were used under emergency compassionate protocols in humans to treat EBOV infections during the 2014 EVD outbreak. Among seven patients treated with ZMapp, five surved, while all six patients treated with ZMAb survived (Davidson et al., 2015; Mora-Rillo et al., 2015; Schibler et al., 2015). In the PREVAIL II study during the 2014-2016 outbreak, a randomized controlled trial performed in the countries of Guinea, Liberia, Sierra Leone and the USA, ZMapp was administered to patients (often in combination with other therapies), however, due to low enrollment numbers, the study did not produce any statistically definitive conclusions concerning the efficacy of ZMapp treatment (Davey et al., 2016).

Most of the advanced therapeutics to counteract EVD are small molecules inhibiting the viral L protein. Among them, GS-5734, a monophosphoramidate prodrug of an adenosine analogue that is rapidly converted to its pharmacologically active triphosphate form, showed anti-EBOV activity (EC_{50} = 0.086-0.14 μM). In a NHP EBOV model an intravenous administration of 10 mg/kg for 12 days resulted in 100% animal survival (Warren et al., 2016). Moreover, Brincidofovir (CMX001), the 3-hexadecyloxy-1-propanol (HDP) lipid conjugate of the acyclic nucleoside phosphonate cidofovir, originally studied as

a treatment for double-stranded DNA viruses, has been demonstrated to inhibit EBOV replication *in vitro* (EC_{50} = 120 nM-1.3 μM) (McMullan et al., 2016). Brincidofovir has been experimentally used in emergency situations to treat one of the first EBOV patients and underwent Phase II clinical trial that was however halted due to the limited number of enrolled patients (Dunning et al., 2016; Florescu et al., 2015; Warren et al., 2014).

Despite the tremendous efforts spent in the discovery of therapeutics, no EBOV-specific therapy has conclusively achieved regulatory approval for use in humans (Bixler et al., 2017). A promising vaccine candidate, the rVSVΔG-ZEBOV-GP, has been granted Breakthrough Therapy Designation by the U.S. Food and Drug Administration (FDA) and PRIority Medicines status from the European Medicines Agency (Merck Press Release, 25 Jul 2016) and is currently awaiting a license (Cardile et al., 2016). The vaccine showed 100% protection during a ring vaccination trial in Guinea, Sierra Leone and Conakry and now it is still in use in the ongoing outbreak of Democratic Republic of Congo (May 2018) (Cardile et al., 2016).

1.6.   EBOV Suppression of the IFN Response

The severity of EVD is mainly due to the massive viral replication and dissemination that are strictly dependent on the EBOV efficiency to evade the host innate immune response, particularly the IFN system (Basler, 2015; Feldmann and Geisbert, 2011). The first evidences were observed in human umbilical vein endothelial cells where the induction of several immunomodulatory genes, including the major histocompatibility complex class I (MHC-I) family of genes, 2′-5′ oligoadenylate synthetase, interleukin-6 (IL-6), PKR, IRF-1, and intercellular adhesion molecule-1 (ICAM-1) by dsRNA polyinosinic acid:polycytidylic acid (PIC) was dramatically suppressed by

infection with EBOV and not by other negative-stranded RNA viruses (Harcourt et al., 1998). In mock-infected cells, PIC induced the formation of protein–DNA complexes that specifically target the ISRE or GAS promoters, while infection with EBOV strongly blocked the formation of these PIC-induced complexes, suggesting a possible inhibition of STAT-1α function (Harcourt et al., 1998). Moreover, the same EBOV infection did not induce these genes (Harcourt et al., 1999, 1998).

Addition of IFN-γ or IFN-α or their combination in EBOV infected cells led to a complete inhibition of IFN induction resulting in a level of MHC protein expression lower than that in the mock-infected not stimulated cells (Harcourt et al., 1999). After these preliminary studies, much work has been done to deeply investigate the viral proteins responsible for the IFN inhibition and now it is well known that they are VP35 and VP24 (Basler, 2015; Basler et al., 2003, 2000; Cannas et al., 2015; Cardenas et al., 2006; Fanunza et al., 2018c; Hartman et al., 2008a; Leung et al., 2010c, 2009; Luthra et al., 2013; Mateo et al., 2010; Prins et al., 2010; Ramanan et al., 2011; Reid et al., 2006, 2007, 2005, Zinzula et al., 2012, 2009; Zinzula and Tramontano, 2013b).

1.6.1. VP35 and IFN Inhibition

The EBOV-encoded protein VP35, whose gene is positioned second on the 19 kb EBOV linear genome, is a protein of 340 amino acid residues long with a molecular mass of ~35 kDa. VP35 is a dsRNA binding protein that fulfills several important functions in the viral life cycle, acting i) as a component of the replication and transcription holoenzyme, ii) as an assembly factor of EBOV viral particles and iii) as a powerful antagonist of the host antiviral innate immune response (Basler et al., 2000; Leung et al., 2010b; Mühlberger, 2007; Mühlberger et al., 1999).

VP35 allows the efficient impairment of the host defenses and the viral replication blocking the IFN-α/β production pathway at several points, both hiding and directly hitting the components of the pathway (Figure 12) (Basler, 2015; Versteeg and García-Sastre, 2010).
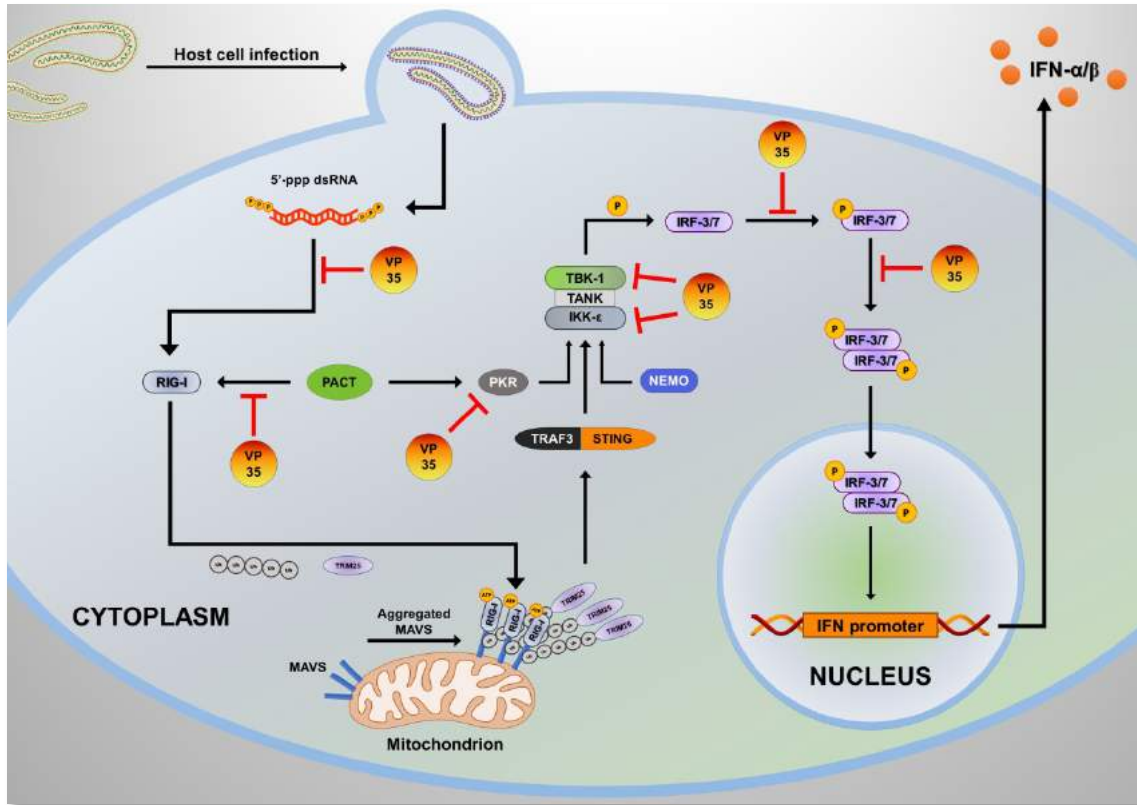
Figure 12. Mechanisms of VP35 inhibition of IFN system (Fanunza et al., 2018b)

The VP35 C-terminal domain is involved in suppression of the IFN response as demonstrated by the fact that this domain alone is sufficient to exert this property; therefore, it was named interferon inhibitory domain (IID) (Leung et al., 2009). In addition, the N-terminal coiled-coil domain provides a critical VP35 oligomerization function enhancing IFN inhibition as its deletion or mutation abrogates IFN suppression (Reid et al., 2005).

VP35 was found to act at the cascade upper levels, hiding the presence of dsRNA replicative intermediates to the sensory action of RIG-I and MDA5. The central basic patch (CBP) of VP35 IID is involved in the interaction with

dsRNAs, differently from the first basic patch (FBP) important for VP35 function in the replication complex. Crystallographic analyses solved the structures of EBOV IID in complex with 8 bp dsRNA (Leung et al., 2010a) and revealed that VP35 uses a bimodal strategy to bind the dsRNA. The terminal nucleotides and the proximal phosphate backbone are bound by a VP35 monomer, while the sugar-phosphate backbone is bound by a second VP35 monomer. The two binding modes, named "end-capping" and "backbone-capping", allow the two VP35 monomers to assemble as an asymmetric dimer that binds with very high affinity to both blunt-ended and 5'-ppp dsRNA molecules and in a sequence-independent mode (Cardenas et al., 2006; Feng et al., 2007; Kimberlin et al., 2010; Zinzula et al., 2012, 2009). The structural characteristics of the VP35 IID revealed the contribution of several amino acids for the dsRNA binding function. Residues lying within the highly conserved CBP R305, K309, R312 and K339 directly interact with the dsRNA phosphate backbone. In addition, protein–protein interactions occur between the R312, K319, R322 and K339 and the dimer interface. In the end-capping monomer I340 and F239 interact with the K339, Q274 and I278 residues, which bind dsRNA terminal nucleotides (Figure 13) (Kimberlin et al., 2010; Leung et al., 2010a). Mutations in residues R305, K309, R312, K319, R322, F239 and K339 correspond to a diminished or abolished suppression of IFN-β induction (Cardenas et al., 2006; Hartman et al., 2008b, 2008a, 2006, 2004; Leung et al., 2010a; Prins et al., 2010; Zinzula et al., 2012). In fact, while upon infection of guinea pigs with wild-type VP35 a massive viral replication with death of all animals is observed within 5 to 7 days postinfection, the VP35 double mutant R319A/ K322A (KRA) EBOV has been shown to be completely avirulent in this model. No viral RNA at 3, 5, or 17 days or later post-infection and any disease symptoms were detected upon infection with EBOV/VP35KRA, suggesting a very low virus replication in animals. Of note, when EBOV/VP35KRA infected guinea
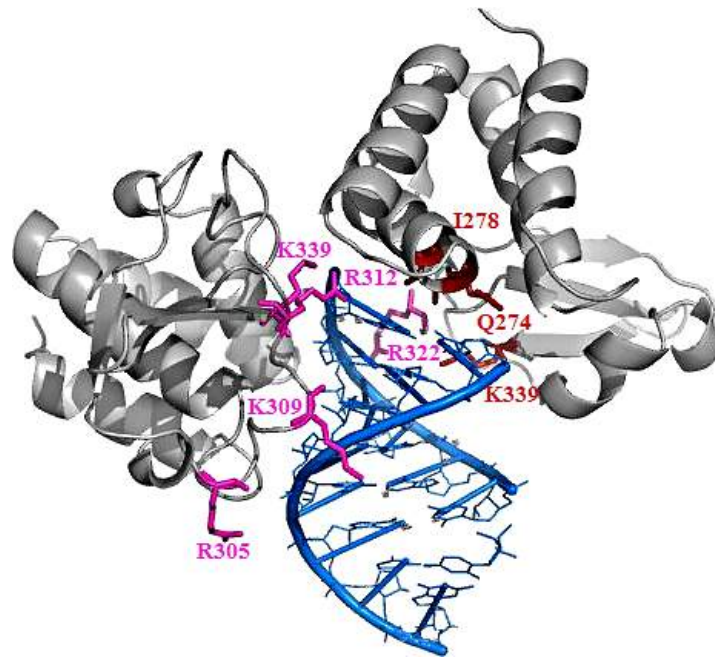
Figure 13. EBOV VP35 IID (gray) in complex with 8 bp dsRNA (blue). The "end-capping" and "backbone-capping" are labelled in red and pink, respectively.

pigs were challenged with lethal EBOV wt, all animals survived through 28 days postchallenge, confirming the EBOV/VP35KRA induction of an anti-EBOV state (Prins et al., 2010).

Beyond the sequestration and hiding of RLR-activating RNAs, VP35 also employs several "hit" strategies to suppress the downstream RIG-I pathway and IFN-α/β induction (Zinzula & Tramontano, 2013). EBOV VP35 was shown to block the Sendai virus-induced activation of ISG54 and ISG56 promoters which are directly activated by IRF-3, whose phosphorylation, dimerization and nuclear accumulation were also inhibited (Basler et al. 2003). Further, it was demonstrated that VP35 blocked IRF-3 phosphorylation and nuclear translocation induced by TBK-1 and IKKε overexpression (Prins et al., 2009). Notably, co-immunoprecipitation (co-IP) studies revealed VP35 ability to directly interact with TBK-1 and IKKε, via their more conserved kinase domains located within the N-terminal domain of the two proteins, decreasing their catalytic activity and, acting as substrate being phosphorylated by these

kinases. The overexpression of VP35 resulted in a disruption of IKK-ε interactions with IRF-3, IRF-7 and MAVS (Prins et al., 2009). In addition, the N-terminal half of VP35 physically interact with both IRF-3 and IRF-7 to promote their ubiquitin (Ub)-like modification by the two members of the small Ub-like modifier (SUMO) cascade PIAS1 (the SUMO E3 ligase protein, inhibitor of activated STAT) and Ubc9 (the SUMO E2 enzyme), thereby inhibiting the IRFs transcriptional function and subsequently suppressing the activation of IFN-β promoter (Chang et al., 2009; Kühl and Pöhlmann, 2012).

VP35 also inhibits the RIG-I-induced TRIM6-mediated IFN-I production by counteracting the host ubiquitin system (Chen and Sun, 2009; Oudshoorn et al., 2012; Rajsbaum and García-Sastre, 2013) (Rajsbaum and García-Sastre, 2013). VP35 IID K309 ubiquitinated interacts with TRIM6, a member of the E3-ubiquitin ligase tripartite motif family that promotes the synthesis of unanchored poly-Ub chains required for activation of IKKε kinase, thus blocking its IFN induction function (Bharaj et al., 2017; Rajsbaum et al., 2014).

Furthermore, VP35 interacts with RNA-activated protein kinase (PKR) activator (PACT), a cellular dsRNA binding protein involved in stimulation of RIG-I ATPase activity thus facilitating its activation by dsRNA (Leung et al., 2010b; Luthra et al., 2013). EBOV VP35 interacts with PACT disabling its interaction with RIG-I so that PACT activation of RIG-I and induction of IFN-α/β gene expression is impaired. Interestingly, mutations of residues that abolished VP35 dsRNA binding activity resulted in the disruption of VP35-PACT interaction and in the VP35 inability to block PACT–RIG-I interaction. This provides evidence that the same VP35 residues mediating the binding with dsRNA are also involved in the direct interaction with PACT (Luthra et al., 2013).

Finally, VP35 counteracts IFN-α/β induction inhibiting the activation of the dsRNA-activated kinase PKR (Feng et al., 2007; Schumann et al., 2009). PKR is

activated by autophosphorylation upon binding to dsRNA or phosphorylation by PACT. In normal conditions, PKR is expressed at basal level, but upon IFN induction its expression is upregulated and acts as an intracellular PRR, enhancing the IFN production (Dalet et al., 2015; McAllister and Samuel, 2009; Zhang and Samuel, 2008). After the interaction with dsRNA, the activated PKR phosphorylates the residue S51 of the α subunit of translation initiation factor eIF-2 (eIF-2α), which blocks protein synthesis (Feng et al., 2007). The VP35 IID involved in dsRNA binding and IRF3 inhibition also mediates the inhibition of PKR enhancing the protein synthesis, but the mechanism seems to be dsRNA-binding independent (Schumann et al., 2009). Despite PACT is a PKR activator, no direct relation has been shown between the VP35 inhibition of PACT and PKR (Basler, 2015).

1.6.2. VP24 and IFN Inhibition

EBOV VP24 is also one of the seven proteins encoded by the viral genome. VP24 has been demonstrated to participate in different levels of the EBOV life cycle, including nucleocapsid formation, assembly and budding of the viral particles and viral replication (Han et al., 2003; Huang et al., 2002; Mateo et al., 2011a; Noda et al., 2007, 2006, Watanabe et al., 2007, 2004). Moreover, VP24 is known to contribute to the EBOV high virulence (Mateo et al., 2011b), in particular for its role in modulating the host response to infection (Ebihara et al., 2006). Using reverse genetics, Ebihara et al. identified VP24 mutations correlated to the ability to evade type I IFN response that were responsible for the acquisition of high virulence of the adapted Mayinga strain in mice (Ebihara et al., 2006). The main mechanism by which VP24 is able to hinder the cellular antiviral defense is the efficient suppression of the both IFN-α/β and IFN-γ signaling (Reid et al., 2006). This reflects the protein ability to interact with a step that is common to both cascades: the binding of karyopherin-α (KPNα) to

phosphorylated STAT1 (P-STAT1) which is essential for the P-STAT1 nuclear translocation and hence activation of transcription of ISGs (Figure 14).
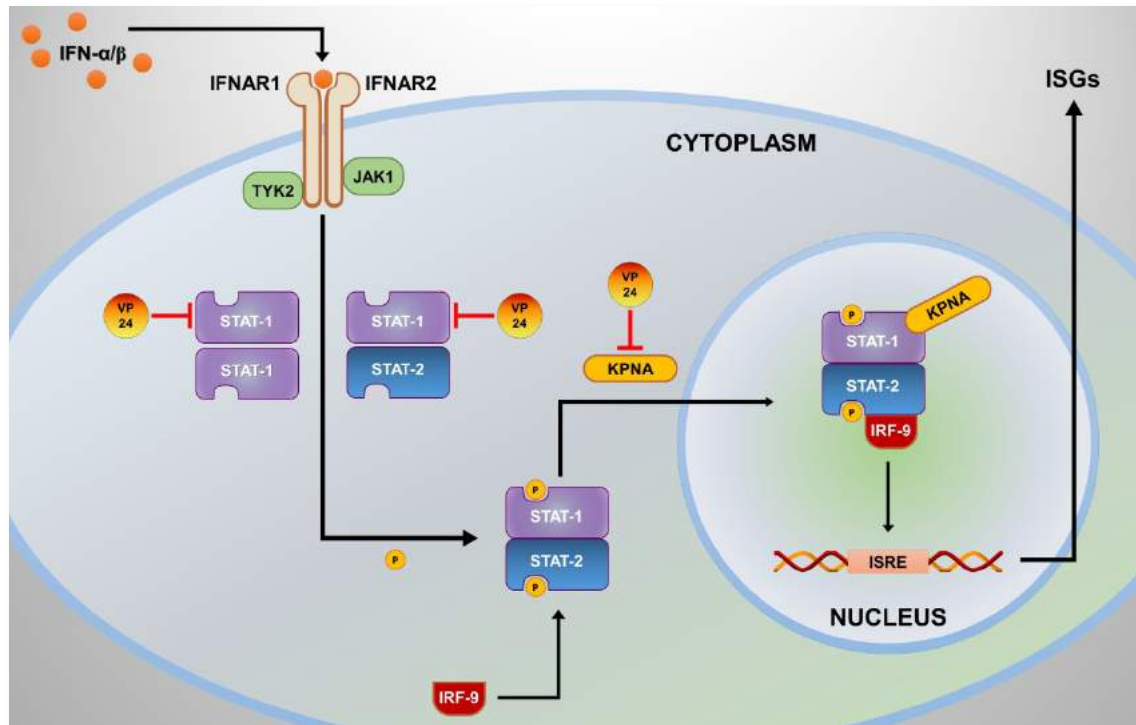
Figure 14. VP24 inhibition of IFN signaling (Fanunza et al., 2018b)

In particular, VP24 binds specifically to the NP1-1 subfamily of KPNα (α1, α5 and α6) while it does not interact with KPNα2, KPNα3 and KPNα4 (Mateo et al., 2010; Reid et al., 2006), which are not involved in STAT1 nuclear transport. Mutation analysis with truncated KPNα1 demonstrated that residues 425 to 538 are implicated with the binding to P-STAT1, while residues 458 to 504 bind VP24, revealing that there is a competition between the two proteins for the binding to the same region of KPNα1 (Reid et al., 2007). Subsequent studies identified two VP24 domains (26 to 50 and 142 to 146) responsible for blocking IFN-β gene expression and P-STAT1 nuclear translocation (Mateo et al., 2010). Combining a mutation in the first domain (W42A) and mutations at residues 142 to 146, ISGs promoter expression was increased more than 90% compared with wtVP24 and the interaction with KPNα1 decreased. Complete loss of binding was observed with the VP24 mutant K142A (Mateo et al., 2010).

The crystal structure of KPNα5 interacting with VP24 has been determined (Xu et al., 2015). Analysis of these residues demonstrated the hydrophobic property of the interface. KPNα5 residues 308-509 (KPNα5C) located in armadillo (ARM) repeats 7-10 are sufficient for binding to VP24 even if the minimal binding region is included within ARMs 8-10. Three clusters of VP24 are mainly involved in the binding to KPNα5C and include residues N130, T131, N135, R137, T138 and R140 (Cluster 1), residues Q184, N185, H186 (Cluster 2) and L201, E203, P204, D205 and S207 (Cluster 3) (Figure 15).
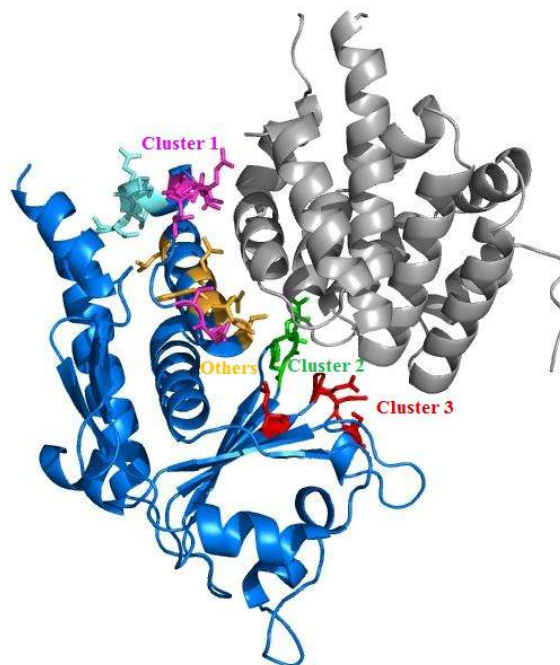
Figure 15. EBOV VP24 (blue) in complex with KPNα5C (gray). Residues implicated in the binding are grouped in Cluster 1 (pink), Cluster 2 (green) and Cluster 3 (red), while the other residues contributing to IFN signaling inhibition are shown in yellow.

Other residues required for the binding are L115, L121, D124, W125, T128 and T129. Mutations of residues 142 to 146 due to their proximity to cluster 1 probably contribute to conformational change of the binding site and consequent loss of IFN inhibitory function.

The ability of VP24 to inhibit the P-STAT1 nuclear transport is explained by the finding that VP24 specifically recognizes a non-classical nuclear localization

signal (ncNLS) binding site on KPNα5 that partially overlaps with the ncNLS binding site for P-STAT1 (Xu et al., 2015). Another suggested mechanism is the direct binding of VP24 with STAT1 (Figure 14) (Zhang et al., 2012). Using an *in vitro* binding assay, Zhang et al. reported that a purified EBOV VP24 bound directly a truncated form of STAT1 lacking the phosphorylation site at Y701, although it was not determined for full length non-phosphorylated STAT1 or P-STAT1 (Zhang et al., 2012). The finding, however, was not confirmed by cell-based experiments that did not detect interaction between VP24 and non-phosphorylated STAT1 or P-STAT1 (Xu et al., 2015).

In addition to its role within the JAK/STAT cascade, it has been shown that VP24 blocks the cellular response to type I IFN also counteracting the p38 MAP kinase pathway inhibiting the IFN-β–induced phosphorylation of p38-α (Halfmann et al., 2011). The p38 MAP kinase cascade is activated after hepatitis C virus infection inducing the cellular antiviral state. The finding that also VP24 blocks this response suggests that at least two mechanisms are possible for the IFN inhibition by VP24. There are, in fact, mutations critical for virulence in mouse-adapted EBOV not affecting the JAK/STAT cascade that might be related to this other IFN inhibitory function (Reid et al., 2007).

1.7.   Zika Virus

1.7.1. Epidemiology

Zika virus (ZIKV) was firstly isolated in 1947 from a Rhesus monkey in the Zika Forest (Uganda) (Figure 16) (Dick, 1952). In 1948, ZIKV was identified in *Aedes africanus* mosquitoes in the same forest. ZIKV has been described as causing sporadic human infections in Africa and Asia (Zanluca and Nunes, 2016). In 2007, the first documented ZIKV outbreak outside of Africa and Asia was reported on Yap Island, Micronesia (Duffy et al., 2009). No deaths were

associated with this outbreak. Other ZIKV infections occurred in Cambodia in 2010 (Heang et al., 2012), Philippines in 2012 (Alera et al., 2015) and Thailand in 2012-2014 (Buathong et al., 2015), but the rate of infection in these countries is unknown. In 2013 an outbreak of ZIKV disease initiated in French Polynesia where about 29.000 people underwent medical care (Paz et al., 2016). It was the first time that ZIKV was associated with severe disease, including neurological or autoimmune complications, although no deaths were observed (Oehler et al., 2014). In 2013, ZIKV was isolated from a German traveller returning from Thailand, representing the first imported case of ZIKV in Europe (Tappe et al., 2014). In 2014, the first autochthonous outbreak of ZIKV with fifty-one cases was reported in Easter Island, South Pacific (Tognarelli et al., 2016).

Figure 16. Zika forest in Uganda (Credit: Isaac Kasamani / Getty)

In 2015, the autochthonous transmission of ZIKV was confirmed by the Ministry of Health of Brazil, where cases of a flu-like illness associated with fever, conjunctivitis and arthralgia were reported (Zanluca et al., 2015). During this epidemic, ZIKV was associated with fetal malformations and death (Zanluca et al., 2015). The autochthonous spread of ZIKV continued in other 30 American countries and territories, being the largest ZIKV outbreak ever reported. On 1st February 2016, the World Health Organization (WHO)

declared the global public health emergency (World Health Organization, 2016b).

1.7.2. ZIKV Genome and Proteins

ZIKV is an arthropod-born virus that belongs to the family of *Flaviviridae* (International Committee on Taxonomy of Viruses, 2015). Like the other flaviviruses, ZIKV has a positive-sense, single-stranded RNA genome (ssRNA+) of approximately 10.7 kb in length, which is in complex with multiple copies of the capsid protein. The genome encodes a single polyprotein that is processed by viral and cellular proteases into three structural proteins, the capsid (C), membrane (prM) and envelope (E) proteins that mediate virus attachment, entry and encapsidation, and seven non-structural (NS) proteins (NS1, NS2A, NS2B, NS3, NS4A, NS4B and NS5), which function in viral replication and polyprotein processing (Figure 17) (Barzon et al., 2016).
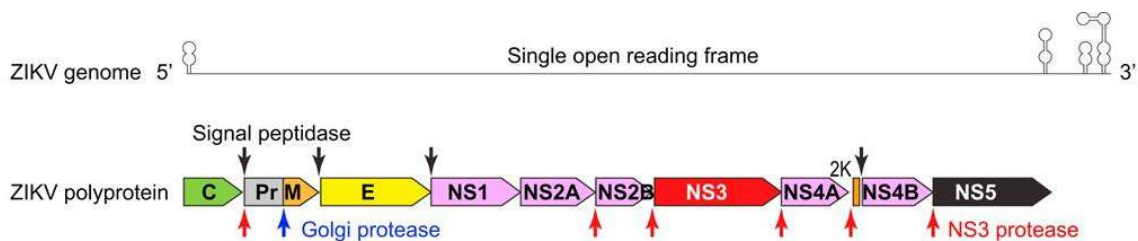
Figure 17. Genome and encoded proteins of ZIKV (Ming et al., 2016)

1.7.3. ZIKV Life Cycle

ZIKV is introduced into the cytoplasm of the target cell after fusion of the envelope with endosomal membranes (Figure 18). ZIKV has been shown to entry into the infecting cells using the lectin DC-SIGN. Additional receptors have been reported such as T-cell immunoglobulin and mucin domain (TIM1) TYRO3, and AXL. During endocytosis, acidification is required to allow the
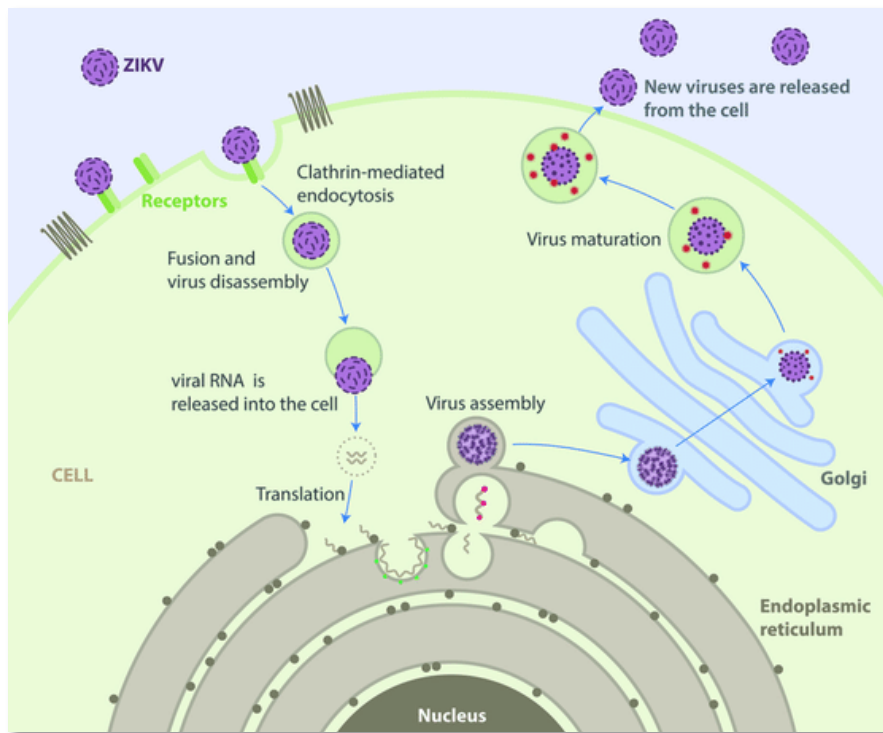
Figure 18. ZIKV life cycle (Acosta-Ampudia et al., 2018)

dissociation of the E protein dimers, exposing the fusion loop, and E monomers are rearranged into trimers. In this active form, they can be inserted into the endosomal membrane, inducing the fusion of the viral envelope and release of the viral RNA into the cytoplasm. At this point, the translation of the ssRNA+ can start. This process occurs at the endoplasmic reticulum membrane. The polyprotein is cleaved by viral and host proteases; most cleavages between nonstructural proteins are catalyzed by the NS2B/3 protease complex. Invaginations of the ER give rise to clusters of vesicles designated vesicle packets (VPs), which are the presumed sites of viral RNA replication. The ssRNA+ genome is copied to give a ssRNA- molecule, which serves as the template for synthesis of the full-length positive-sense genomic RNA. During this process, a replicative intermediate of double-stranded RNA is formed. Synthesis of viral genome is mediated by a replication complex that includes the NS5 RNA-dependent RNA polymerase and other NS proteins. The new genomes are packaged by the C protein which contains an RNA-interacting

domain and acquire the envelope while budding from the ER. These immature virions are transported through the acidic compartment of the trans-Golgi network, where E glycosylation and cleavage of prM by host protease furin occurs resulting in the rearrangement of the virion surface and formation of mature virions that are released by exocytosis (Barzon et al., 2016; Medin and Rothman, 2017).

1.7.4. ZIKV Transmission

ZIKV is maintained in a sylvatic environment, in a zoonotic cycle between mosquitoes (Aedes spp. and other species) and non-human primates (Figure 19) (Paz et al., 2016). ZIKV has been isolated from different mosquito species: *Aedes africanus, Aedes aegypti, Aedes furcifer, Aedes hirsutus, Aedes luteocephalus, Aedes taylori, Aedes metalicus, Aedes vittatus, Aedes unilineatus, Aedes dalzieli, Anopheles coustani, Mansonia uniformis* and *Culex perfuscus* (Zanluca and Nunes, 2016). In the urban transmission (mosquito-human-mosquito) ZIKV is transmitted to humans through the bite of an infected female of Aedes spp mosquitoes. The virus is acquired by the arthropod during a blood meal, and after replication in the body of the mosquito, it reaches the salivary gland and is transferred at the subsequent meal into the skin of the new host. Also cases of perinatal transmission have been reported and viral RNA has been detected in breast milk (Besnard et al., 2014). ZIKV has been isolated from the semen of a patient various weeks after the acute phase of the disease and a case of sexual transmission has been recorded (Musso et al., 2015b). Moreover, viral RNA and proteins has also been detected in urine, saliva, amniotic fluid and placental tissues, suggesting the possibility of multiple mechanisms of transmission (Gourinat et al., 2015; Hiller et al., 2015; Musso et al., 2015a; Oliveira Melo et al., 2016).
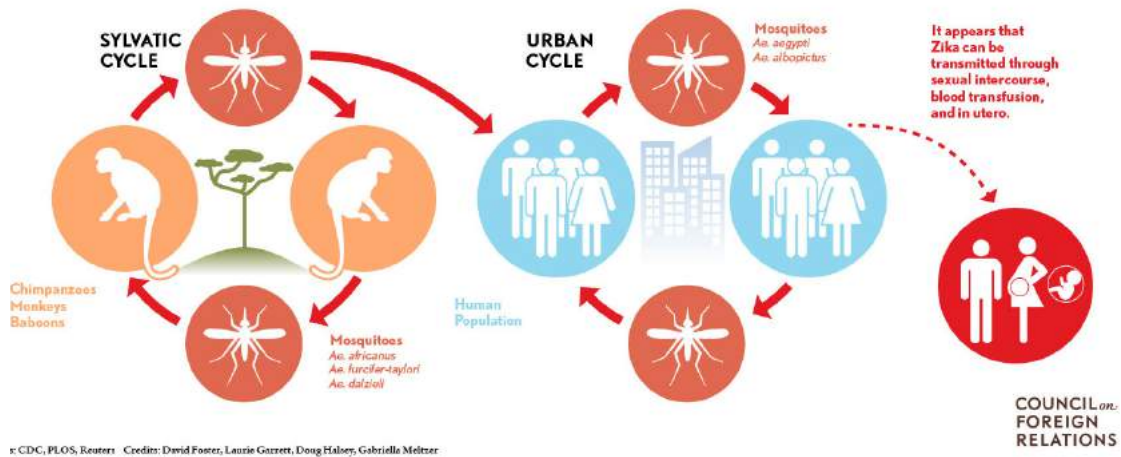
Figure 19. ZIKV sylvatic and urban cycles (Renwick, 2016)

1.7.5. ZIKV Pathogenesis

The first site of viral replication is represented by the skin at the site of inoculation. Human primary dermal fibroblasts, epidermal keratinocytes and immature dendritic cells have been demonstrated to permit ZIKV infection and replication (Hamel et al., 2015). From the skin, the virus circulates to the draining lymph node and the bloodstream, disseminating to peripheral tissues and visceral organs. ZIKV has also been shown to infect placental macrophages, cytotrophoblasts and human neural progenitor cells (Bayer et al., 2016; Quicke et al., 2016).

ZIKV infection is asymptomatic in the 80% of the cases. However, when symptoms occur, they appear 3-11 days after the mosquito bite. ZIKV disease is similar to a febrile illness without severe complications. Papular rash, fever, arthralgia, fatigue, conjunctivitis, myalgia and headache are the frequent symptoms (Barzon et al., 2016).

During the outbreaks in French Polynesia and in Brazil high incidences of neurological complications have been registered. It has been observed a temporal association between the increase in cases of microcephaly in fetus

born from women presenting ZIKV-compatible clinical symptoms during early pregnancy (Figure 20).

Figure 20. A father holds his son who is affected by microcephaly (VOA, 2016)

The first trimester of pregnancy represented the period of major risk for microcephaly. Some of the typical malformations reported in infected fetuses and newborns include intrauterine growth restriction, cerebral and placental calcifications, agenesis of corpus callosum, hydrocephalus and brain atrophy. ZIKV infection has also been linked with the Guillain–Barré syndrome, an autoimmune disease causing flaccid paralysis, acute meningoencephalitis and myelitis in adults (Barzon et al., 2016).

1.7.6. ZIKV Therapeutics

Nowadays, no antiviral agents against ZIKV have been approved. However, a great effort has been carried out to test several drug candidates directed against viral or host targets (da Silva et al., 2018). Among compounds targeting the early stages of the ZIKV life cycle, Chloroquine, also mentioned as anti-EBOV agent, has been reported to inhibit ZIKV with EC_{50} values between 9.8 and 14.2 μM, possibly acting during the fusion of the E protein to the endosome membrane (Delvecchio et al., 2016). Chloroquine was also reported to protect fetal mice from microcephaly caused by ZIKV infection (Li et al., 2017). Antivirals directed against the RNA-dependent RNA polymerase NS5 have also been investigated. Among them, the nucleoside analog BCX4430 has been

reported to inhibit ZIKV replication with EC_{50} values of 3.8 to 11.7 μM, andadministration of 300 mg/kg/day of compound protected 7 out of 8 ZIKV-infected AG129 mice compared with vehicle-treated animals (Julander et al., 2017). Sofosbuvir, a nucleotide analog approved by the FDA for the treatment of HCV, efficiently blocked ZIKV replication with EC_{50} values between 0.4 and 1.9 μM. Treatment with Sofosbuvir at 33 mg/kg/day for 7 days to ZIKV-infected mice resulted in a 50% survival rate compared with the 20% of vehicle-treated mice (Mesci et al., 2018). Due to the relevance of its function in the ZIKV life cycle, also the protease NS2B/3, represents a target for anti ZIKV treatment (Kang et al., 2017). Analyzing 71 small molecules already screened for HCV infection, it was found that 10 of them showed IC_{50} values ≤ 50 μM, with IC_{50} values of compounds named 2 and 3 of 5.2 μM and 4.1 μM, respectively (H. Lee et al., 2017). Furthermore, Bromocriptine, used to treat Parkinson's disease, was tested for the ability to block ZIKV infection showing to be active against NS2B-NS3 protease activity in a dose-dependent manner (Chan et al., 2017).

1.8.   ZIKV and IFN Response

ZIKV infection results in the production of type I, II and III IFNs as well as the activation of several ISGs (Bayer et al., 2016; Chaudhary et al., 2017; Hamel et al., 2016, 2015; Quicke et al., 2016). Secretion of type III IFNs by placental trophoblasts was reported to provide protection against ZIKV infection in placenta and neuroinvasion in other related flaviviruses (Bayer et al., 2016; Lazear et al., 2015). Infection of human fibroblasts resulted in the increased expression levels of RIG-I, MDA-5, TLR3 and IRF7 as well as ISGs (ISG15, OAS2 and MX1) transcription (Hamel et al., 2016). The expression of ISGs such as IFITM1 and IFITM3 led to the inhibition of ZIKV replication (Savidis et al., 2016). Additionally, another ISG named viperin is able to restrict infection in

human hepatoma cells; and viperin knockout mouse embryonic fibroblast cells produce higher ZIKV titers than wt infected cells (Van Der Hoek et al., 2017).

However, dependent on cell type and viral strain, ZIKV infection can result in induction or evasion of the IFN system. For example, human dendritic cells are permissive to productive infection by the contemporary ZIKV strain Puerto Rican (Bowen et al., 2017). Treatment with a highly specific RIG-I agonist, strongly restricted ZIKV replication, suggesting that this strain was acting on the IFN signaling cascade, in particular at level of STAT1/STAT2 phosphorylation (Bowen et al., 2017). ZIKV, like the other member of its family, is able to dampen the IFN system employing different mechanisms to interfere at both level of the cascade: IFN production and IFN signaling (Figure 21).
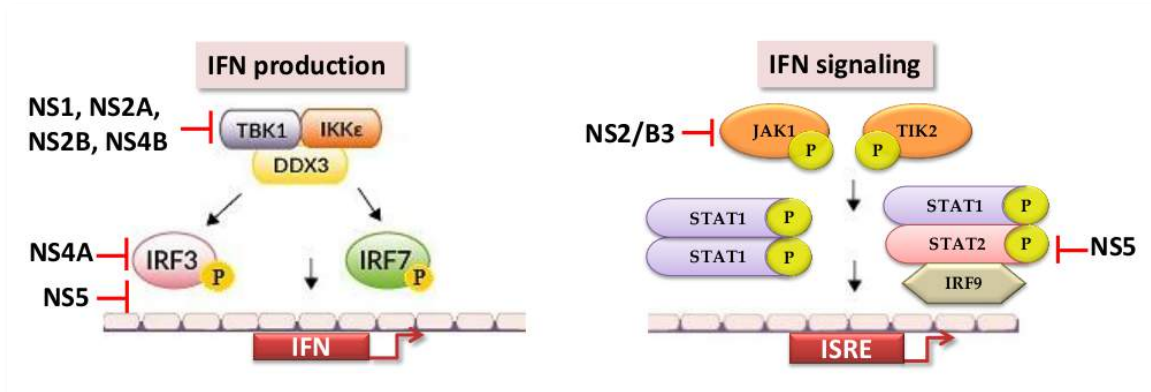
Figure 21. ZIKV evasion of IFN system

1.8.1. ZIKV Evasion of IFN Production

ZIKV NS1 and NS4B proteins are able to block type I IFN induction through inhibition of RIG-I-like receptor signaling. Overexpression of both proteins inhibited induction of IFN-β reporter activation mediated by cytoplasmic poly(I:C), poly(dA:dT) as well as Sendai Virus (SeV) in 293T cells. Phosphorylation of TBK1 and IRF3 and the expressions of IFNβ and ISGs were also inhibited by NS1 and NS4B after SeV infection. Co-immunoprecipitation studies demonstrated that NS1 and NS4B directly interacted with TBK1

impairing its function by blocking its oligomerization (Wu et al., 2017). Five non-structural proteins, NS2A, NS2B, NS4A, NS4B, and NS5 were also reported to significantly block the IFN-β promoter expression (Kumar et al., 2016; Xia et al., 2018). All five proteins inhibited the promoter transcription induced by ectopic expression of RIG-I (2CARD), MAVS, IKK-ε, or TBK1, while only NS5 was also able to block IRF3 induced IFN-β promoter activation. In fact, NS2A, NS2B, and NS4B were reported to inhibit TBK1 phosphorylation; NS4A suppresses IRF3 phosphorylation; while NS5 counteracts a step downstream of IFR3 phosphorylation by binding it (Xia et al., 2018).

1.8.2. ZIKV Evasion of IFN Signaling

A recent study reported the ability of the ZIKV protease complex, NS2B3, to suppress the IFN signaling pathway. NS2B3, in fact, has shown shown to be able to interact with JAK1 promoting its degradation, resulting in the inhibition of STAT1 phosphorylation and in the reduced expression of ISGs such as ISG15, IFIT1, IFIT2 and viperin in NS2B3 overexpression cells upon stimulation with IFNβ (Wu et al., 2017).

The JAK/STAT cascade is targeted also by ZIKV NS5. As observed for DENV, ZIKV NS5 is able to bind and degrade STAT2 (Grant et al., 2016; Kumar et al., 2016). However, the two proteins act through a different mechanism. In the case of DENV NS5, it binds to STAT2 and co-opts the host E3 ubiquitin ligase UBR4, which mediates the specific NS5 N-terminus degradation. By contrast, proteolytic processing of ZIKV NS5 did not require an authentic N terminus and UBR4 interaction (Grant et al., 2016).

1.8.3. Correlation between ZIKV IFN Antagonism and Virulence

The 2016 outbreak ZIKV strains have accumulated mutations in residues involved in anti-host countermeasures that promote the viral antagonism of innate response, resulting in increased viral replication and pathogenesis in humans. These mutations occur faster than others in the flavivirus genome. A report by Mlakar et al. described that a full-length ZIKV genome isolated during the recent Brazil outbreak had polymorphisms within the ORF compared with the 2013 French Polynesian isolate. Interestingly, the amino acid changes were found in NS1 and NS4B, known to be involved in immune evasion, and in the FtsJ-like methyltransferase region (M2634V) of NS5, a domain involved in hiding the viral RNAs from host recognition in WNV (Mlakar et al., 2016). The A188V substitution in the NS1 gene of the ZIKV strains isolated after 2012 enabled the protein to inhibit the IFN-β induction, in contrast with NS1 of the pre-epidemic strains. The mutation allows the binding between NS1 and TBK1 resulting in decreased IRF3 phosphorylation. Massive viral replication, high brain viral titers, neurovirulence and increased mortality rate were observed after intracranial infection of mice with A188V mutant virus, compare to that infected with wt (Xia et al., 2018). A mouse-adapted strain of ZIKV with a substitution (G18R) in the NS4B protein was generated by Gorman et al. The introduction of the mutation was associated with reduced IFN-β production and ISGs expression and resulted in increased viral replication in neuronal stem cells and greater brain infection in mice infected with the mutant strain (Gorman et al., 2018).

1.9. Objectives

This thesis explores the details of the molecular mechanisms at the base of the IFN signaling inhibition mediated by i) EBOV and ii) ZIKV, with a final common objective for the two different types of viruses: the identification of a novel and specific antiviral strategy based on the restoration of the IFN response. However, the gained knowledge on understanding IFN evasion is undoubtedly different comparing both viruses. While the modes of EBOV IFN escape have been deeply investigated, very little is known about a new emergent virus such as ZIKV. The process of antivirals identification involves the following steps: target identification and validation, assay development, screening, lead optimization, preclinical testing and clinical trials (Figure 22). Even though EBOV and ZIKV lines of research converge in the same objective, they necessary initiate from different starting points (arrows in Figure 22). In the context of EBOV, the viral protein responsible for IFN signaling inhibition is VP24, which has been validated as pharmacological target. Thus, the EBOV project will address the following points: i) development of a drug screening assay able to quantify the effect of VP24 on the IFN induction cascade (Chapter 3); ii) screening of natural compounds as potential inhibitors of VP24 (Chapter 4). The ZIKV project (Chapter 5), instead, aims to exploit the details of ZIKV IFN signaling evasion bringing to light novel potential pharmacological targets, which is the first step directed toward the development of an anti-ZIKV therapeutic strategy.
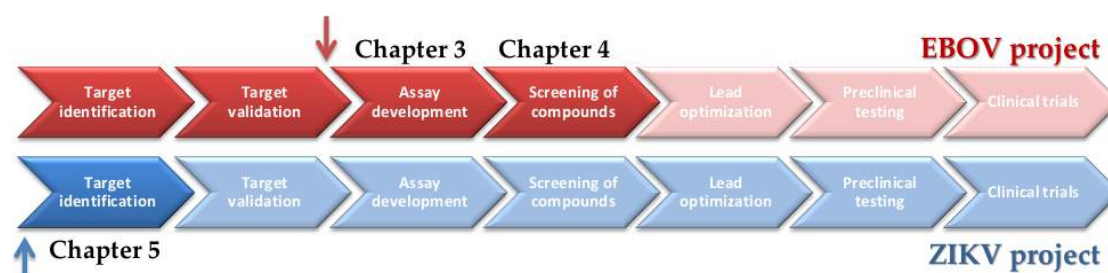
Figure 22. Work flow diagram of the thesis

Chapter 2

Materials and Methods

2.1. Cells and Reagents

HEK293T cells were grown in Dulbecco's modified Eagle's medium (Gibco) supplemented with 10% fetal bovine serum (Gibco) and 1% penicillin/streptomycin (Sigma). Cells were incubated at 37 °C in a humidified 5% CO_2 atmosphere. Plasmid pISRE-luc was kindly provided by Prof Ian Goodfellow (University of Cambridge, UK). Plasmid pcDNA3-V5-VP24 was a kind gift of Dr St Patrick Reid (University of Nebraska Medical Center, USA). pcDNA3-NS1 was kindly given by Prof Stephan Ludwig (University of Münster, Germany). pRL-TK was purchased from Promega. T-Pro P-Fect Transfection Reagent was from T-Pro Biotechnology. Human Recombinant IFN-α was purchased from PeproTech. Gossypetin, Taxifolin, Tricetin were purchased from Extrasynthese. Myricetin and Dihydromyricetin were kindly provided by Prof Lijia Xu (IMPLAD, Beijing, China), Luteolin, Apigenin, Quercitrin and Quercetin by Prof. Mauro Ballero (University of Cagliari, Italy), Wogonin and Baicalein by Prof. Ming Ye (University of Beijing, China). Mouse monoclonal anti-FLAG M2 was obtained from Sigma. Rabbit antibodies against P-STAT1, P-STAT2, GAPDH and the anti-rabbit HRP-linked IgG were purchased from Cell Signaling. Rabbit anti-STAT1 and P-JAK1, HRP-linked anti-mouse IgG, goat anti-mouse IgG Alexa Fluor 488, goat anti-rabbit IgG Alexa Fluor 594 and Pierce ECL Western Blotting Substrate were from Thermo Fischer Scientific.

2.2.   Construction of Mammalian Expression Plasmids

The EBOV VP24 expression plasmid was kindly given us by Marco Sgarbanti (Superior Institute of Health, Rome, Italy). The VP24 cDNA, was obtained by de novo gene synthesis (GenScript USA Inc. Piscataway, NJ) using the sequence of VP24 from the Zaire Ebolavirus isolate H.sapiens-wt/GIN/2014/Gueckedou-C05, Sierra Leone/guinea. The FLAG epitope, present in frame at the NH_2 terminus of VP24 sequence, and the HindIII and EcoRV restriction sites at both ends, used for the sub-cloning in the pcDNA 3.1 (+) (Invitrogen), were also part of the entire sequence obtained by de novo gene synthesis. Each ZIKV NS gene was amplified from the strain Brazil/ 2016/INMI1, an Asian lineage isolated at the Spallanzani hospital (Rome) from sera of a traveller returning from Brazil to Italy. The coding sequences with a C-terminal Flag tag were subcloned into the pcDNA3.1 (+) using NheI and EcoRI as restriction enzymes. Our library included the non-structural proteins: NS1, NS2A, NS4B and the fusion proteins NS2B/3 and NS3/4A. The NS4B construct used in these studies contains the 2K signal peptide. The primer pairs used for subcloning are listed in Table 1.

Table 1. Primers for subcloning

Primer name[a]	Sequence (5' to 3')
NS1_F	GTGGGGTGTTCGGTGGACTTC
NS1_R	AAGGGAGAAGTGATCCATGTG
NS2A_F	GGAGTGCTTGTGATTCTGCTC
NS2A_R	GGGCCAGCTCCGCTTCCCACT
NS2/B3_F	CCTAGCGAAGTACTCACAGCT
NS2/B3_R	AGCCGCTCCTCTTTTCCCAGC
NS3/4A_F	ACCACAGATGGAGTGTACAGA
NS3/4A_R	TCTTTGCTTTTCTGGCTCAGG
2K/NS4B_F	TCTCCCCAGGACAACCAAATG
2K/NS4B_F	ACGTCTCTTGACCAAGCCAGC

[a]F, forward; R, reverse.

2.3. Luciferase Reporter Gene Assay

HEK293T cells (1.5×10^4 cells/well) were seeded in 96-well plates 24 h before transfection. Plasmids pISRE-luc, pRL-TK were mixed in reduced serum medium Optimem (Gibco) and incubated with T-Pro P-Fect Transfection Reagent for 20 min at room temperature (RT). Transfection complexes were then gently added into individual wells of the 96-well plate. For inhibition assay the construct pISRE-luc was cotransfected with EBOV VP24 or ZIKV NS proteins expression plasmids. 24 h after transfection, cells were stimulated with IFN-α and incubated for 8 h at 37 °C in 5% CO_2. Then, cells were harvested with 50 μL of lysis buffer (50 mM Na-MES [pH 7.8], 50 mM Tris-HCl [pH 7.8], 1 mM dithiothreitol, and 0.2% Triton X-100). To lysates were added 50 μL of luciferase assay buffer (125 mM Na-MES [pH 7.8], 125 mM Tris-HCl [pH 7.8], 25 mM magnesium acetate, and 2.5 mg/mL ATP). Immediately after addition of 50 μL of 1 mM D-luciferin, the firefly luminescence was measured in Victor3 luminometer (Perkin Elmer). An equal volume, 50 μL, of coelenterazine assay buffer (125 mM Na-MES [pH 7.8], 125 mM Tris-HCl [pH 7.8], 25 mM magnesium acetate, 5mM KH_2PO_4, 10 μM coelenterazine) was added and the bioluminescence was read. The relative light units (RLU) were normalized as the fold induction over unstimulated controls. Luciferase activity was expressed as the percentage of ISRE expression in viral proteins transfected samples normalized to the empty vector samples (indicated as 100% of activation). Each assay was performed in triplicate.

2.4. Drug Screening EBOV VP24 Assay

After transfection with pISRE-luc, pRL-TK and VP24 expression plasmid, cells were stimulated with 1 ng/mL of IFN-α and treated with 10 μM of either Gossypetin, Taxifolin, Tricetin, Myricetin, Dihydromyricetin, Quercitrin,

Quercetin, Wogonin, Luteolin, Baicalein or Apigenin. After 8 h of stimulation, cells were harvested and luciferase assay buffer and D-luciferin were added. The firefly luminescence was measured. After addition of coelenterazine assay buffer the renilla luminescence was read. Luciferase activity was expressed as the percentage of ISRE inhibition in VP24 cells treated with compounds normalized to the VP24 not treated cells (indicated as 100% of inhibition). Each assay was performed in triplicate.

2.5.   Luciferase Assay Data Analysis

2.5.1. IC_{50} Calculations

To determine the concentration of IFN-α that provide the maximal activation of JAK-STAT pathway, the concentration of EBOV VP24, ZIKV NS2A and NS4B plasmid required to inhibit 50% of IFN-α stimulation (IC_{50}) and IC_{50} of Quercetin, we used the log agonist concentration versus response, variable slope algorithm in GraphPad Prism software where:

$$Y = Bottom + (Top - Bottom)/(1 + 10\hat{}((LogIC50))) \qquad (1)$$

IC_{50} values were calculated based on three independent experiments performed in triplicate.

2.5.2. Z- and Z'-factor Calculations

The Z- and Z'-factor values were calculated from the following equations developed by *Zhang et al* (Zhang et al., 1999)

$$Z = 1 - \frac{(3 * SD_s + 3 * SD_c)}{|M_s - M_c|} \qquad (2)$$

$$Z' = 1 - \frac{(3 * SD_{c+} + 3 * SD_{c-})}{|M_{c+} - M_{c-}|} \qquad (3)$$

where SD and M are standard deviation and mean, s and c represent sample and control, c+ and c- positive and negative controls, respectively. For ISRE activation assay we calculated the Z'-factor, considering c+ and c- as stimulated control and not stimulated control respectively. For VP24 assay we considered the Z-factor, where s are samples cotransfected with pISRE-luc and VP24 and c are cells cotransfected with pISRE-luc and empty vector. All experiments were repeated at least three times. Quantitative data were expressed as the mean ± SD.

2.6. Quercetin Cytotoxicity assay

HEK293T (1.5×10^4 cells/well) were seeded in 96-well plates. After 24 h, cells were treated with 3-100 μM of Quercetin and incubated 8 h at 37 °C in 5% CO_2. Then, 15 μL of PrestoBlue Cell Viability Reagent (Thermo Fisher Scientific) were added to each well. The plate was incubated for 1 h at 37 °C in 5% CO_2 and fluorescence was read in the Victor3 luminometer.

2.7. Immunoblot Analysis

To detect EBOV VP24 expression levels, HEK293T cells were seeded in 6-well plates (4×10^5 cell/mL) and transfected with pISRE-luc and increasing concentrations of EBOV FLAG-VP24 plasmid. 24 h post-transfection, the medium was replaced with IFN-α. 8 h post-IFN addition, cells were harvested and lysed in radioimmunoprecipitation (RIPA) buffer (50 mM Tris-HCl [pH 8], 150 mM NaCl, 1% Triton X-100, 0.5% sodium deoxycholate, 0.1% sodium dodecyl sulfate, 1 mM phenylmethylsulfonyl fluoride, 1x Roche complete

protease inhibitor cocktail, 1 mM sodium orthovanadate). Total cell extracts were analyzed by sodium dodecyl sulfate-polyacrylamide gel electrophoresis (SDS-PAGE) and then transferred to a polyvinylidene difluoride (PVDF) membrane by standard methods. Membranes were blocked with 3% nonfat dry milk in TBS (50 mM Tris-HCl, 0.138 M NaCl, 2.7 mM KCl, pH 8.0) and probed with mouse monoclonal anti-FLAG M2 and rabbit monoclonal anti-GAPDH. Secondary antibodies were HRP-linked anti-mouse IgG and HRP-linked anti-rabbit IgG. Detection was performed using Pierce ECL Western Blotting Substrate and Chemidoc MP Imaging System (Biorad).

2.8.   Immunofluorescence

For immunostaining, HEK293T cells were seeded in 6-well plates (3 x 10^5 cell/well) and cotransfected with Lipofectamine 2000 transfection reagent (Invitrogen) with 2.5 μg/well of pcDNA3.1 or plasmids for EBOV VP24 and ZIKV proteins. After 24 h of transfection, cells were treated with IFN-α for 30 minutes and then fixed with 4% paraformaldehyde in PBS for 15 minutes at RT. Permeabilization was performed with ice-cold 100% methanol for 10 minutes, washed three times for 5 minutes with PBS, and blocked in blocking buffer (PBS containing 0.2% Triton X-100, 10% normal goat serum and 3% bovine serum albumin) for 1 h at RT. The cells were then incubated with the primary antibodies: anti-Flag (1:500), anti-P-STAT1 (1:400), anti-P-STAT2 (1:200), anti P-JAK1 (1:250), anti-STAT1 (1:100) for 1 h. After three washes with PBS, cells were incubated with secondary antibodies conjugated to Alexa Fluor 488 and Alexa Fluor 594 (1:500; Invitrogen) for 1 h and then 1 min with Hoechst (Thermo Fischer Scientific). Stained cells were mounted on glass slides with Glycerol Mounting Medium with DABCO as anti-fade reagent and observed with an Olympus BX61 microscope, equipped with epifluorescence illumination, and

digital images were captured with a Leica DF 450C camera. The cultures were examined at 40x magnification. At this magnification, the total number of microscopic fields per culture was between 30 and 50.

2.9.   RNA Extraction and Quantitative Real-Time PCR

To determine the effect of VP24, NS2A and NS4B on the expression of ISGs, ISG15 and OAS1, HEK293T cells in 6-well plates (3 x 10^5 cell/well) were transfected with 2.5 µg/well of empty vector or expression plasmids for EBOV and ZIKV proteins using Lipofectamine 2000 transfection reagent (Invitrogen). After 24 h, the cells were treated with IFN-α (10 ng/mL) for 24 h. Total RNA was extracted from transfected cells with TRIzol reagent (Invitrogen). RNA was then reverse transcribed and amplified using Luna Universal One-Step RT-qPCR kit (New England Biolabs). Quantitative real-time PCR (RT-qPCR) experiments were performed in triplicate. mRNA expression levels were normalized to the level of glyceraldehyde-3-phosphate dehydrogenase (GAPDH). For ZIKV experiments, results are shown as folds induction of stimulated over not stimulated samples. Results of Quercetin experiment are expressed as percentage of mRNA transcript levels of treated cells versus not treated cells. All qPCR primers used in this study are listed in Table 2.

Table 2. Primers used for RT-qPCR

Primer name[a]	Sequence (5′ to 3′)
GAPDH_F	GAGTCAACGGATTTTGGTCGT
GAPDH_R	TTGATTTTGGAGGGATCTCG
ISG15_F	TCCTGGTGAGGAATAACAAGGG
ISG15_R	CTCAGCCAGAACAGGTCGTC
OAS1_F	AGCTTCATGGAGAGGGGCA
OAS1_R	AGGCCTGGCTGAATTACCCAT

[a]F, forward; R, reverse.

2.10. Docking Ligand Preparation

The 2D coordinate structure-data file (SDF) file of Quercetin ligand was downloaded from Pubchem compound repository. Then, it was prepared with Maestro GUI and subject to conformational analysis by means of MacroModel program version 9.2 (Mohamadi et al., 1990). Merck molecular force fields (MMFFs) (Halgren, 1996) was applied as force field and it was considered the implicit solvation model Generalized Born/Surface Area (GB/SA) water (Kollman et al., 2000). Therefore the compound geometry was energy minimized using Polak-Ribier Conjugate Gradient (PRCG) method, 5000 iterations and a convergence criterion of 0.05 kcal/(mol Å). The compound global minimum conformation was considered for the docking studies.

2.11. Docking Protein Preparation

The coordinates for VP24 were taken from the RCSB Protein Data Bank (Berman, H. M.; Westbrook, J.; Feng, Z.; Gilliland, G.; Bhat, T. N.; Weissig, H.; Shindyalov, I. N.; Bourne, 2000) considering the pdb model 4M0Q (Edwards et al., 2014). The protein was prepared by means of Maestro Protein Preparation Wizard (Maestro, Schrödinger L. L. C., New York, N., USA, 2018). Original water molecules were removed. The bond orders, hydrogen atoms and formal charges were added in the structure. After preparation, the structure was refined in order to optimize the hydrogen bond network using OPLS_2005 force field (Kaminski et al., 2001).

2.12. Docking Experiments

Docking inner and outer grids were defined around the refined structure by calculating the centroid of clustered residues interacting with KPNα5 (Xu et al.,

2015). The coordinates Grid point's level for x, y, z axis are -2,06, -21,53, -12,16. The inner box side was increased to 15 Å while the outer was left of 20 Å. The box resulted a cube of 35 Å for side.

The extra precision (XP) docking algorithm was applied for scoring theoretical poses (Friesner et al., 2006). The other settings were left as default.

2.13. Post-Docking

In order to better take into account the induced fit phenomenon occurring at the ligand binding domain, the most energy favored generated complexes were fully optimized with 10000 steps of the Polak-Ribier conjugate gradient (PRCG) minimization method considering OPLS_2005 force field and GB/SA implicit water. The optimization process was performed up to the derivative convergence criterion equal to 0.1 kJ/(mol*Å).

2.14. Graphics

The resulting complexes were considered for the binding modes graphical analysis with Pymol (The PyMOL Molecular Graphics System Version1.7, Schrödinger, L. L. C.) and Maestro Ligand Interaction visualization (Maestro, Schrödinger L. L. C., New York, N., USA, 2018). Graphics of other experiments were performed using GraphPad Prism software 6.01 (GraphPad software, Inc, 2012).

2.15. Multiple Alignments

Pairwise and multiple alignments of Flaviviridae amino acid sequences (from UniProt database) were generated with Geneious bioinformatics software

platform, version 8.1.4 (Kearse et al., 2012) using MAFFT algorithm FFT-NS-i x1000 (Katoh and Standley, 2013) with default parameters.

2.16. Phylogenetic Analysis

All phylogenetic trees were built from manually optimized multiple alignments using Mega Software, version 6 (Tamura et al., 2013) and neighbor joining statistical method. Amino acid sequences NJ trees were built using the Poisson model and applying pairwise deletion option. Phylogenies were tested by the bootstrap method with 1000 replicates.

Chapter 3

Development and Validation of a Novel Dual Luciferase Reporter Gene Assay to Quantify EBOV VP24 Inhibition of IFN Signaling

3.1.　Introduction

EBOV VP24 inhibits signaling downstream of both IFN-α/β and IFN-γ by sequestering KPNα proteins (α1, α5 and α6) and preventing nuclear transport of activated P-STAT1 (Mateo et al., 2010; Reid et al., 2006, 2007). In addition, VP24 also binds directly P-STAT1 (Zhang et al., 2012). EBOV evasion of IFN signaling by VP24 is a critical event in the pathogenesis of the infection. Mutations in VP24 correlated to IFN evasion are responsible for the acquisition of high virulence in animal models (Ebihara et al., 2006). Being a key factor in the EBOV virulence, VP24 is a potential target for the development of new drugs. In the absence of approved drugs specific for VP24, the identification of molecules able to inhibit VP24, restoring and possibly enhancing the IFN response, is a goal of concern. We describe here the development of a novel artificial dual cell-based gene reporter screening assay able to quantify IFN induction and its inhibition by VP24. HEK293T cells transiently express the ISRE promoter driving a luciferase reporter gene. Stimulation with IFN-α activates the IFN signaling cascade leading to the expression of ISGs genes. This system may be a suitable cellular model to reproduce the effect of VP24 on IFN signaling and to test VP24 inhibitors. The enzymatic activity of firefly luciferase provides a susceptible, stable and rapid mean to quantify transcriptional activity of ISRE. We optimized the assay evaluating different parameters to achieve excellent signal. Further, the normalization with a Renilla luciferase

control allows to minimize variability between experiments providing an high reproducibility of our dual drug screening assay.

3.2. Results

3.2.1 Establishment of a Miniaturized Cell-Based Assay for Evaluating VP24 Inhibition of JAK/STAT Cascade Activation

To monitor the activation status of IFN signaling, we transfected HEK293T cells with pISRE-luc, a reporter plasmid that is widely used to evaluate the transcription effect of activated JAK/STAT pathway by type I IFNs (Strnadova et al., 2015; Subba-Reddy et al., 2011). Treatment with human recombinant IFN-α of the transiently transfected HEK293T cells activates the IFN signaling pathway leading to a luminescent signal. To use this assay to test a considerable number of compounds, we performed it in 96-well plates. For initial assay development, we analyzed the concentration of luciferase plasmid to use for transfection. Hence, HEK293T cells were transfected with various amounts of plasmid per well. Results showed that the optimal concentration for reporter vector was 60 ng/well (Figure 23a). To assess the optimal time of stimulation, we performed a time-course analysis. HEK293T cells exhibited an IFN-α treatment time for maximal signal between 12 and 24 h (Figure 23b). We chose the 8 h time point that allows to have a strong stimulation, with a luciferase activity increased by 27-fold compared to the no IFN treated cells.

It has been demonstrated the ability of EBOV VP24 to inhibit the IFN signaling pathway (Mateo et al., 2010; Reid et al., 2006, 2007). Given the contribution of VP24 to EBOV virulence (Ebihara et al., 2006; Mateo et al., 2011b), the protein could be a very important target for drug development. For this reason, we wanted to evaluate its inhibitory effect in our system, to provide a suitable model for screening a large quantity of potential inhibitors. HEK293T were
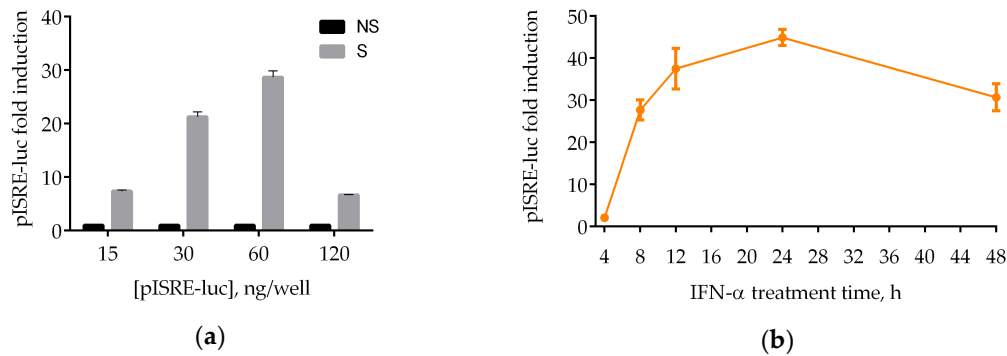
Figure 23. Miniaturized luciferase reporter gene assay in 96-well plates. (**a**) HEK293T cells were transfected with 15, 30, 60 and 240 ng of pISRE-luc per well. 24 h after transfection, cells were stimulated (S) or not (NS) with IFN-α for JAK/STAT pathways activation. After 8 h, cells were lysed and luciferase activity was measured. (**b**) HEK293T cells were transfected with pISRE-luc (60 ng/well). 24 h after transfection, cells were stimulated with IFN-α. After 4, 8, 12, 24, 48 h, cells were harvested and luciferase activity was measured. Results are shown as pISRE-luc fold induction of stimulated cells over not stimulated control. Error bars indicate the mean ± SD.

cotransfected with pISRE-luc reporter and empty vector pcDNA3.1(+), or expression plasmid for the FLAG- or V5-tagged VP24. We cotransfected cells also with the expression plasmid for IAV NS1, a previously demonstrated inhibitor of IFN signaling, as positive control (Jia et al., 2010). Cells were stimulated with IFN-α for 8 h. A 30-fold induction in ISRE activity was observed in IFN-α treated samples transfected with pISRE-luc with or without empty vector. This activation was inhibited in cells expressing either FLAG- or V5-tagged VP24 protein and in cells expressing NS1, but with different percentages (Figure 24a). In order to demonstrate that the inhibitory effect of ISRE transcription was effectively due to VP24 expression at protein level, we performed a western blot of the samples transfected with EBOV VP24-FLAG or empty vector treated or not with IFN-α and, in parallel, assayed the luciferase activity. Results clearly showed that higher amounts of expressed VP24 corresponded to higher inhibition of the pathway (Figure 24b), demonstrating that the dose-dependent inhibition of the luciferase activity was due to the dose-dependent expression of VP24.
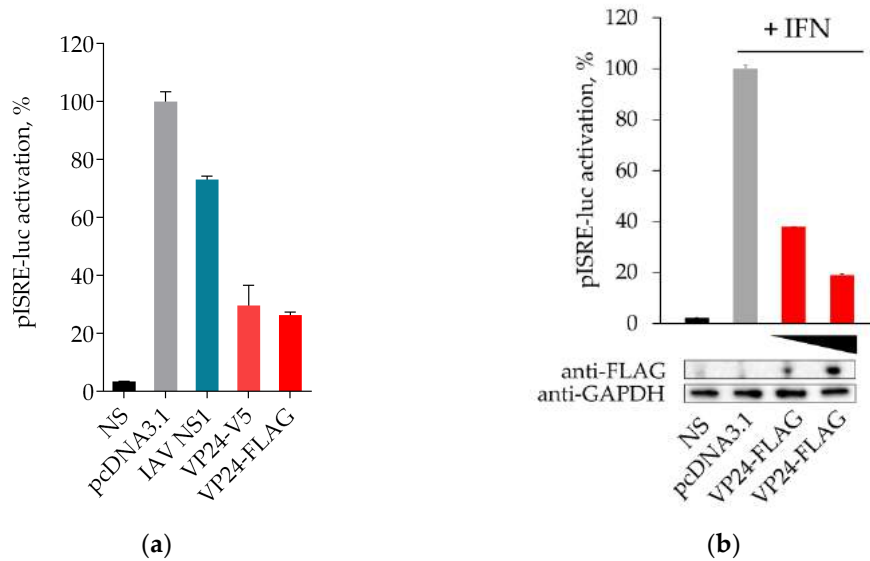
Figure 24. **EBOV VP24 inhibition assay.** (**a**) HEK293T cells were transfected with pISRE-luc and 60 ng/well of empty vector pcDNA3.1(+), or expression plasmid for EBOV FLAG- or V5-tagged VP24 and IAV NS1. 24 h after transfection, cells were stimulated with 10 ng/mL of IFN-α or left untreated (NS). After 8 h, cells were lysed and luciferase activity was measured. (**b**) Expression of EBOV VP24 at protein level. HEK293T were seeded in 6-well plate. After 24 h, cells were transfected with pISRE-luc and pcDNA3.1 (1 µg/well) and 0.25 and 1 µg/well of EBOV VP24-FLAG. The day after cells were incubated or not with IFN-α for 8 h and subsequently lysed and examined for luciferase activity and protein expression by Western blotting. Results are shown as percentage of pISRE-luc activation in VP24 transfected cells over empty vector transfected controls. Each experiment was done in triplicate. Error bars indicate the mean ± SD.

3.2.2 Optimization of Stimulation Conditions and Evaluation of VP24 IC$_{50}$

Normalization with an internal control is crucial to reduce variability between experiments and to develop a drug screening assay. In order to assess the optimal concentration of IFN-α to use for quantifying the dose-dependent effect of VP24 in our inhibition assay, we performed a curve of IFN-α using Renilla luciferase as internal control for transfection. As shown in Figure 25a, IFN-α activated the ISRE reporter gene expression concentration dependently. For inhibition assay the concentration of agonist required to achieve a "maximum" signal response corresponds to the 80% of stimulation, accordingly with acceptance criteria for assay validation (P. W. Iversen et al., 2012). Hence, we

used the concentration at the initial inflexion of the IFN curve (1 ng/mL), to perform the VP24 dose-response assay. Cotransfection of HEK293T with concentrations between 0.46 and 120 ng/well were utilized to create the dose-dependence inhibition curve (Figure 25b) and the IC_{50} value was calculated (30 ng/well). Thus, we chose this concentration for further drug screening assay development.

(a) (b)
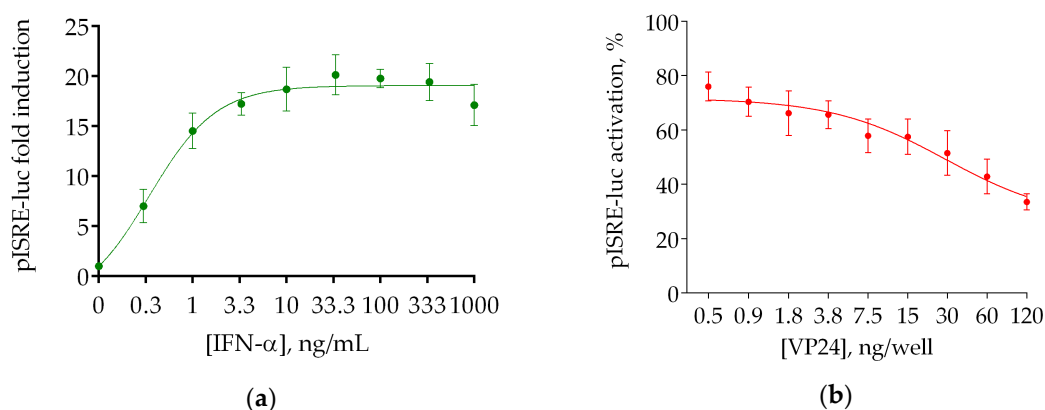
Figure 25. **IFN stimulation assay and VP24 inhibition curve.** (**a**) HEK293T cells were transfected with pISRE-luc (60 ng/well), RL-TK (10 ng/well) and pcDNA3.1 (30 ng/well). 24 h after transfection, cells were stimulated with different concentrations of IFN-α between 0.3 and 1000 ng/mL or left unstimulated. The medium was changed after 8 h, and luciferase activity was measured. Results are shown as pISRE-luc fold induction of stimulated cells over not stimulated control. Firefly luciferase activity is normalized to the Renilla luciferase internal control. Error bars indicate the mean ± SD. (**b**) Regression curve of VP24 inhibition was obtained transfecting HEK293T cells with reporter vector at the fixed concentration of 60 ng/well, RL-TK (10 ng/well) and EBOV VP24-FLAG or empty vector in concentrations between 0.46 and 60 ng/well. Results are shown as percentage of pISRE-luc activation in VP24 transfected cells over empty vector transfected controls. Firefly luciferase activity is normalized to the Renilla luciferase internal control. Error bars indicate the mean ± SD.

3.2.3. Luciferase Assay Signal Stability

The stability of luciferase signal is a rilevant factor supporting drug screening applications. The time-dependent decay of RLU generated from our firefly luciferase activity was explored. After adding D-luciferin, the luminescent signal generated from cells transfected with ISRE alone and

with ISRE and VP24 was recorded every 5 minutes. As it is shown by the luminescence decay curve (Figure 26a) the maximum level of bioluminescence was reached 5 minutes after substrate addition, followed by slow decay during 1 h.
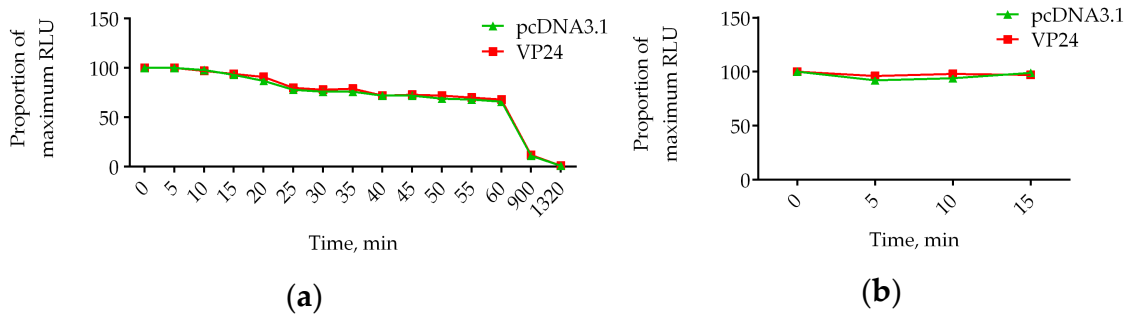
Figure 26. Time-dependent decay of luciferase activity. HEK293T cells cotransfected with pISRE-luc and empty vector or pISRE-luc and VP24 were lysed. (**a**) After addition of D-luciferin, luciferase signal was read over 1320 minutes. The relative decay is reported by plotting RLU as a proportion of the RLU at t_0(100%). (**b**) Addition of D-luciferin was performed at 0, 5, 10, 15 minutes after incubation with luciferase assay buffer. The luciferase signal is reported by plotting RLU as a proportion of the RLU at t = 0 minutes after addition of luciferase buffer (100%).

Because of reading a 96-well plates requires the readout signal to be stable for about 20 minutes (10 sec/well), to minimize timing effects we decided to read lines two by two, avoiding the problem of decay of the signal. The time needed by the luminometer for reading two lines is 4.30 minutes, time in which the signal is perfectly stable. We wanted to verify that the addition of luciferase substrate at 0, 5, 10, 15 minutes after the incubation with luciferase assay buffer for lines 1-2, lines 3-4, lines 5-6, lines 7-8 respectively do not affect the intensity of signal obtained. In figure 26b we show that even if harvesting and luciferase assay buffer are present for longer time in the other lines compared to the first two, the intensity of the signal does not change. Luminescence signal is expressed as percentage over the time = 0 minutes (t_0) value (100%) that represents the lines 1-2 where D-luciferin is immediately added.

3.2.4. Assay Validation

To achieve optimization, coefficients of variation (CV) were calculated for the not stimulated controls (Min signal), for cells cotransfected with pISRE-luc and pcDNA3.1 (Max signal) or VP24 (IC_{50}) (Mid signal) after stimulation with the maximum signal response concentration of IFN-α (1 ng/mL). Representative results are provided in Table 3. CV's for each signal are less than 20% indicating achieved acceptance criteria (P. W. Iversen et al., 2012).

Table 3. Well to well reproducibility of VP24 inhibition assay

Signal	Coefficients of Variation, CV (%)
Min	6.1
Mid	4.6
Max	3.3

In order to assess the plate uniformity and to evaluate the signal variability between different days, we performed inter-plate and inter-day tests. Plate-to-plate or day-to-day variation in the 50% percent activity needs to be assessed during a validation of a drug screening assay (P. W. Iversen et al., 2012). Thus, we performed the tests evaluating as mid-point the signal obtained transfecting cells with 30 ng/well of VP24 plasmid corresponding to the IC_{50} value. In Table 4 are indicated the percentages of ISRE expression in presence of VP24 (IC_{50} value). The fold shift is not higher than 2 for both inter-day and inter-plate test, confirming acceptance criteria for validation.

Table 4. Inter-plate and Inter-day tests for VP24 inhibition assay

Inter-plate Test	pISRE-luc activation (%)	Inter-day Test	pISRE-luc activation(%)
Plate 1	52.4	Plate 1	49.3
Plate 2	50.8	Plate 2	49.0

Using the optimized reaction conditions previously calculated, the assay procedures were validated in a Z-factor experiment. The Z-factor is a measure

of assay quality that takes into account the standard deviation, the dynamic range between positive and negative controls and the signal variation amongst replicates. A scale of 0-1 is used, with values greater than or equal to 0.5 indicative of an excellent assay. For ISRE activation assay we calculated the Z'-factor using HEK293T cells untreated or treated with IFN-α as negative and positive controls, respectively. For inhibition assay, the Z-factor was measured considering the difference in signal between cells cotransfected with pISRE-luc and empty vector or pISRE-luc and VP24 expression plasmid. As shown in Figure 27, the Z'- and Z-value for each assay plate were 0.62 for stimulation assay and 0.53 for inhibition assay, indicating the robustness of the system.
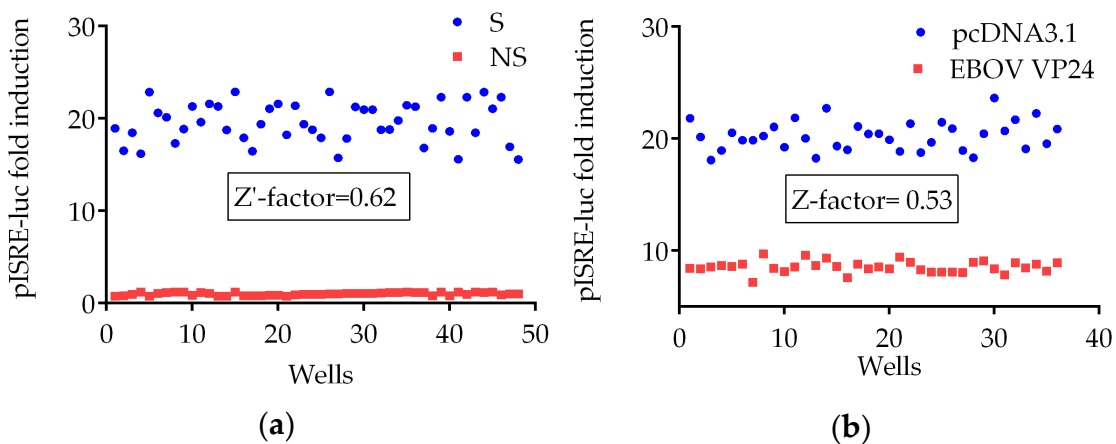
Figure 27. Z' and Z-factor determination for IFN-α stimulation and VP24 inhibition assays. Firefly luciferase activity is normalized to the Renilla luciferase internal control. Results are expressed as pISRE-luc fold induction over the unstimulated control. Z'- and Z-factor were calculated as described in methods. (**a**) HEK293T cells were seeded in 96-well plate and transfected with pISRE-luc (60 ng/well) and pcDNA3.1 (30 ng/well). 24 h post-transfection, 48 wells (S) were incubated with 1 ng/mL of IFN-α and 48 wells were left untreated (NS). (**b**) HEK293T cells seeded in 48 wells were transfected with pISRE-luc (60 ng/well) and pcDNA3.1 (30 ng/well), and the ones in other 48 wells were transfected with pISRE-luc and expression plasmid for VP24 (60 ng/well). 35 wells for each sample were stimulated with 1 ng/mL of IFN-α and 12 were not stimulated.

3.2.5. Designing the Drug Screening Assay

For drug screening assay, HEK293T cells (1.5×10^4 cells/well) are cotransfected with pISRE-luc and empty vector or VP24 expression plasmid. At 24 h post transfection, the cells are mocked treated or treated with IFN-α in the presence of compound at three different concentrations or DMSO. The concentration of IFN-α (0.3 ng/mL) in the linear range of the IFN-α dose response curve is used. At 8 h post-treatment, cells are harvested, and firefly and renilla luciferase activities are measured. Positive controls of inhibition are cells cotransfected with pISRE-luc and VP24 in presence of DMSO, negative controls of inhibition are cells cotransfected with pISRE-luc and empty vector in presence of DMSO. Luciferase activity is calculated as folds induction of stimulated versus not stimulated controls as well as percentage of pISRE-luc activation in VP24 transfected cells over empty vector transfected controls. A plate map illustrating the layout of the screening plate, including well locations of compounds, positive and negative controls, is represented in Figure 28.
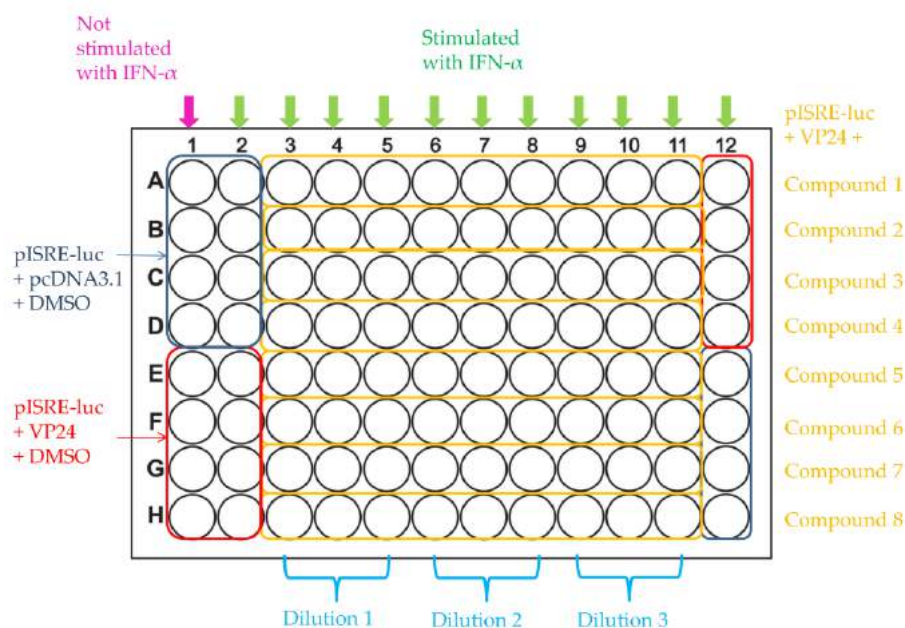
Figure 28. Representative scheme of 96-well plate for drug screening

3.2.6. IFN-α Partially Reverts VP24 Inhibition of JAK/STAT Cascade

The lack of inhibitors for VP24 inhibition of the JAK/STAT cascade does not allow to have a positive control of restoration of the JAK/STAT cascade activation in presence of VP24. However, to investigate the suitability of the assay for drug screening, we evaluated the reversion of the effect of VP24 on pISRE-luc activation mediated by IFN-α. HEK293T cells were cotransfected with pISRE-luc and empty vector or VP24 expression plasmid at 30 ng/ml (IC$_{50}$ value). In addition to the standard amount of IFN-α (0.3 ng/mL), we added increasing concentrations of IFN-α (0.7, 3, 9.7 ng/mL). As shown in Figure 29, IFN-α is able to partially revert the ISRE expression in presence of VP24, demonstrating its inhibitory effect against the viral protein.
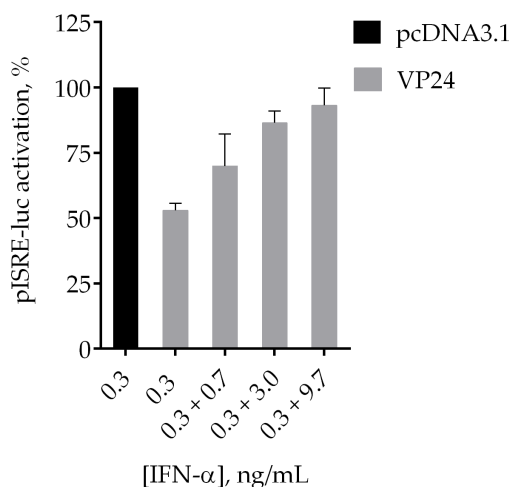
Figure 29. Effect of IFN-α on VP24 inhibition of IFN signaling. HEK293T cells were cotransfected with pISRE-luc (60 ng/well), RL-TK (10 ng/well) and pcDNA3.1 (30 ng/well). 24 h after transfection, cells were stimulated with 0.3 ng/mL of IFN-α. Then, increasing concentrations of IFN-α were added. After 8 h of stimulation, the medium was changed and luciferase activity was measured. Results are shown as percentage of ISRE expression in VP24 transfected cells over empty vector transfected control. Firefly luciferase activity is normalized to the Renilla luciferase internal control. Error bars indicate the mean ± SD.

3.3. Discussion

Ebola virus has evolved multiple strategies to antagonize the IFN-α/β responses in target cells such as macrophages, monocytes and dendritic cells, resulting in total impairment of the innate immune system. An important contribution to EBOV virulence is given by the protein VP35 through its suppression of IFN production (Basler et al., 2003; Cárdenas et al., 2006; Luthra et al., 2013; Prins et al., 2009; Ramanan et al., 2011), but a crucial role is exerted by another viral protein, VP24, that disables cells to contrast viral replication and propagation by interfering with the IFN signaling (Basler and Amarasinghe, 2009; Ebihara et al., 2006; Mateo et al., 2010; Reid et al., 2006, 2007; Wong et al., 2017; Zhang et al., 2012). The early control of viremia is one of the keys for survival, thus blocking EBOV VP24 action on the cellular immune response, is an important subject for investigation and, hence, a validated pharmacological target.

Much work has been done in the last years to elucidate the function of EBOV VP24 in IFN antagonism. These efforts have been conducted employing different methods. Immunofluorescence analysis with multiple epitope tags, such as phospho-specific antibodies for P-STAT1 or STAT1 fused to green fluorescent protein (GFP), were used to demonstrate the ability of VP24 to inhibit IFN-induced nuclear localization and tyrosine phosphorylation of human STAT1. An equivalent effect was confirmed after EBOV infection of cells (Mateo et al., 2010; Reid et al., 2006, 2007). Coimmuonoprecipitation studies revealed that VP24 selectively interacts with KPNA (α1, α5 and α6), competing with P-STAT1 for the same binding (Reid et al., 2006, 2007) and in vitro ELISA assays were used to show that purified EBOV VP24 could also bind directly to purified truncated STAT1 (Zhang et al., 2012). Subsequently, characterization of the binding of EBOV VP24 to KPNα was performed by isothermal titration calorimetry (ITC), in vitro pull down assay with recombinant expressed proteins and computational analysis (Xu et al., 2015). In addition, X-ray

crystallization analysis allowed the determination of the complex structure (Xu et al., 2015). Affinity tagging coupled to label-free quantitative mass spectrometry was used to identify potential interacting partners of VP24 and confirmed the binding with KPNα (Garcia-Dorival et al., 2014). Reverse genetics was used to identify the mutations correlated with the ability to evade type I IFN responsible for the acquisition of the high virulence of adapted EBOV Mayinga strain in mice (Ebihara et al., 2006). Among the variety of techniques, the use of luciferase reporter assays to measure viral antagonist activity against the IFN system has long been established to be robust and biologically relevant (Mateo et al., 2010; Reid et al., 2006, 2007).

Our group has previously developed a luciferase assay gene reporter able to quantify the inhibition of IFN system by EBOV VP35 that is used for testing compounds against this protein (Cannas et al., 2015). Since with such system we could study the inhibition of the first cascade of IFN production, the RIG-I pathway, we decided to develop a new miniaturized luciferase assay that could be used to study the second cascade of the IFN system, the JAK-STAT pathway. We report here its use to measure the EBOV VP24 inhibition of the IFN signaling in HEK293T cells, to be used as a screening system to identifying EBOV VP24 inhibitors as well as to dissecting the interaction between EBOV VP24 and its cellular partners.

Experiments were carried out in 96-well plates always at least in triplicates allowing good statistical evaluation of the results and showing good reproducibility. In addition, the use of 96-well plates allows to perform the entire assay in only one plate avoiding a more complex experimental approach. Luciferase assays done in 6-, 12-, 24-, 48- well plates imply that cell lysates are moved from a big plate to another with more passages and the risk to lose material. One advantage of this assay is that the luminescence signal derives

effectively from all cells in the well and that the technique is absolutely faster than traditional methods.

Various parameters of the microtransfection method were optimized: amount of plasmids, amount of IFN-α and stimulation time. Measurements of luciferase activity performed at various times yielded optimal results between 8 and 24 h post transfection. Thus, the shorter 8 h incubation was chosen. In literature, luciferase assay performed to evaluate EBOV VP24 inhibition requires at least 16 h of stimulation to measure the luminescence signal (He et al., 2017; Mateo et al., 2011b; Reid et al., 2006, 2007; Schwarz et al., 2017). The present method allows data to be obtained more rapidly. Conventional transfection assays also require the use of high quantities of plasmids and reagents (Mateo et al., 2011b; Reid et al., 2006, 2007), while in the present system, as little as 60 ng/well for plasmid reporter can be used, compared to 1- 0.5 µg/well in 6-well plate (Mateo et al., 2011b; Reid et al., 2006). Hence, the present method appears to be extremely sensitive and allows a considerable economy of all reagents. Moreover, the use of home-made reagents for reading luciferase activity is a convenient and ultra-low-cost system compared to the use of highly expensive commercial kits.

Our assay provides a convenient tool for large scale screening studies to identify selective EBOV VP24 inhibitors as well as compounds subverting VP24 block of the IFN cascade. In fact, all acceptance criteria for drug screening validation, including the Z'-factor analysis, were satisfied. In addition, the expression of Renilla luciferase offers an internal control value with which the firefly luciferase reporter gene is normalized, providing a decrease in variability and an increase in consistency. We confirmed the feasibility of the present assay to be used for a rapid and quantitative evaluation of anti-EBOV VP24 agents. Indeed, the experiment with the increasing concentrations of IFN-α suggested

that it is possible to override the inhibitory effect of VP24 and partially restore the IFN signaling in our system.

In conclusion, the development of a new dual cell-based assay able to quantify the inhibition of IFN signaling by EBOV VP24 could have important implications for future studies since it represents a suitable model for screening compounds against a viral target for which no drugs are currently approved. The enzymatic activity of luciferase and its normalization with the Renilla internal control allows to achieve a robust assay performance as Z- and Z'-factor calculations demonstrate. Overall, the present method offers multiple advantages such as 100- to 1000-fold reduction in cells, plasmids and reagents required, shorter time assay, reduced costs and rapid detection of molecules anti-EBOV VP24.

Chapter 4

Flavonoid Derivatives Inhibit EBOV VP24 Impairment of the IFN Signaling Pathway

4.1. Introduction

It has been demonstrated that mutations of EBOV VP24 residues principally involved in its IFN antagonism function, such as the substitution T50I, are critical for the acquisition of the high virulence in animal models and thus can contribute to the progression of the infection even in humans (Ebihara et al., 2006). Finding a therapy targeting the IFN inhibitory function of VP24 leading to the restoration of the IFN response has an obvious impact in the treatment of EVD. Although the increasing and constant effort in the identification of VP24 inhibitors and despite recent progresses have been made in developing novel techniques to test its function, nowadays no approved drugs are available against such promising pharmacological target (Fanunza et al., 2018c). Several *in vitro*, *in vivo* and *in silico* approaches have been attempted to identify potential inhibitors among FDA-approved drugs, oligomers, peptides and natural compounds (Daino et al., 2018; P. L. Iversen et al., 2012; Pleško et al., 2015; Qiu et al., 2016; Raj and Varadwaj, 2016; Setlur et al., 2017; Shah et al., 2015; Song et al., 2017; Tanaka et al., 2018; Zhao et al., 2016).

4.1.1. Repositioning of FDA Approved Drugs

Using a pharmacophore based virtual screening and docking study, the FDA-approved Deslanoside and Digoxin with their respective analogues (ZINC85911633 and ZINC77291634) have been identified, among 56 FDA-

approved drugs, to possess *in silico* high binding affinity for VP24 (Shah et al., 2015). Another FDA approved drug, Indinavir, known to inhibit the HIV protease, was identified *in silico* to potentially interact with VP24 (PDB ID: 4M0Q) (Edwards et al., 2014) involving the same atoms to form hydrogen bonds with both HIV protease and VP24 (Zhao et al., 2016).

4.1.2. Oligomers and Peptides

AVI-7537, a Phosphorodiamidate Morpholino Oligomer containing five positively charged linkages (PMO*plus*) was designed based on the EBOV VP24 sequence (P. L. Iversen et al., 2012). AVI-7537 acts as steric inhibitor of gene expression by physically blocking the binding of translation complex elements to the VP24 transcript RNA. The suppression of VP24 translation by AVI-7537 resulted in mice and guinea pigs protection against EBOV lethal challenge (P. L. Iversen et al., 2012). AVI-6003, a combination of PMOs AVI-7287 (targeting VP24) and AVI-7288 (targeting NP) led to a survival of 100% in NHPs (P. L. Iversen et al., 2012). Another strategy to identify novel viral proteins inhibitors is the use of the RaPID system that allows the selection of high-affinity binders from an mRNA library of non-standard peptides (Song et al., 2017). By this approach, recently, a macrocyclic peptide binder for VP24, namely eVpeD2, has been identified. It represents the first molecule that has been shown to inhibit the VP24–KPNA5 protein–protein interaction (PPI) in a biochemical study with an IC_{50} value of 9 μM (Song et al., 2017).

Furthermore, Tanaka et al. used the capillary electrophoresis-systematic evolution of ligands by exponential enrichment (CE-SELEX) to generate natural and artificial nucleic acid aptamers with high-affinity for VP24. Since the aptamers shared a common binding site with KPNA1 for the interaction with

VP24, they showed to antagonize VP24 binding to KPNA1 at sub-nanomolar range ($K_d \approx 0.1$ nM) (Tanaka et al., 2018).

4.1.3. Natural Compounds

Three small molecules extracted from Indian medicinal plants, Limonin, Samarcandin and Gummosin were reported to have *in silico* high docked energy in complex with VP24 (Setlur et al., 2017). In addition, docking studies revealed a high binding affinity of the VP24-KPNα5 complex (PDB ID: 4U2X) to plant polyphenols such as Epigallocatechin gallate, 1,2,3,6-Tetragalloyl glucose (1,2,3,6-TGG) and Theaflavin-3,3'-digallate (Pleško et al., 2015).
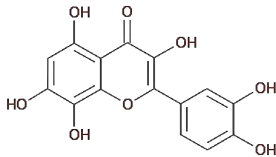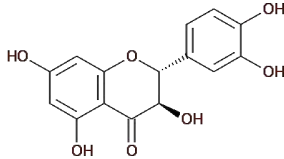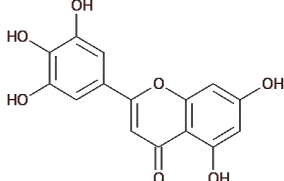
4.1.3.1. Flavonoids

Flavonoids are polyphenol chemical compounds characterized by a benzo-γ-pyrone structure (C6-C3-C6) in which the two aromatic rings are joined by a three carbon chain, typically organized as an oxygenated heterocycle. The interest in the research on flavonoids from plant sources is increasing due to their versatile health benefits. In fact, among plant components, they have been shown to possess a wide range of biological properties: antioxidant, hepatoprotective, antibacterial, anti-inflammatory (Kumar and Pandey, 2013; Umesh et al., 2018) and also antiviral activity (Cushnie and Lamb, 2005; Sritularak et al., 2013). It has been shown that they are active against different viruses such as Japanese encephalitis virus (Johari et al., 2012), Hepatitis B virus (Guo et al., 2007), Dengue virus type-2 (Zandi et al., 2011), Herpes simplex virus (S. Lee et al., 2017), Influenza virus (Bang et al., 2017; Liu et al., 2008) and Human immunodeficiency virus (Esposito et al., 2013; Pasetto et al., 2014; Sanna et al., 2018). Flavonoids have been reported to be active against EBOV entry or to directly target EBOV viral proteins (Daino et al., 2018; Qiu et al., 2016).

While no single flavonoid molecule has been tested against VP24 *in vitro*, recent *in silico* studies reported that a number of them are potentially able to bind different EBOV targets, including VP24 (Plesko et al., 2015; Raj and Varadwaj, 2016). In particular, Raj et al. described that Gossypetin (ST059622), Taxifolin (ST060285) and Tricetin (ST101866) (Table 1) possess high docked energy in complex with VP24, being potentially able to impair VP24 ability to disrupt the JAK/STAT signaling pathway.

Starting from this observation we evaluated their activity in the biological assay described in the previous chapter and we also performed a screening of flavonoids with similar structure to Gossypetin, Taxifolin and Tricetin finding some of them able to block VP24 leading to the restoration of the IFN signaling cascade. They are the first compounds able to interfere specifically with the IFN inhibitory function of VP24 *in vitro*.

Table 5. Chemical structures of Gossypetin, Taxifolin and Tricetin

Compounds	Structure
Gossypetin	
Taxifolin	
Tricetin	

4.2. Results

4.2.1. Gossypetin, Taxifolin and Tricetin Suppress VP24 IFN Inhibitory Function

Using the dual-luciferase reporter system previously described in Chapter 3 (Fanunza et al., 2018c), we firstly wanted to verify whether Gossypetin, Taxifolin and Tricetin were effectively able to affect VP24 anti-IFN function *in vitro*. In brief, HEK293T cells were cotransfected with pISRE-luc, pRL-TK and the expression plasmid for VP24. The stimulation with IFN-α resulted in 100% of ISRE expression in cells not cotransfected with VP24, while VP24 cotransfected cells showed about 50% of inhibition of the IFN response. The treatment of VP24 cotransfected cells with 10 µM of Gossypetin, Taxifolin and Tricetin resulted in the partial restoration of the ISRE expression, demonstrating that all three compounds were able to block VP24 inhibitory effect on IFN signaling cascade *in vitro* (Figure 30).
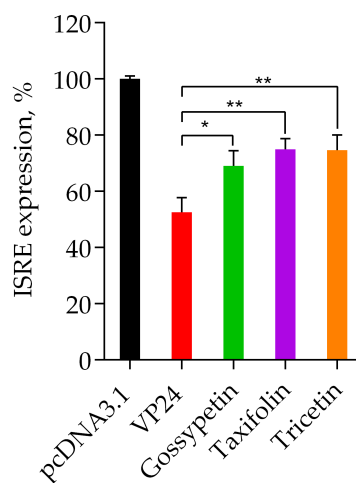
Figure 30. Inhibition of VP24 by Gossypetin, Taxifolin and Tricetin. HEK293T cells were seeded in 96-well plate and cotransfected with pISRE-luc (60 ng/well), RL-TK (10 ng/well) and pcDNA3.1 (30 ng/well) or VP24 expression plasmid (30 ng/well). 24 h after transfection, cells were stimulated for 8 h with 1 ng/mL of IFN-α and 10 µM of Gossypetin, Taxifolin, Tricetin were added. Then, luciferase activity was measured. Results are shown as percentage of ISRE expression in VP24 transfected cells over empty vector transfected control. Firefly luciferase activity is normalized to the Renilla luciferase internal control. Error bars indicate the mean ± SD. *P< 0.05, **P< 0.01, asterisks indicate a significant difference (two-tailed unpaired Student's t-test, n=3).

4.2.2. Quercetin and Wogonin Are Active Compounds Against VP24

To the aim of identifying more active compounds, we decided to screen a series of other flavonoids such as Myricetin, Dihydromyricetin, Quercitrin, Quercetin, Wogonin, Luteolin, Baicalein and Apigenin (Table 6) that share a similar structure with Gossypetin, Taxifolin and Tricetin. Results showed that, when tested in our dual-luciferase reporter system, two out of eight of the tested flavonoids, namely Quercetin and Wogonin, significantly suppressed the IFN inhibitory function of VP24 restoring IFN stimulation (Figure 31). In particular, quercetin was able to restore, at 10 μM concentration, the ISRE expression from ~ 50% up to ~ 80%, in VP24 cotransfected cells, while Wogonin restored the

Table 6. Chemical structures of screened flavonoids

Compounds	Structure	Compounds	Structure
Myricetin		Wogonin	
Dihydromyricetin		Luteolin	
Quercitrin		Baicalein	
Quercetin		Apigenin	

pathway up to ~ 70% (Figure 31). Overall, among all tested flavonoids Quercetin was the most effective in restoring the IFN stimulation at 10 μM concentration.
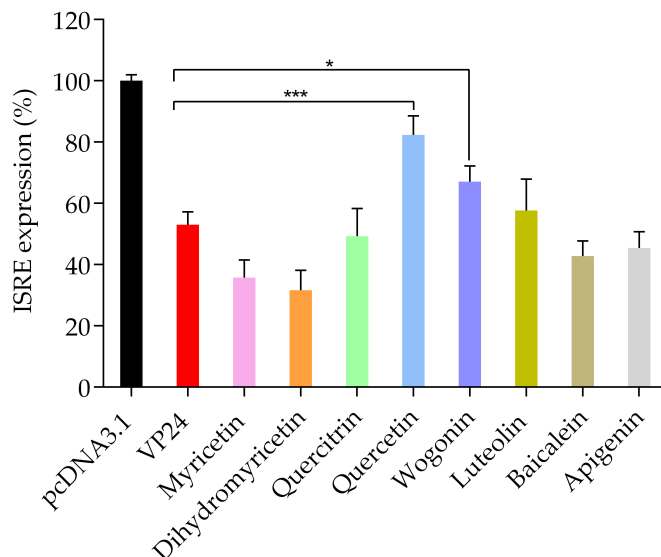
Figure 31. Effect of screened flavonoids on EBOV VP24 inhibition of IFN signaling. HEK293T cells were transfected with pISRE-luc (60 ng/well), RL-TK (10 ng/well) and pcDNA3.1 (30 ng/well) or EBOV VP24 expression plasmid (30 ng/well). 24 h after transfection, cells were treated with 1 ng/mL of IFN-α and 10 μM of Myricetin, Dihydromyricetin, Quercitrin, Quercetin, Wogonin, Luteolin, Baicalein or Apigenin. After 8 h of stimulation, the medium was changed and luciferase activity was measured. Results are shown as percentage of ISRE expression in VP24 transfected cells over empty vector transfected control. Firefly luciferase activity is normalized to the Renilla luciferase internal control. Error bars indicate the mean ± SD. *$P < 0.05$, **$P < 0.01$ and ***$P < 0.005$, asterisks indicate a significant difference (two-tailed unpaired Student's t-test, n=3).

4.2.3. Active Compounds Specifically Target VP24 Not Altering ISRE Expression

In order to verify whether these flavonoids acted by targeting specifically VP24 and not by enhancing the IFN response employing some VP24-independent mechanisms, we tested them in the absence of the viral protein (Figure 32a and 32b). Results showed that none of the screened compounds enhanced the ISRE expression in HEK293T cells, confirming that active compounds could specifically interact with VP24. Of note, Myricetin and Dihydromyricetin

reduced ISRE activation (Figure 32b). Indeed, Myricetin has been reported to inhibit STAT1 phosphorylation (Scarabelli et al., 2009), and this can explain the inhibition of the ISRE transcription. While no direct data are available for Dihydromyricetin, and considering its structural diversity from Myricetin, further studies are needed to understand its mechanism of action.

(a)   (b)
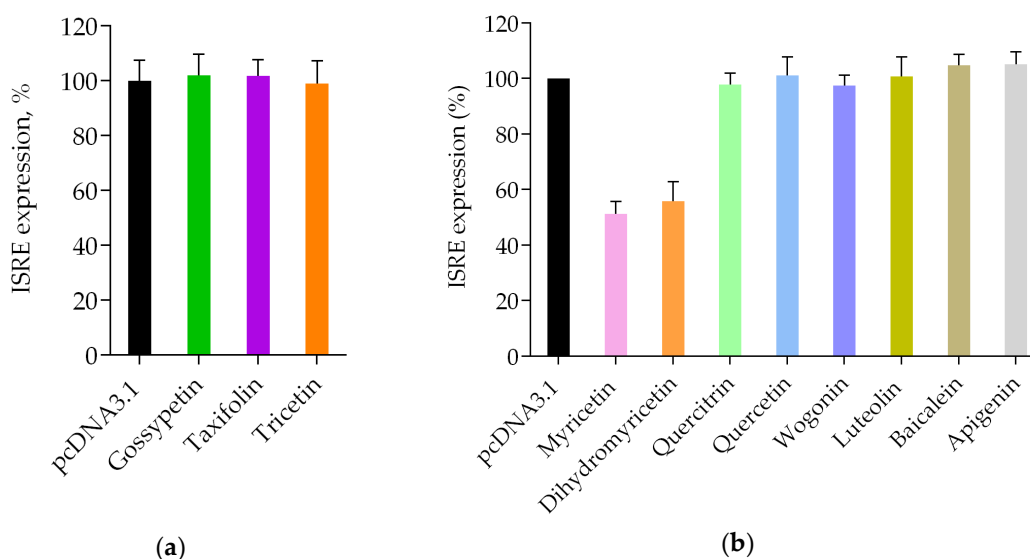
Figure 32. Effect of screened compounds on ISRE expression. After 24 h of cotransfection with pISRE-luc (60 ng/well), RL-TK (10 ng/well) and pcDNA3.1 (30 ng/well), HEK293T were stimulated for 8 h with 1 ng/mL of IFN-α and 10 µM of Gossypetin, Taxifolin, Tricetin (**a**), Myricetin, Dihydromyricetin, Quercitrin, Quercetin, Wogonin, Luteolin, Baicalein or Apigenin (**b**). Then, luciferase activity was read. Results are shown as percentage of ISRE expression in compounds treated cells over not treated control. Firefly luciferase activity is normalized to the Renilla luciferase internal control. Error bars indicate the mean ± SD of three independent experiments.

4.2.4. Dose-dependent Effect of Quercetin on VP24 Inhibition

Next, we wanted to better evaluate the effect of the most active compound, Quercetin, on the VP24 block of the IFN signaling by performing a dose-response curve in the presence of the same amount of VP24 plasmid. Of note, Quercetin exhibited a dose-dependent reversion of the VP24 inhibition of the ISRE IFN-dependent stimulation (Figure 33a) showing an EC$_{50}$ value of 7.4 µM (Figure 33a). Quercetin cytotoxicity in HEK293T cells was also assessed,

yielding 100% cell viability at concentrations between 3 μM and 30 μM and a CC50 value >100 μM (Figure 33b), hence Quercetin showed a selectively index (SI, CC_{50}/IC_{50}) >13.

(a) (b)
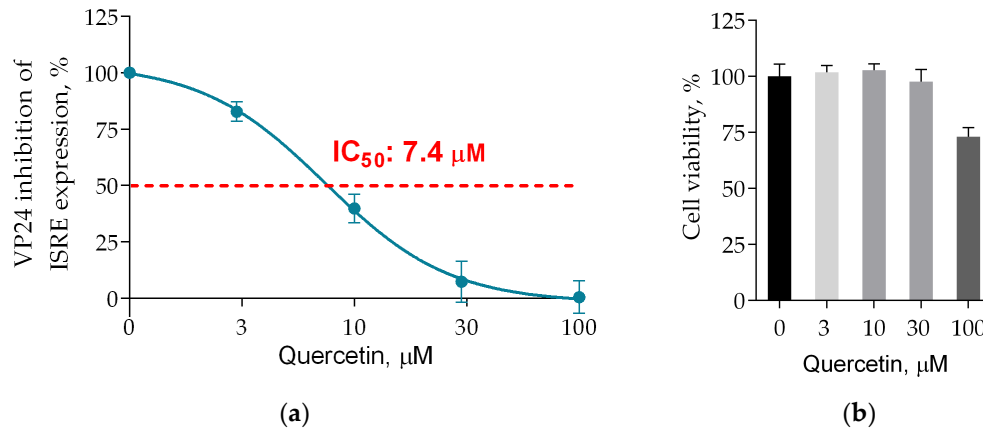
Figure 33 Quercetin dose-dependently inhibits VP24 IFN inhibitory function. (**a**) HEK293T cells were cotransfected with pISRE-luc (60 ng/well), RL-TK (10 ng/well) and VP24 plasmid (30 ng/well). 24 h after transfection, cells were stimulated with 1 ng/mL of IFN-α and Quercetin (3 μM, 10 μM, 30 μM, 100 μM) was added to VP24 cotrasfected cells. After 8 h, cells were lysed and luciferase was read. Results are shown as percentage of VP24 inhibitory activity on ISRE expression using as positive control of inhibition (100%) cells not treated with Quercetin. Firefly luciferase activity is normalized to the Renilla luciferase internal control. Error bars indicate the mean ± SD of three independent experiments. (**b**) HEK293T cells were seeded in 96 well plate. After 24 h, cells were treated with Quercetin (3 μM, 10 μM, 30 μM, 100 μM) and cytotocicity was measured. Results are shown as percentage of cells counts treated with Quercetin over not treated cells. Error bars indicate the mean ± SD of three independent experiments.

4.2.5. Quercetin Treatment Affects ISG15 mRNA Expression

We then wanted to examine the effect of Quercetin on the VP24 block of the IFN signaling by using a different end-point, i.e. by assessing its efficacy on the ISG15 gene expression. The high induction of ISG15 in response to IFN stimulation suggests an important role for ISG15 in antiviral defense and, in fact, ISG15 has been demonstrated to have a broad antiviral effect including suppression of EBOV viral particles budding (Skaug and Chen, 2010). For this reason ISG15 has been used as marker for IFN stimulation in a number of

studies (Au et al., 1995; Loeb and Haas, 1992; Reich et al., 1987). Indeed, the inhibition of the IFN signaling by viral proteins has been shown to determine to the down-regulation of ISGs expression levels, including ISG15 (Guerra et al., 2008; Jia et al., 2010; Mesman et al., 2014). Accordingly, our analysis confirmed that VP24 was effectively able to inhibit ISG15 mRNA transcription in IFN-stimulated cells as compared to cells transfected with an empty vector (Figure 34). Results also showed that Quercetin significantly restored the IFN-induced ISG15 gene expression down-regulated by VP24 confirming that the compound was effectively blocking VP24 function (Figure 34).
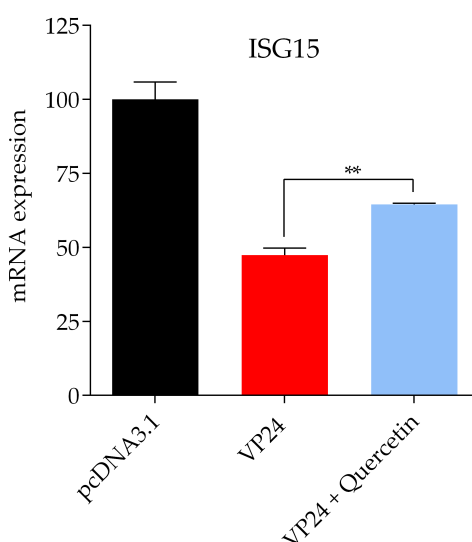
Figure 34. Effect of Quercetin on ISG15 mRNA expression. HEK293T cells were seeded in 6-well plate and transfected with pcDNA3.1 (30 ng/well) or VP24 plasmid (30 ng/well). After 24 h, cells were stimulated with 1 ng/mL of IFN-α and treated or not with 30 µM of Quercetin. After 24 h, total RNA was extracted and RT-qPCR was performed. Results are shown as percentage of ISG15 mRNA expression in VP24 cotrasfected cells (treated or not with Quercetin) over empty vector control. Error bars indicate the mean ± SD of three independent experiments. **P< 0.01, two-tailed unpaired Student's t-test, n=3.

4.2.6. Evaluation of Quercetin Binding Mode on VP24-KPNα Complex

Asking for more details on Quercetin/VP24 interaction, in cooperation with Prof. Simona Distinto of the University of Cagliari, we performed *in silico* molecular docking experiments to evaluate the putative binding mode of

Quercetin on VP24. Among the available VP24 crystal structures, 4M0Q (Edwards et al., 2014) currently has the best resolution (1.92 Å) and, therefore, we selected it for docking experiments performed by means of Glide-XP (Friesner et al., 2006). The grid was set on the centroid of clustered residues (reported above) interacting with KPNα5 (coordinates Grid point's level for x, y, z axis: -2,06, -21,53, -12,16). The default size of the box was increased of 5Å for both inner and outer box covering almost the whole protein. Then, the best docking complexes were subjected to a post-docking procedure based on energy minimization applying molecular mechanics generalized Born/surface area (MM-GBSA) method and continuum solvation models (Kollman et al., 2000). The most stable binding mode was analyzed showing that Quercetin occupies a central position in the reported contact area between VP24 and KPNα5 (Figure 35).
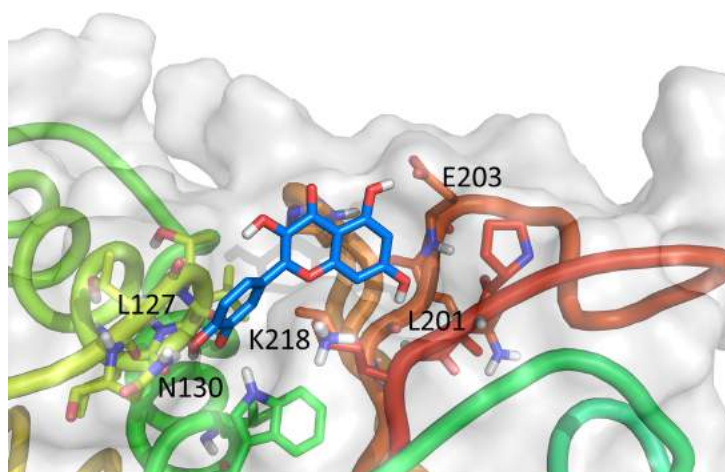
Figure 35. Three-dimensional representation of the putative binding mode obtained by blind docking experiments of Quercetin into VP24.

The complex VP24- Quercetin resulted to be stabilized by hydrogen bonds with the VP24 key residues N130, L201, E203, while additional residues are involved in anchoring the compound i.e L127, W92 by hydrogen bonds and K218 by cation–π interaction (Figure 36).
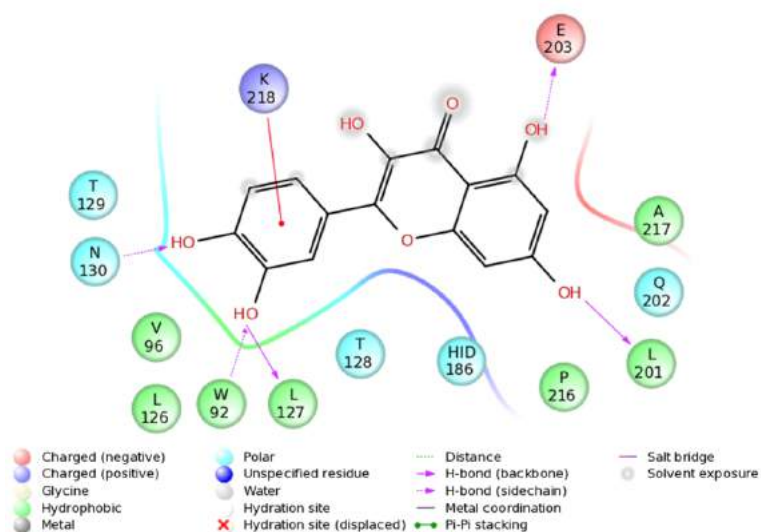
Figure 36. Relative 2D representation of the complexes stabilizing interactions

Such *in silico* analysis allowed us to propose that the presence of Quercetin in such a VP24 pocket, would prevent KPNα5 ARMs 7-10 to move close to VP24, ultimately inhibiting the VP24 binding to KPNα5 (Figure 37).
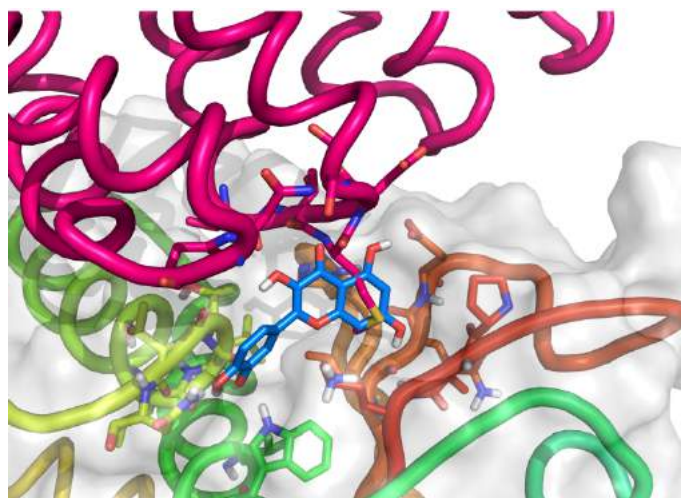
Figure 37. Alignment of Quercetin-VP24 complex obtained by docking experiment with VP24 – KPNα5 reported in 4U2X PDB model (Xu et al., 2015)

4.2.7. Quercetin Blocks VP24 Inhibition of P-STAT1 Nuclear Transport

It is well known that KPNα5 is required for P-STAT1 transport to the nucleus and the induction of the ISGs transcription. To demonstrate that, as suggested by our *in silico* model, Quercetin was able to effectively interfere with the binding between VP24 and KPNα5, we evaluated the effect of the compound on

P-STAT1 nuclear transport after a rapid (30 min) and massive stimulation with IFN-α (150 ng/mL). As expected, in empty vector transfected cells, 100% of IFN-stimulated cells were positive for nuclear P-STAT1, indicating the activation of the IFN signaling cascade after IFN-α stimulation (Figure 38a and 38b). Differently, in IFN-stimulated VP24 transfected cells P-STAT1 nuclear transport was inhibited so that no P-STAT1 was detectable in the nuclei of these cells (Figure 38a). Notably, in IFN-stimulated VP24 transfected cells treated with Quercetin, there was a significant 20% of cells positive for nuclear P-STAT1 (Figure 38a and 38b). The fact that the compound was incubated only for 30 min (instead of 8 h as in the dual-luciferase reporter assay) and with a robust dose of IFN-α confirms that Quercetin rapidly blocks VP24 anti-IFN function.

(a)

(**b**)
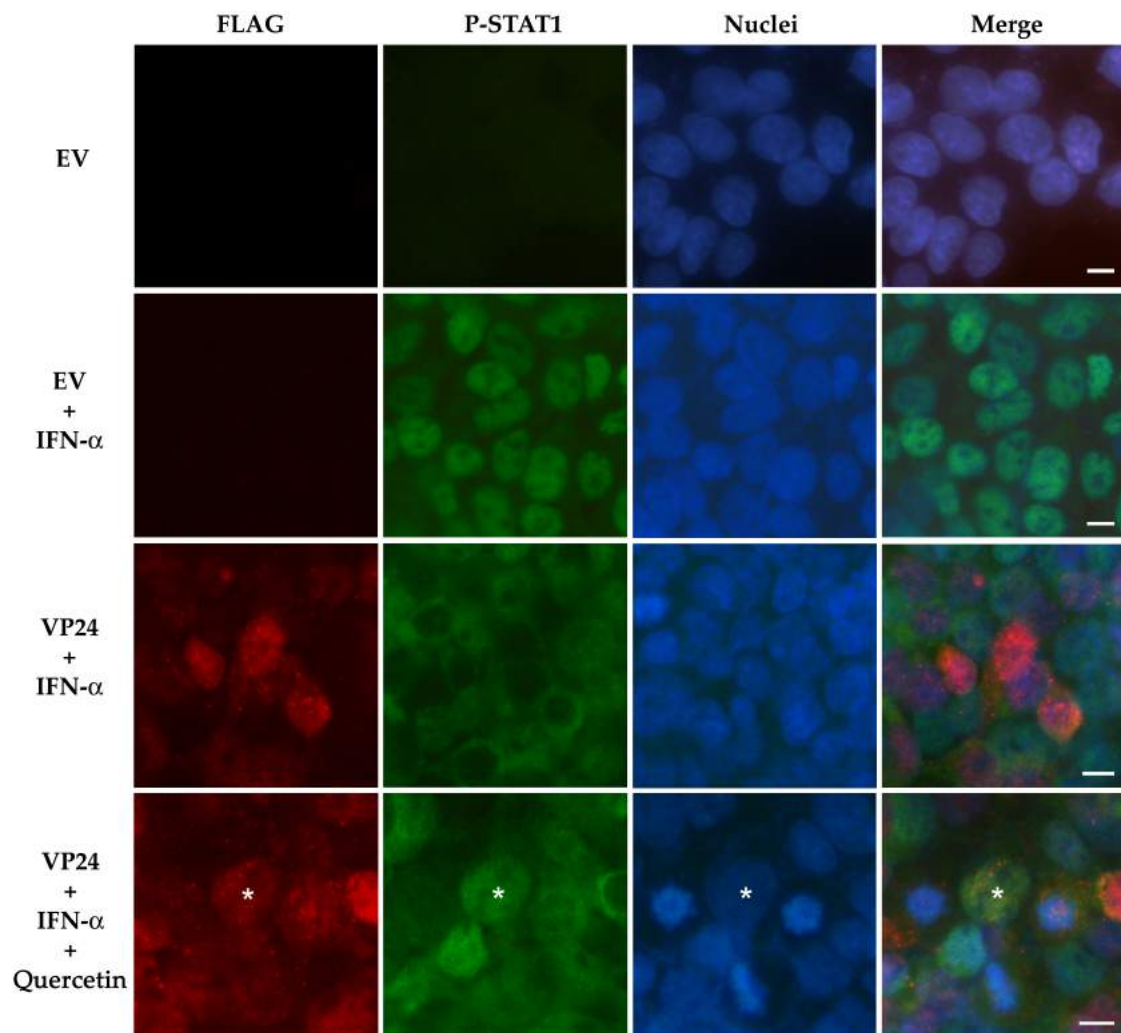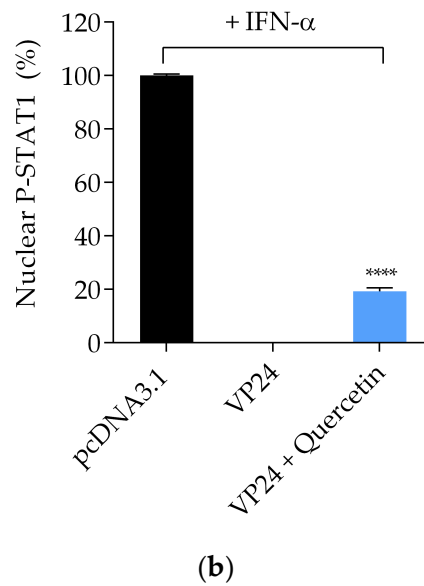
Figure 38. Effect of Quercetin on VP24 inhibition of P-STAT1 nuclear translocation. (**a**) Row 1-2: Immunofluorescence of HEK293T cotrasfected with 2.5 μg/well of empty vector (EV) not stimulated (row 1) or stimulated (row 2) with IFN-α (150 ng/mL) for 30 min. Row 3-4: Immunofluorescence of HEK293T cotrasfected with 2.5 μg/well of VP24 plasmid stimulated with IFN-α (150 ng/mL) for 30 min and not treated (row 3) or treated (row 4) with Quercetin. Asterisk indicated P-STAT1 in the nucleus of a VP24 cell treated with Quercetin. All cells were stained for P-STAT1. Scale bar, 10 μm. (**b**) Percentage of positive cells for nuclear P-STAT1. Error bars represent the mean of three individual experiments. ****$P < 0.0001$, two-tailed unpaired Student's t-test, n=3.

4.3. Discussion

Among the diversified antiviral strategies developed to contrast the different steps of the viral life cycle, (Abner et al., 2018; Esposito and Tramontano, 2014; Gastaminza et al., 2010; Sheahan et al., 2017; Van De Klundert et al., 2016), interfering with the initial phases of the infection, such as the viral evasion of the IFN system, is an attractive therapeutic approach against several types of viruses (Jones et al., 2017; Khiar et al., 2017; Pizzolla et al., 2017; Zinzula and Tramontano, 2013b). Since the EBOV inhibition of IFN response massively contributes to the viral pathogenesis (Ebihara et al., 2006; Prins et al., 2010), restoring the IFN system could represent an ideal strategy for EBOV control. Several mutational studies confirm, in fact, VP24 as a therapeutic target

(Darapaneni, 2014; Pinto et al., 2015; Plesko et al., 2015; Raj and Varadwaj, 2016; Setlur et al., 2017; Zhao et al., 2016). However, few antiviral agents have been tested *in vitro* against VP24 and only two molecules have been reported to interfere with its binding to KPNα5 (Garcia-Dorival et al., 2014; P. L. Iversen et al., 2012; Song et al., 2017; Tanaka et al., 2018; Warren et al., 2015). In this study we showed for the first time that flavonoids are able to interfere with the ability of VP24 to block the IFN signaling in cellular systems, and that Quercetin is the most active compound among the ones that have been tested.

While the majority of the studies on Quercetin and its derivatives focused on their therapeutic use against inflammation and cancer, also an antiviral activity has been demonstrated on different viruses, including HCV (Khachatoorian et al., 2012), Mayaro virus (Dos Santos et al., 2014), IAV (Kim et al., 2010), CHIKV (Lani et al., 2015) and EBV (Lee et al., 2015). In this study, Quercetin was shown to inhibit EBOV VP24 effects on IFN-induced stimulation with IC_{50} value in the low macromolar range, and to significantly restore the ISRE expression and the ISG15 mRNA transcription. Docking studies on its putative binding mode suggest that Quercetin locates in the interface between VP24 and KPNα5 preventing their binding. This was confirmed by the ability of Quercetin to rapidly affect the VP24 inhibition of P-STAT1 nuclear transport even in presence of a high amount of IFN. Overall, given its anti-VP24 properties and its selective index, Quercetin surely represents a very promising lead compound for the development of novel EBOV therapeutics.

Chapter 5

ZIKV NS2A and NS4B Inhibition of the Interferon Signaling

5.1. Introduction

As described in the introduction, ZIKV is able to escape the IFN response using different mechanisms and adopting multiple viral proteins to overcome the host defense. While much work has been done to characterize the role of ZIKV proteins in the inhibition of the IFN production cascade, little is known about the proteins involved in the evasion of the IFN signaling pathway. ZIKV NS2B/3 (Wu et al., 2017) and NS5 (Grant et al., 2016; Kumar et al., 2016) are the only proteins already known to interfere with the JAK/STAT cascade, acting by degradation of JAK1 and STAT2, respectively. In the attempt to identify potential ZIKV-encoded IFN signaling antagonists, we evaluated the effect of individual non-structural protein of ZIKV in our luciferase assay (see Chapter 3). We identified two novel ZIKV proteins able to inhibit the IFN signaling pathway, NS2A and NS4B, and we further characterized their molecular mechanism of action.

5.1.1. NS2A protein

NS2A is a small protein (20 kDa) associated with the endoplasmic reticulum. It is implicated in multiple steps of the viral life cycle including virion assembly (Leung et al., 2008) and genome replication (MacKenzie et al., 1998). In ZIKV, NS2A relevantly contributes to the developing of the pathogenesis, disrupting

mammalian cortical neurogenesis by degradation of adherens junction proteins (Yoon et al., 2017). As already mentioned in Chapter 1, flaviviral NS2A is implicated in the modulation of the host IFN response. Its role as interferon antagonist has been described for DENV-2 (Munoz-Jordan et al., 2003), KUNV (Liu et al., 2006, 2005, 2004), JEV (Tu et al., 2012) and also ZIKV (Kumar et al., 2016; Wu et al., 2017; Xia et al., 2018). NS2A is responsible for the suppression of IFN-β transcription, being an important determinant of virulence in KUNV (Liu et al., 2006). In ZIKV, NS2A is known to interfere at the level of TBK1 phosphorylation blocking the IFN production (Kumar et al., 2016; Xia et al., 2018). In JEV, it acts blocking PKR (Tu et al., 2012), while in DENV and WNV, it is reported to inhibit the IFN-α/β signaling (Liu et al., 2005; Munoz-Jordan et al., 2003).

5.1.2. NS4B protein

NS4B is a highly hydrophobic protein with a molecular weight of about 27 kDa and, like NS2A, it is integrated in the endoplasmic reticulum membrane. NS4B is a component of the viral replication complex (Westaway et al., 1997; Zou et al., 2014). In addition, it mediates the virus-host interactions, by suppression of the host RNA interference (Kakumani et al., 2013) and the IFN responses (Cumberworth et al., 2017). NS4B is known to block RIG-I pathway through an interaction with STING during YFV infection (Ishikawa et al., 2009). Also in ZIKV NS4B counteracts the via of RIG-I (Wu et al., 2017). It has been demonstrated that a single mutation in ZIKV NS4B that causes greater disease in mice was associated with a decreased IFNβ production and diminished ISGs expression, confirming the importance of NS4B as determinant of pathogenesis (Gorman et al., 2018). Flaviviral NS4B is also implicated in IFN signaling inhibition. DENV NS4B acts by suppressing the phosphorylation and nuclear

transport of STAT1/STAT2. This function has also been reported for YFV and WNV (Muñoz-Jordán and Fredericksen, 2010). The first N-terminal 125 amino acids are requested for IFN-I inhibition in DENV. It has been suggested that residues 77-103 interact with cellular components involved in the IFN antiviral defense (Munoz-Jordan et al., 2003; Muñoz-Jordán and Fredericksen, 2010). In addition, the anti-IFN function of NS4B depends on the presence of an N-terminal signal peptide, named 2K. However, the 2K segment is not directly involved in blocking IFNβ signaling, since its sequence is not specific and can be substituted without loss of the IFN inhibitory function (Muñoz-Jordán et al., 2005). In WNV NS4B amino acids 22 and 24 have been shown to be essential for inhibition of the IFN response (Cumberworth et al., 2017).

5.2. Results

5.2.1. Effect of ZIKV Proteins on the IFN-α-induced ISRE Expression

To the aim of identifying ZIKV proteins able to inhibit the IFN signaling pathway, we prepared a library of expression plasmids for the individual proteins of ZIKV (NS1, NS2A, NS2B/3, NS3/4A, NS4B) and tested them for their ability to suppress the IFN-α-induced ISRE-driven transcription in our dual-luciferase reporter assay. In brief, HEK293T were cotransfected with pISRE-luc, RL-TK and each plasmid for the ZIKV proteins. Then, cells were stimulated with IFN-α and the luciferase activity was read (see Chapter 2 for details). As positive control of inhibition, we used EBOV VP24 and ZIKV NS2B/3, known inhibitors of the JAK/STAT cascade (Reid et al., 2006; Wu et al., 2017). Results showed that, as expected, transfection with empty vector did not have any effect on IFN-α-induced ISRE-driven transcription, while transfection with the positive controls VP24 and NS2B/3 showed a high suppression of the luciferase reporter activity (Figure 39). Notably, substantial suppression of IFN-α-induced

ISRE expression was observed in cells expressing the NS2A and NS4B genes but not in cells expressing the NS1 or NS3/4A genes (Figure 39). NS2A resulted more efficient than NS4B reducing the ISRE transcription (~ 40% versus ~ 55% of ISRE activation, respectively, with 60 ng/well of plasmid).
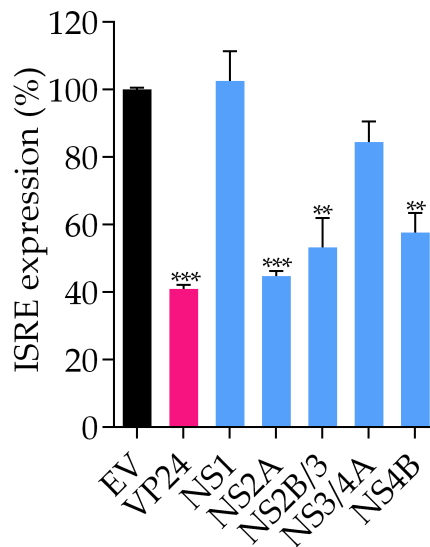
Figure 39. Cotransfection with ZIKV NS2A and NS4B results in inhibition of ISRE expression. HEK293T cells were transfected with pISRE-luc (60 ng/well), RL-TK (60 ng/well) and 60 ng/well of empty vector (EV) pcDNA3.1(+), or expression plasmid for EBOV VP24 or ZIKV proteins. After 24 h, cells were stimulated with 10 ng/mL of IFN-α for 8 h. Then, luciferase activity was read. Results are shown as percentage of pISRE-luc activation in VP24/ZIKV proteins transfected cells over EV control. Each experiment was done in triplicate. Error bars indicate the mean ± SD. **P< 0.01 and ***P< 0.005, (two-tailed unpaired Student's t-test, n=3).

5.2.2. NS2A and NS4B Suppress ISG15 and OAS1 mRNA Transcription

To confirm the inhibitory effect of NS2A and NS4B on ISRE transcription, mRNA expression levels of two common ISGs, ISG15 and OAS1, were detected by qRT-PCR in HEK293T cells cotransfected with the two proteins. Results showed that the mRNA levels of ISG15 and OAS1 induced by IFN-α were significantly reduced in cells cotransfected with NS2A and NS4B, compared to empty vector cotransfected cells (Figure 40). NS2A expression resulted in the

most dramatic reduction in both ISG15 and OAS1 mRNAs levels (Figure 40), confirming the higher efficiency compared to NS4B in inhibiting the pathway.
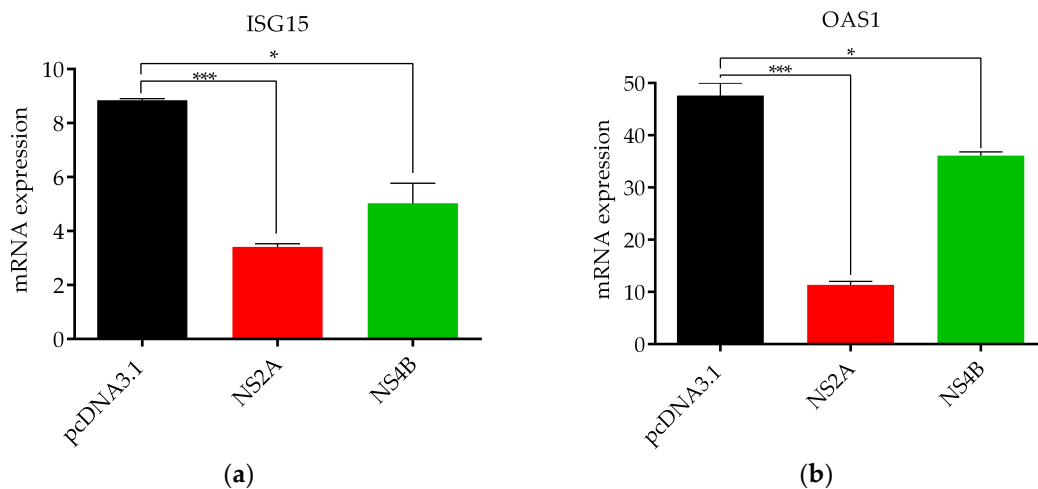
Figure 40. Effect of NS2A and NS4B on ISGs mRNA expression. HEK293T cells were transfected with pcDNA3.1 (2.5 µg/well) or ZIKV NS2A or NS4B plasmid (2.5 µg/well). After 24 h, cells were stimulated with 10 ng/mL of IFN-α. After 24 h, total RNA was extracted and RT-qPCR was performed for evaluation of (**a**) ISG15 or (**b**) OAS1 transcript levels. Results are shown as fold inductions of ISG15/OAS1 mRNA expression in IFN-α stimulated over not stimulated cells. Error bars indicate the mean ± SD of three independent experiments. *P< 0.05 and ***P< 0.005, two-tailed unpaired Student's t-test, n=3.

5.2.3. NS2A and NS4B Inhibit the IFN-α-induced ISRE Transcription Dose-Dependently and with Addictive Effect

Our gene reporter assay showed that transfection with NS2A resulted in the strongest inhibition of IFN-α stimulation of ISRE compared to NS4B protein. We performed a dose-response curve cotransfecting cells with increasing concentration of each expression plasmid for the two proteins (1.8- 120 ng/well). Calculating the EC$_{50}$ value, we found that NS2A and NS4B were able to dose-dependently suppress the ISRE transcription, showing a EC$_{50}$ values of 40.15 ng/well and 93 ng/well, respectively (Figure 41), suggesting a higher potency of NS2A inhibiting the system. In addition we tested the combined effect of the two proteins and observed that the antagonistic effects of these proteins in the

IFN signaling was stronger when these proteins were coexpressed with an EC_{50} value of 14.42 ng/well for both plasmids (synergistic effect).

(a)

(b)
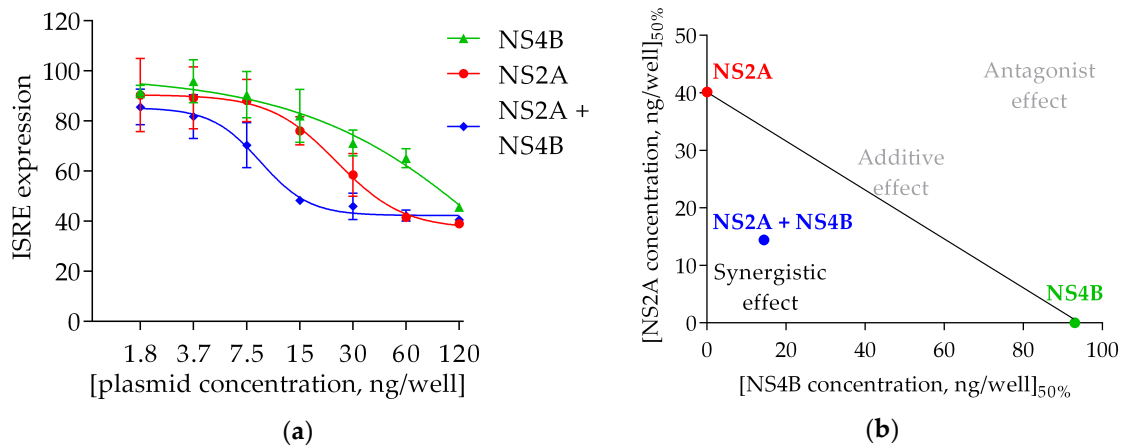
Figure 41. Dose-response curve of NS2A, NS4B and their combination. (a) Cells were transfected with pISRE-luc (60 ng/well), RL-TK (60 ng/well) and empty vector (EV) or NS2A/NS4B or both plasmids together (1.8-120 ng/well). After 8 h of IFN-α stimulation, luciferase activity was read. Results are shown as percentage of ISRE activation in viral proteins transfected cells over EV control. Each experiment was done in triplicate. Error bars indicate the mean ± SD. **(b)** Isobolographic analysis diagram of the interaction between NS2A and NS4B. The EC_{50} values (red point for NS2A and green point for NS4B) were the dose at 50% of ISRE inhibition. The straight line (additive line) is made by dose NS2A and dose NS4B (EC_{50} values). A value of combination (EC_{50} NS2A + NS4B) (blue point above additive line) indicated that the interaction is synergistic.

5.2.4. NS2A Inhibits the IFN-α-Mediated STAT1 Phosphorylation

ZIKV NS2A exhibited the highest inhibitory effects on ISRE promoter activation. Thus, given its impact on IFN signaling, we firstly focused on NS2A for detailed analyses of its mechanism of action. As detailed in the introduction, the induction of type I IFN occurs through the activation of a signal cascade which results in the phosphorylation and translocation of the transcription factors, STAT1 and STAT2, from cytoplasm to the nucleus where they switch on the ISRE promoter. To identify the key cellular targets of NS2A in the IFN response pathway, we firstly examined phosphorylation of STAT1 at Tyr701 and its subcellular localization by immunofluorescence. HEK293T were transfected with empty vector or expression plasmids for NS2A or EBOV VP24,

known inhibitor of STAT1 nuclear transport (Reid et al., 2006). After transfection, cells were incubated with IFN-α for 30 min and then were stained for FLAG and P-STAT1 (green and red signals, respectively) (Figure 42). Results showed that in cells transfected with empty vector and stimulated with IFN-α, P-STAT1 was detectable in the nuclei (Figure 42, row 2), while - as expected - in not stimulated cells no P-STAT1 was observed (Figure 42, row 1). Notably, in cells transfected with NS2A plasmid, P-STAT1 was not detectable upon IFN-α stimulation (Figure 42, row 3), while in cells transfected with EBOV VP24 plasmid P-STAT1 was observed only in the cytoplasm (Figure 42, row 4). This clearly demonstrated that ZIKV NS2A is acting differently from EBOV VP24, inhibiting STAT1 phosphorylation and not only P-STAT1 nuclear transport.

5.2.5. NS2A Suppress STAT1 Phosphorylation Not Degrading STAT1

The inhibition of STAT1 phosphorylation can be due to two events: the NS2A binding and/or degradation of (i) STAT1 or (ii) inhibition of P-JAK1, the IFNAR associated kinase responsible for the tyrosine phosphorylation of STAT1. To test the first hypothesis, we evaluated the presence of STAT1 in stimulated or not stimulated empty vector/NS2A transfected cells, incubating them with an antibody for total STAT1. Non-phosphorylated STAT1 is a constitutive transcription factor expressed in the cytoplasm, even without IFN stimulation (Ramana et al., 2000), as observed in empty vector cotransfected cells (Figure 43, row 1). Upon IFN stimulation, STAT1 is activated and P-STAT1 enters into the nucleus to promote the ISGs transcription (Figure 43, row 2). If NS2A was inducing STAT1 degradation, a reduction in STAT1 signal would have been observed in both stimulated and not stimulated NS2A cotransfected cells. However, our results showed that in NS2A cotransfected cells STAT1 signal
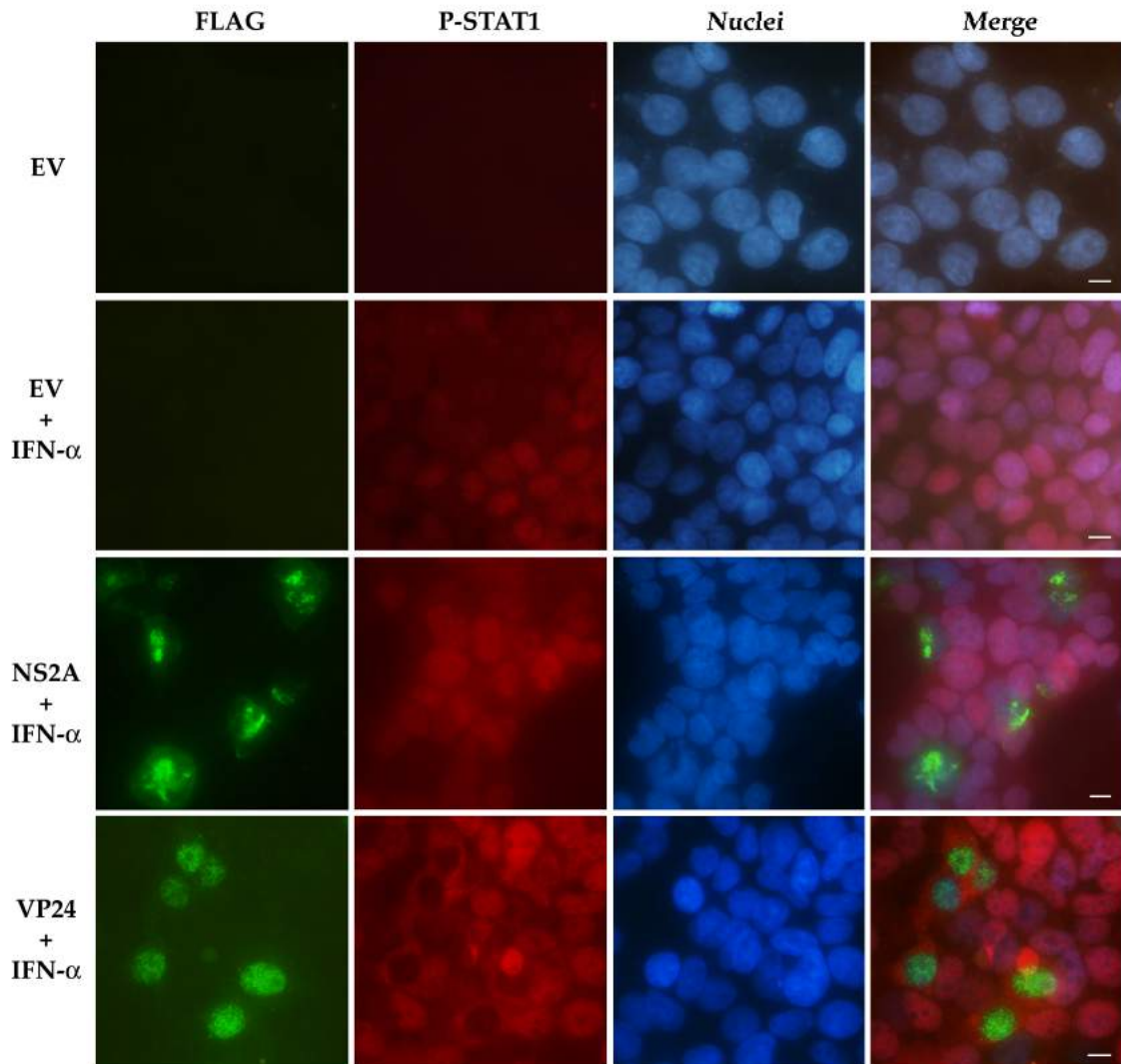
Figure 42. Inhibition of STAT1 phosphorylation mediated by NS2A. Immunofluorescence of HEK293T cells with empty vector (EV) stimulated (row 2) or not (row 1) with IFN-α. NS2A (row 3) and VP24 (row 4) transfected cells were stimulated with IFN-α. FLAG (green) and P-STAT1 (red) signals were detected. Nuclei (blue) were stained with Hoechst. Scale bar, 10 µm.
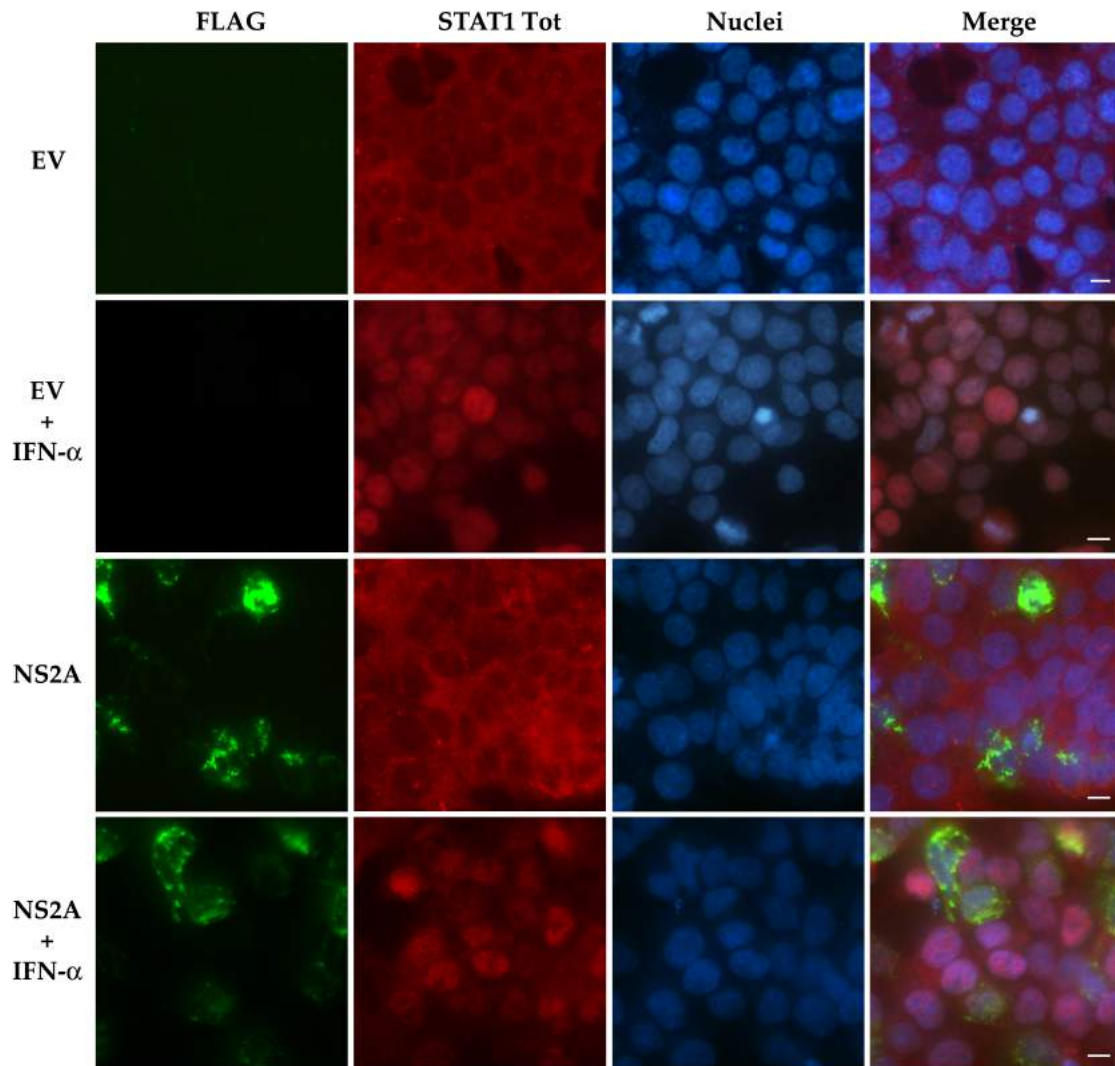
Figure 43. NS2A was not degrading STAT1. Immunofluorescence of HEK293T cells with empty vector (EV) stimulated (row 2) or not (row 1) with IFN-α. NS2A transfected cells were stimulated (row 4) or not (row 3) with IFN-α. FLAG (green) and total STAT1 (red) signals were detected. Nuclei (blue) were stained with Hoechst. Scale bar, 10 μm.

was detectable, as in the sample cotransfected with the empty vector, regardless of which stimulated condition was considered (Figure 43, rows 3 and 4). Of note, in stimulated cells transfected with the NS2A plasmid the STAT1 signal was detectable only in the cytoplasm, indicative of the presence of only non-phosphorylated STAT1, since its nuclear transport did not occur (Figure 43, row 4). Thus, we confirmed that NS2A was blocking STAT1 phosphorylation but not by the degradation of STAT1.

5.2.6. NS2A Directly Targets P-JAK1

To further trace the upstream steps of NS2A inhibition of the IFN signaling cascade, we examined whether JAK1 phosphorylation was also suppressed by NS2A. The IFN-α binding to the IFNAR receptor results in activation through phosphorylation of JAK1 to catalyze the sequential phosphorylation of STAT1. We incubated IFN-α stimulated or not stimulated cells with the antibody for P-JAK1 (Figure 44). As expected, P-JAK1 was distributed in the cytoplasm of only stimulated cells, confirming the IFN-α-mediated activation of the JAK/STAT pathway (Figure 44 row 2). Results also showed that in cells expressing NS2A P-JAK1 was detectable, confirming that NS2A is not inhibiting the phosphorylation of JAK1 or mediating its degradation. However, P-JAK1 was found in colocalization with the NS2A signal (Figure 44 row 3), strongly suggesting that NS2A is directly interacting with P-JAK1.

5.2.7. NS2A Blocks Nuclear Translocation of P-STAT2

To further analyze the inhibition of IFN signaling by NS2A, we tested whether NS2A was affecting the IFN-α-mediated phosphorylation of STAT2. We probed HEK293T cells with the antibody for P-STAT2. Results showed that, while no P-
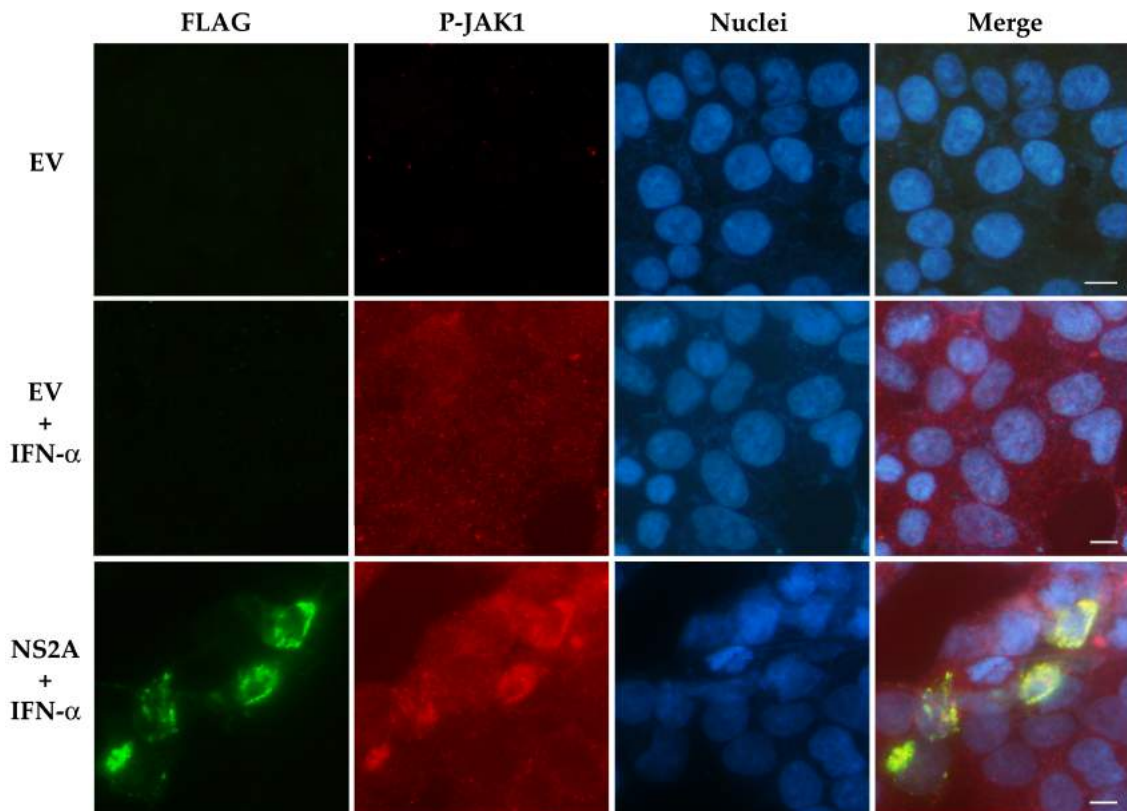
Figure 44. NS2A colocalizes with P-JAK1. Immunofluorescence of HEK293T cells with empty vector (EV) stimulated (row 2) or not (row 1) with IFN-α. NS2A transfected cells were stimulated (row 3) with IFN-α. NS2A FLAG (green) and P-JAK1 (red) signals were detected. Nuclei (blue) were stained with Hoechst. Scale bar, 10 µm.

STAT2 was present in not stimulated cells (Figure 45, row 1), STAT2 was phosphorylated in both IFN-α-stimulated empty vector (Figure 45, row 2) and NS2A cells (Figure 45, row 3). This indicates that STAT2 phosphorylation is not suppressed by the ZIKV NS2A protein. However, in cells transfected with NS2A P-STAT2 was localized in the cytoplasm and not in the nucleus (Figure 45, row 3), in contrast with cells transfected with empty vector in which P-STAT2 had a nuclear localization (Figure 45, row 2). A possible explanation of this result is that the inhibition of STAT1 phosphorylation impedes the assembly of the heterotrimeric complex, ISGF3, constituted by P-STAT1, P-STAT2 and IRF9, thus P-STAT2 alone cannot enter into the nucleus (Banningeri and Reich, 2004). Notably, our results revealed also that P-STAT2 was colocalizing with the NS2A signal, suggesting a potential interaction also between NS2A and P-STAT2.
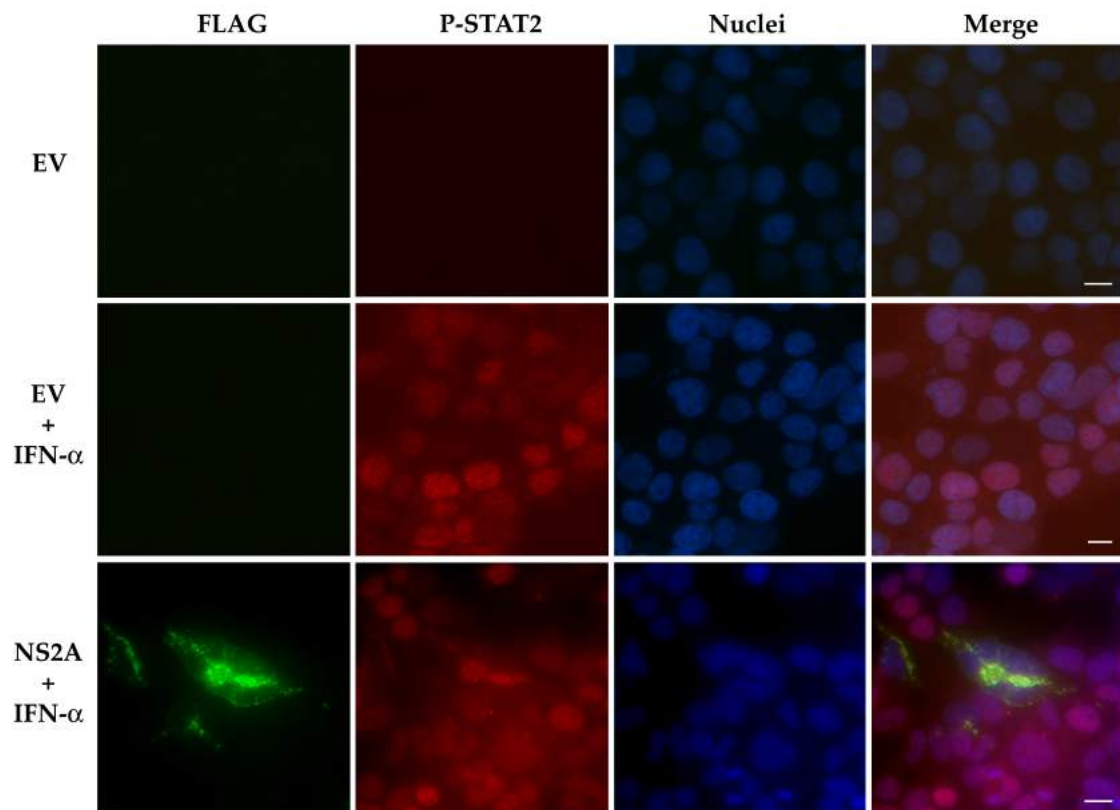
Figure 45. Nuclear transport of NS2A is blocked after NS2A expression. Immunofluorescence of HEK293T transfected with empty vector (EV) (rows 1 and 2) or NS2A (row 3) plasmids. After stimulation with IFN-α, cells were probed for FLAG (green) and P-STAT2 (red). Nuclei (blue) were stained with Hoechst. Scale bar, 10 μm.

5.2.8. NS4B Effect on STAT1 and STAT2 Phosphorylation

Subsequently, the NS4B mechanism of IFN signaling inhibition was examined. We evaluated the effect of NS4B on the IFN-mediated STAT1 and STAT2 phosphorylation. Results showed that, while NS4B weakly inhibit the STAT1 phosphorylation (data not shown), it was able to strongly inhibit the STAT2 phosphorylation (Figure 46 row 2).
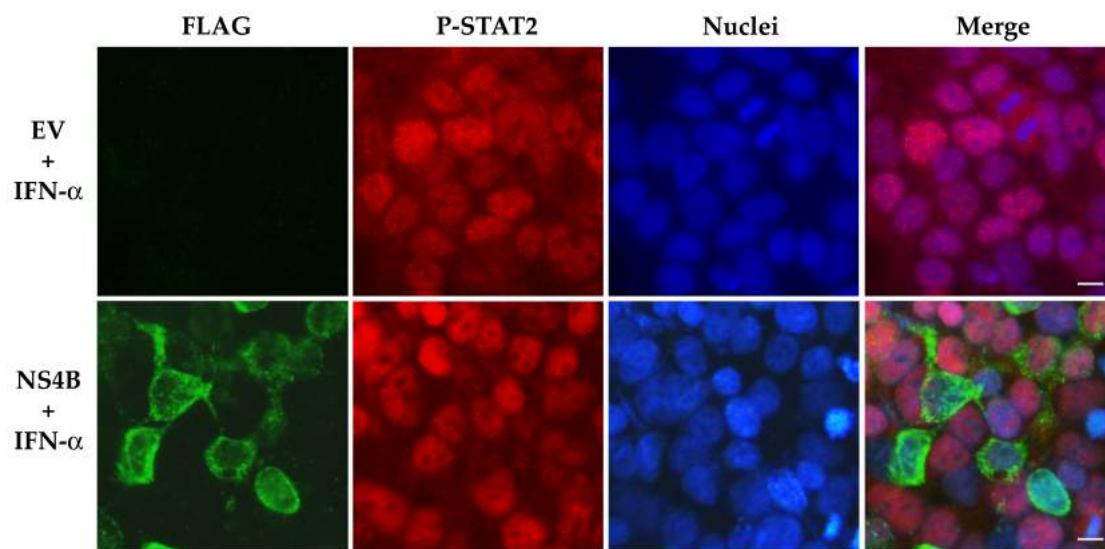
Figure 46. Effect of NS4B on IFN signaling cascade. Immunofluorescence of HEK293T cells transfected with empty vector (EV) (row 1) and NS4B (row 2) expression plasmids, stimulated with IFN-α and stained for P-STAT2. Scale bar, 10 μm.

5.3. Discussion

Our results showed two novel mechanisms adopted by ZIKV to hinder the IFN signaling cascade. Viral proteins NS2A and NS4B were found to be responsible for that effect. In fact, expression of NS2A and NS4B resulted in the dose-dependent inhibition of the ISRE transcription and in the significant reduction of the transcript levels of ISG15 and OAS1. NS2A was demonstrated to be more efficient than NS4B in blocking the IFN-α-induced ISRE in the dual-luciferase assay as well as the ISGs mRNA transcription. In addition, the combination of the two proteins resulted in a substantial reduction of the ISRE transcription, revealing a synergistic effect of the two viral proteins. This was also observed

after coexpression of DENV-2 NS2A, NS4A and NS4B that implicated an enhanced replication of an IFN-sensitive virus (Munoz-Jordan et al., 2003). Examining the mechanism of action of NS2A, it was observed that it counteracts with two steps of the JAK/STAT pathway: (i) interacting with P-JAK1, thus blocking the STAT1 phosphorylation, (ii) interacting with P-STAT2, thus blocking its nuclear transport. The observation that NS2A targets multiple steps of the cascade may explain the stronger effect in inhibiting the IFN signaling as compared to NS4B, which was shown to strongly inhibit only the STAT2 phosphorylation.

NS2A is a known antagonist of the IFN-α/β signaling in other flaviviruses. The only reported NS2A mechanism of action is the suppression of the nuclear translocation of P-STAT2 by KUNV (Liu et al., 2005). Immunofluorescence analysis with anti-STAT2 antibody revealed no presence of STAT2 in the nucleus after IFN-β treatment in A549 cells transfected with KUNV NS2A, demonstrating its ability to interfere not a level of STAT2 phosphorylation but at the step of P-STAT2 nuclear transport (Liu et al., 2005). This is consistent with our results, in which also ZIKV NS2A is able to block the same step. The phylogenetic analysis of ZIKV NS2A and the other flaviviruses, including KUNV, supported the strong correlation between ZIKV NS2A and KUNV, showing a 97% bootstrap value (Figure 47). However, the alignment of ZIKV and KUNV NS2A amino acid sequence showed a low identity (34.26%) that could be explained by the fact that such identity was calculated taking into consideration the entire protein and not only the isolated anti-IFN function domain, which was not possible since it is not well characterized yet.

In regards to the flaviviral protein NS4B, it has been shown that it is able to interfere with both STAT1 and STAT2 phosphorylation. NS4B of DENV-2 (16681 strain), WNV (NY strain), and YFV (YF vaccine 17D, YFV1) were found

Figure 47. Neighbor joining tree of flaviviral NS2A. The phylogenetic relationship between flaviviral NS2A was analyzed through the construction of phylogenetic trees using a neighbor-joining (NJ) method. The red lines belong to the subgroup of ZIKV NS2A, which includes our NS2A sequence and KUNV NS2A (red triangles).

to block STAT-1 phosphorylation and thus ISG induction (Munoz-Jordan et al., 2003; Muñoz-Jordán et al., 2005). In KUNV, NS4B was reported to block STAT1 but also STAT2 phosphorylation (Liu et al., 2005) with E22 and K24 residues reported to control IFN resistance in cells expressing subgenomic replicons (Evans and Seeger, 2007). In fact, substitution of these residues with alanine exhibited stimulation of the IFN pathway in cells transfected with the mutant NS4B, as seen by induced STAT1 phosphorylation. The residue E22 (but not K24 that in ZIKV lysine substituted with alanine) is present also in ZIKV NS4B sequence, suggesting that this residue could be involved in the IFN inhibition.

However, the characterization of the IFN signaling inhibition mediated by NS4B in different flaviviruses is complicated because of the strain-specific differences. For example, some DENV strains with different serotypes (TSV01-DENV-2, SG167-DENV-1, MY02569-DENV-1, MY10340-DENV-2) were not reported to block STAT1 IFN-β-mediated phosphorylation, while NGC-DENV-2, MY10245-DENV-1, MY22563-DENV-2, and MY22713-DENV-4 serotypes showed this inhibitory activity. Our phylogenetic analysis of ZIKV NS4B showed a statistical correlation with DENV with 84% of bootstrap value, even if the amino acid conservation was moderate, being the sequence identity between the entire ZIKV NS4B protein and DENV-1, DENV-3 and DENV-4 NS4B proteins in the range of 25-33% (Figure 48). A higher NS4B amino acid identity (41-45%) was observed between ZIKV and different strains of DENV-2. It would be important to deeply investigate NS4B domains involved in P-STAT1 or P-STAT2 inhibition since the full scenario is still missing (Figure 48).

Overall, these results give significant insights into the role of ZIKV NS2A and NS4B proteins as IFN signaling antagonists. Given that the IFN inhibition contributes to ZIKV pathogenicity, NS2A and NS4B proteins may be potential targets for the development of new antiviral agents.
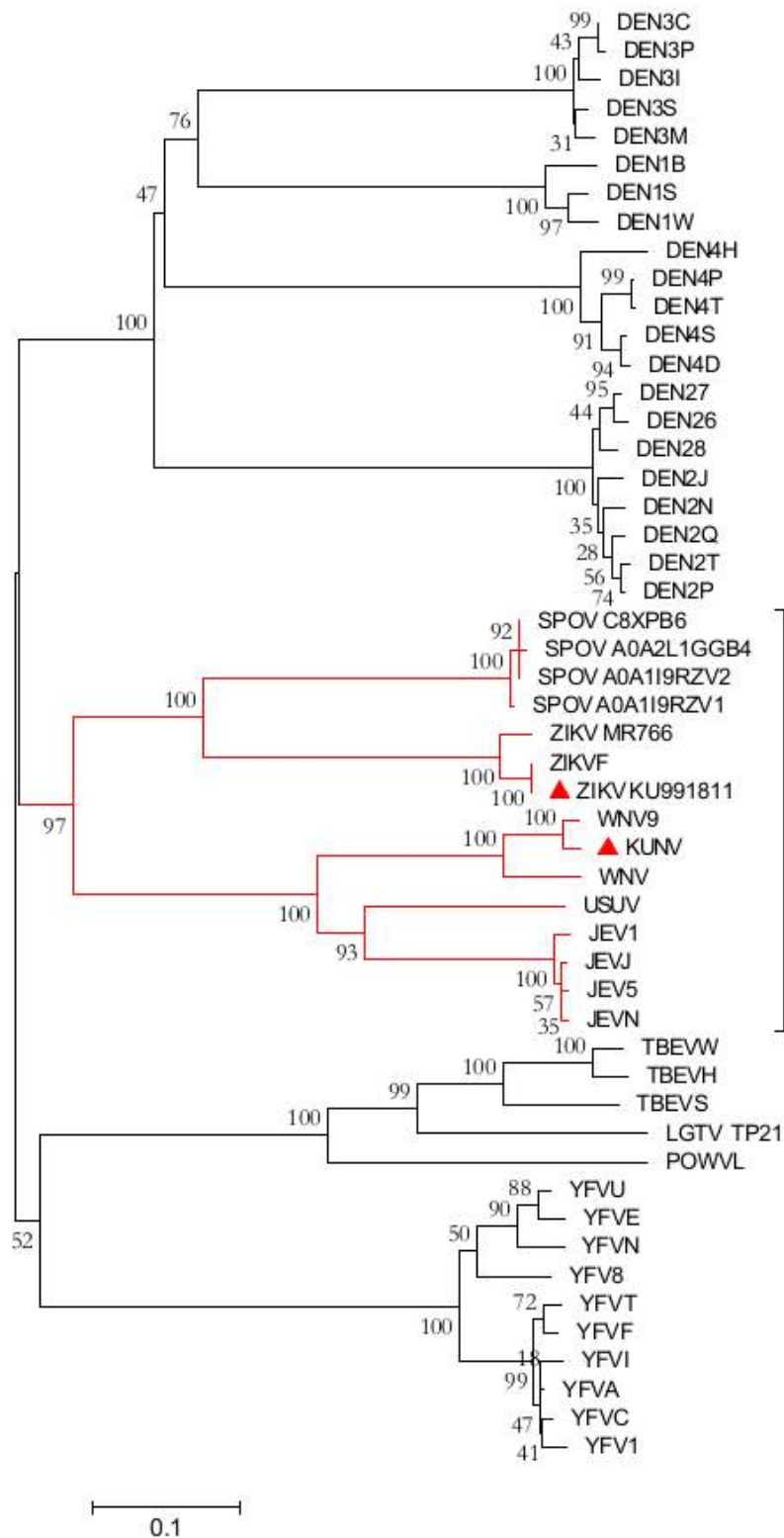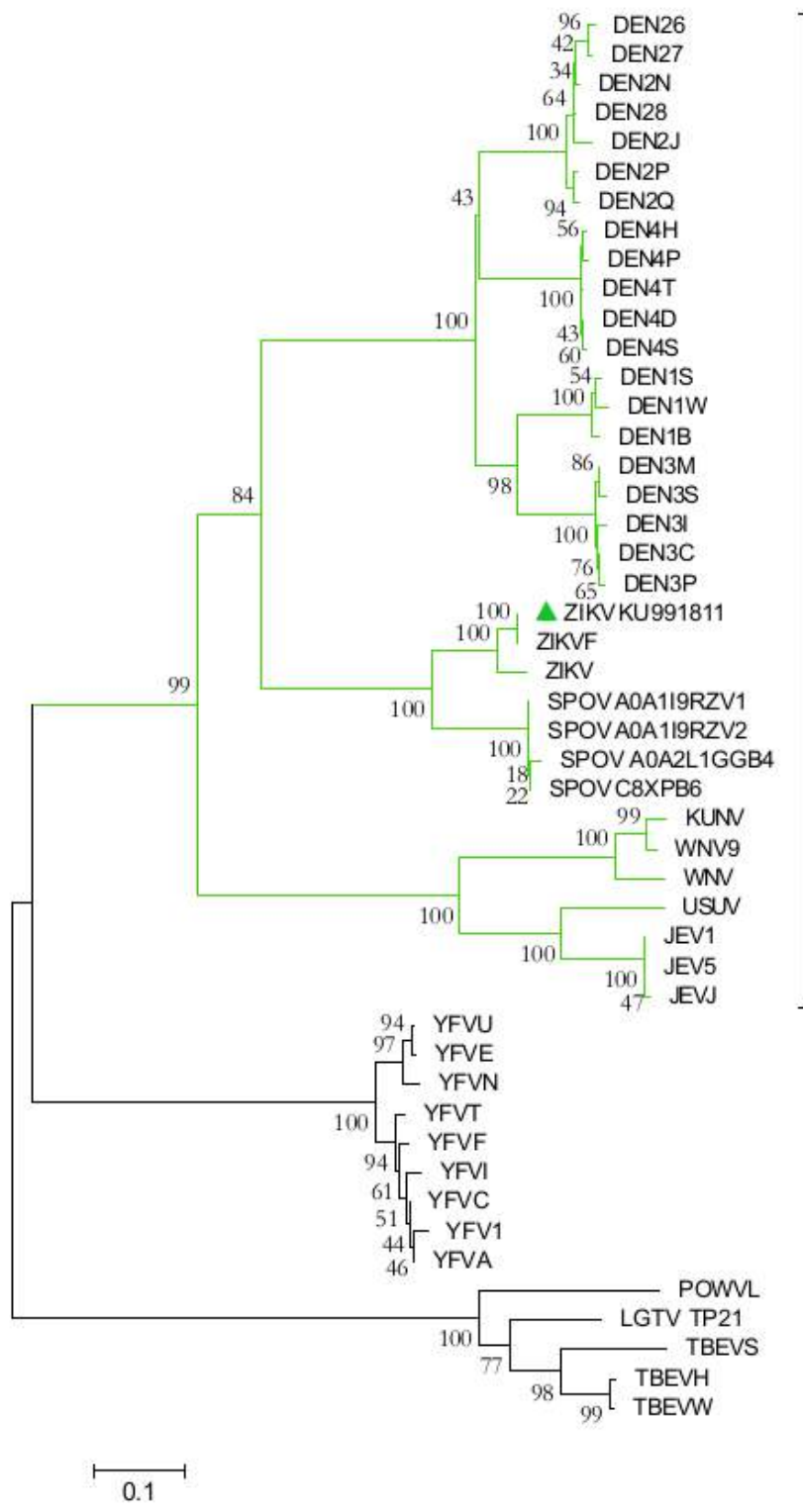
Figure 48. Neighbor joining tree of flaviviral NS4B. The phylogenetic relationship between flaviviral NS4B was analyzed through the construction of phylogenetic trees using a NJ method. The green lines belong to the subgroup of ZIKV NS4B.

Chapter 6

Conclusions

The IFN system is of crucial importance preventing viral recognition and thus the progression of infection. A number of RNA viruses, including EBOV and ZIKV, encode proteins that display IFN-antagonism properties circumventing the host innate immune system. The impact of this counteraction is particularly evident for EBOV since the fatal outcome has been related to the viral ability to subvert the type I IFN response helping the systemic spread of the virus and causing the excessive production of cytokines and mediators that lead to the impairment of the vascular system and failure of adaptive immunity (Bray, 2005). Also ZIKV impairment of the IFN response contributes to the severity of the disease (Gorman et al., 2018; Xia et al., 2018). This is clear since it has been demonstrated that the more virulent strains of ZIKV have evolved several mutations in proteins involved in IFN evasion resulting in an increased virulence compared to old strains.

Several antiviral agents have been tested against EBOV and ZIKV (da Silva et al., 2018; Fanunza et al., 2018a). They are mainly directed against viral entry and replication. However, none of them has been approved. The lack of efficacious therapies highlights the need to identify novel antiviral approaches especially targeting the initial stages of the viral infection. The aim of my project was to focus on the EBOV and ZIKV host interactions, characterizing their molecular mechanisms of IFN evasion in order to develop a specific antiviral strategy based on the restoration of the IFN response.

To this aim, a novel dual gene reporter assay was firstly established. This cell-based assay represents an efficient model to evaluate the IFN induction and its

inhibition by viral proteins. In brief, HEK293T cells are transfected with the pISRE-luc, in which firefly luciferase gene expression is regulated through the ISRE element, and the activation of the ISRE expression is mediated by the exogenous stimulation with IFN-α. This system provides excellent specificity and high reproducibility that allowed to validate the assay for drug screening (Fanunza et al., 2018c).

Among EBOV encoded proteins, VP24 is a valuable pharmacological target (Ebihara et al., 2006). In fact, its suppression of type I IFN signaling is of great importance since it crucially contributes to the EBOV high virulence (Ebihara et al., 2006). Hence, we firstly tested the effect of VP24 in the ISRE stimulation assay in order to optimize all the conditions to use the system for screening compounds against VP24. Results showed that VP24 was inhibiting dose-dependently the ISRE transcription with a VP24 plasmid IC_{50} value of 30 ng/well. The assay validation included the observation that the strong pathway inhibition by VP24 could be restored by adding increasing amounts of IFN-α, confirming the possibility to revert the effect of VP24 by compounds (Fanunza et al., 2018c).

It is well known that plants have shown promise to treatment of a number of viral infections (Di Petrillo et al., 2017; Sanna et al., 2018). Among plants' components, flavonoids exert several biological properties: anti-inflammatory, antioxidant, hepatoprotective, antibacterial (Kumar and Pandey, 2013; Umesh et al., 2018) and also antiviral activity (Cushnie and Lamb, 2005; Sritularak et al., 2013). Flavonoids have been shown to be active against EBOV entry and also to directly target EBOV viral proteins such as VP35 (Qiu et al., 2016; Daino et al., 2018). Based on *in silico* studies, a few flavonoid compounds have been proposed to be potentially active on VP24 (Raj and Varadwaj, 2016), however none of them has been tested against VP24 *in vitro*. Hence, in order to identify

potential VP24 inhibitors, we screened different flavonoids and found for the first time compounds effectively targeting VP24 *in vitro* blocking its function on IFN signaling. Among them, Quercetin was the most active compound. Combining cell-based and computational analysis, we demonstrated that Quercetin was specifically blocking the VP24 IFN inhibitory function. The compound almost completely restored the IFN signaling cascade, showing an IC$_{50}$ value of 7.4 μM in the dual-luciferase assay, and reverted the ISG15 transcript levels expression. We showed that the binding of Quercetin to VP24 compromised the interaction between the viral protein and KPNα5, which is the key element for VP24 IFN inhibitory effect (Mateo et al., 2010; Reid et al., 2006, 2007). This was confirmed by the fact that in presence of Quercetin the nuclear transport of STAT1 was significantly restored in VP24 expressing cells. Based on these evidences, Quercetin represents a very promising hit for the development of anti-EBOV drugs.

Finally, the third part of the thesis comprises the first study describing a novel function for the accessory proteins of ZIKV NS2A and NS4B and shows that they play an important role in viral antagonism of the type I IFN response. In fact, NS2A and NS4B dose-dependently inhibited the ISRE transcription and the mRNA transcription of ISG15 and OAS1 interfering at the levels of STAT1 and STAT2 phosphorylation. The two proteins are known antagonists of the IFN signaling in other member of the same family of ZIKV, including DENV, WNV and YFV (Ye et al., 2013). However, since the entire NS2A and NS4B sequence are not highly conserved among flaviruses, further studies are requested to understand if at least their IFN-inhibitory domains are well conserved.

In conclusion, this thesis exploits diverse strategies of IFN evasion adopted by two viruses, EBOV and ZIKV, belonging to different families, *Filoviridae* and

Flaviviridae, displaying both IFN antagonist properties. To the best of our knowledge, for the first time, results from this dissertation identified new antiviral candidates against EBOV VP24 and novel pharmacological targets among ZIKV proteins. These studies provide the groundwork for a new prospective area in the field of EBOV and ZIKV research, in particular in the development of an antiviral countermeasure addressed to the restoration of IFN response as a powerful approach to early control viral infections.

References

Ablasser, A., Bauernfeind, F., Hartmann, G., Latz, E., Fitzgerald, K.A., Hornung, V., 2009. RIG-I-dependent sensing of poly(dA:dT) through the induction of an RNA polymerase III-transcribed RNA intermediate. Nat. Immunol. 10, 1065–1072. https://doi.org/10.1038/ni.1779

Abner, E., Stoszko, M., Zeng, L., Chen, H.-C., Izquierdo-Bouldstridge, A., Konuma, T., Zorita, E., Fanunza, E., Zhang, Q., Mahmoudi, T., Zhou, M.-M., Filion, G.J., Jordan, A., 2018. A new quinoline BRD4 inhibitor targets a distinct latent HIV-1 reservoir for re-activation from other 'shock' drugs. J. Virol. JVI.02056-17. https://doi.org/10.1128/JVI.02056-17

Acosta-Ampudia, Y., Monsalve, D.M., Castillo-Medina, L.F., Rodríguez, Y., Pacheco, Y., Halstead, S., Willison, H.J., Anaya, J.-M., Ramírez-Santana, C., 2018. Autoimmune Neurological Conditions Associated With Zika Virus Infection. Front. Mol. Neurosci. 11, 116. https://doi.org/10.3389/fnmol.2018.00116

Aebi, M., Fäh, J., Hurt, N., Samuel, C.E., Thomis, D., Bazzigher, L., Pavlovic, J., Haller, O., Staeheli, P., 1989. cDNA structures and regulation of two interferon-induced human Mx proteins. Mol. Cell. Biol. 9, 5062–72. https://doi.org/10.1128/MCB.9.11.5062

Aguirre, S., Maestre, A.M., Pagni, S., Patel, J.R., Savage, T., Gutman, D., Maringer, K., Bernal-Rubio, D., Shabman, R.S., Simon, V., Rodriguez-Madoz, J.R., Mulder, L.C.F., Barber, G.N., Fernandez-Sesma, A., 2012. DENV Inhibits Type I IFN Production in Infected Cells by Cleaving Human STING. PLoS Pathog. 8. https://doi.org/10.1371/journal.ppat.1002934

Akira, S., Uematsu, S., Takeuchi, O., 2006. Pathogen recognition and innate immunity. Cell 124, 783–801. https://doi.org/10.1016/j.cell.2006.02.015

Al-Khatib, K., Williams, B.R.G., Silverman, R.H., Halford, W., Carr, D.J.J., 2003. The murine double-stranded RNA-dependent protein kinase PKR and the murine 2′,5′-oligoadenylate synthetase-dependent RNase L are required for IFN-β-mediated resistance against herpes simplex virus type 1 in primary trigeminal ganglion culture. Virology 313, 126–135. https://doi.org/10.1016/S0042-6822(03)00298-8

Alera, M.T., Hermann, L., Tac-An, I.A., Klungthong, C., Rutvisuttinunt, W., Manasatienkij, W., Villa, D., Thaisomboonsuk, B., Velasco, J.M., Chinnawirotpisan, P., Lago, C.B., Roque, V.G., Macareo, L.R.,

Srikiatkhachorn, A., Fernandez, S., Yoon, I.K., 2015. Zika virus infection, Philippines, 2012. Emerg. Infect. Dis. https://doi.org/10.3201/eid2104.141707

Andersson, I., Bladh, L., Mousavi-Jazi, M., Magnusson, K.-E., Lundkvist, A., Haller, O., Mirazimi, A., 2004. Human MxA protein inhibits the replication of Crimean-Congo hemorrhagic fever virus. J. Virol. 78, 4323–9. https://doi.org/10.1128/JVI.78.8.4323-4329.2004

Ank, N., West, H., Paludan, D.S.R., 2006. IFN-λ: Novel Antiviral Cytokines. J. Interferon Cytokine Res. 379, 373–379. https://doi.org/10.1089/jir.2006.26.373

Arnaud, N., Dabo, S., Maillard, P., Budkowska, A., Kalliampakou, K.I., Mavromara, P., Garcin, D., Hugon, J., Gatignol, A., Akazawa, D., Wakita, T., Meurs, E.F., 2010. Hepatitis c virus controls interferon production through PKR activation. PLoS One 5, e10575. https://doi.org/10.1371/journal.pone.0010575

Ashkar, A. a, Rosenthal, K.L., 2002. Toll-like receptor 9, CpG DNA and innate immunity. Curr. Mol. Med. 2, 545–56. https://doi.org/10.2174/1566524023362159

Au, W.C., Moore, P.A., Lowther, W., Juang, Y.T., Pitha, P.M., 1995. Identification of a member of the interferon regulatory factor family that binds to the interferon-stimulated response element and activates expression of interferon-induced genes. Proc. Natl. Acad. Sci. 92, 11657–11661. https://doi.org/10.1073/pnas.92.25.11657

Bang, S., Li, W., Ha, T.K.Q., Lee, C., Oh, W.K., Shim, S.H., 2017. Anti-influenza effect of the major flavonoids from Salvia plebeia R.Br. via inhibition of influenza H1N1 virus neuraminidase. Nat. Prod. Res. 32, 1224–1228. https://doi.org/10.1080/14786419.2017.1326042

Banningeri, G., Reich, N.C., 2004. STAT2 nuclear trafficking. J. Biol. Chem. 279, 39199–39206. https://doi.org/10.1074/jbc.M400815200

Barzon, L., Trevisan, M., Sinigaglia, A., Lavezzo, E., Palu, G., 2016. Zika virus: from pathogenesis to disease control. FEMS Microbiol. Lett. https://doi.org/10.1093/femsle/fnw202

Baseler, L., Chertow, D.S., Johnson, K.M., Feldmann, H., Morens, D.M., 2017. The Pathogenesis of Ebola Virus Disease. Annu. Rev. Pathol. Mech. Dis. 12, 387–418. https://doi.org/10.1146/annurev-pathol-052016-100506

Basler, C.F., 2015. Innate immune evasion by filoviruses. Virology 479–480, 122–130. https://doi.org/10.1016/j.virol.2015.03.030

Basler, C.F., Amarasinghe, G.K., 2009. Evasion of interferon responses by Ebola and Marburg viruses. J. Interferon Cytokine Res. 29, 511–20. https://doi.org/10.1089/jir.2009.0076

Basler, C.F., Mikulasova, A., Martinez-Sobrido, L., Paragas, J., Mühlberger, E., Bray, M., Klenk, H.D., Palese, P., García-Sastre, A., 2003. The Ebola virus VP35 protein inhibits activation of interferon regulatory factor 3. J. Virol. 77, 7945–56. https://doi.org/10.1128/JVI.77.14.7945

Basler, C.F., Wang, X., Muhlberger, E., Volchkov, V., Paragas, J., Klenk, H.D., Garcia-Sastre, A., Palese, P., 2000. The Ebola virus VP35 protein functions as a type I IFN antagonist. Proc. Natl. Acad. Sci. 97, 12289–12294. https://doi.org/10.1073/pnas.220398297

Bayer, A., Lennemann, N.J., Ouyang, Y., Cherry, S., Sadovsky, Y., Coyne Correspondence, C.B., Bramley, J.C., Morosky, S., De, E.T., Marques, A., Coyne, C.B., 2016. Type III Interferons Produced by Human Placental Trophoblasts Confer Protection against Zika Virus Infection. Cell Host Microbe 19, 1–8. https://doi.org/10.1016/j.chom.2016.03.008

Belgnaoui, S.M., Paz, S., Samuel, S., Goulet, M.L., Sun, Q., Kikkert, M., Iwai, K., Dikic, I., Hiscott, J., Lin, R., 2012. Linear ubiquitination of NEMO negatively regulates the interferon antiviral response through disruption of the MAVS-TRAF3 complex. Cell Host Microbe 12, 211–222. https://doi.org/10.1016/j.chom.2012.06.009

Berman, H. M.; Westbrook, J.; Feng, Z.; Gilliland, G.; Bhat, T. N.; Weissig, H.; Shindyalov, I. N.; Bourne, P.E., 2000. The protein data bank. Nucleic Acids Res. 28, 235–242. https://doi.org/10.1093/nar/28.1.235

Besnard, M., Lastère, S., Teissier, A., Cao-Lormeau, V., Musso, D., 2014. Evidence of perinatal transmission of Zika virus, French Polynesia, December 2013 and February 2014. Eurosurveillance 19, 20751. https://doi.org/10.2807/1560-7917.ES2014.19.13.20751

Bharaj, P., Atkins, C., Luthra, P., Giraldo, M.I., Dawes, B.E., Miorin, L., Johnson, J.R., Krogan, N.J., Basler, C.F., Freiberg, A.N., Rajsbaum, R., 2017. The host E3-Ubiquitin ligase TRIM6 ubiquitinates the Ebola virus VP35 protein and promotes virus replication. J. Virol. JVI.00833-17. https://doi.org/10.1128/JVI.00833-17

Bixler, S.L., Duplantier, A.J., Bavari, S., 2017. Discovering Drugs for the Treatment of Ebola Virus. Curr. Treat. Options Infect. Dis. 9, 299–317. https://doi.org/10.1007/s40506-017-0130-z

Bowen, J.R., Quicke, K.M., Maddur, M.S., O'Neal, J.T., McDonald, C.E.,

Fedorova, N.B., Puri, V., Shabman, R.S., Pulendran, B., Suthar, M.S., 2017. Zika Virus Antagonizes Type I Interferon Responses during Infection of Human Dendritic Cells. PLoS Pathog. 13, 1–30. https://doi.org/10.1371/journal.ppat.1006164

Bray, M., 2005. Pathogenesis of viral hemorrhagic fever. Curr. Opin. Immunol. https://doi.org/10.1016/j.coi.2005.05.001

Buathong, R., Hermann, L., Thaisomboonsuk, B., Rutvisuttinunt, W., Klungthong, C., Chinnawirotpisan, P., Manasatienkij, W., Nisalak, A., Fernandez, S., Yoon, I.K., Akrasewi, P., Plipat, T., 2015. Detection of zika virus infection in Thailand, 2012-2014. Am. J. Trop. Med. Hyg. 93, 380–383. https://doi.org/10.4269/ajtmh.15-0022

Bui, T.T., Moi, M.L., Nabeshima, T., Takemura, T., Nguyen, T.T., Nguyen, L.N., Pham, H.T.T., Nguyen, T.T.T., Manh, D.H., Dumre, S.P., Mizukami, S., Hirayama, K., Tajima, S., Le, M.T.Q., Aoyagi, K., Hasebe, F., Morita, K., 2018. A single amino acid substitution in the NS4B protein of dengue virus confers enhanced virus growth and fitness in human cells in vitro through IFN-dependent host response. J. Gen. Virol. 99, 1044–1057. https://doi.org/10.1099/jgv.0.001092

Cannas, V., Daino, G.L., Corona, A., Esposito, F., Tramontano, E., 2015. A Luciferase Reporter Gene Assay to Measure Ebola Virus Viral Protein 35 – Associated Inhibition of Double-Stranded RNA – Stimulated , Retinoic Acid – Inducible Gene 1 – Mediated Induction of Interferon β. J. Infect. desease 212, S277–S281. https://doi.org/10.1093/infdis/jiv214

Cardenas, W.B., Loo, Y.-M., Gale, M., Hartman, A.L., Kimberlin, C.R., Martinez-Sobrido, L., Saphire, E.O., Basler, C.F., 2006. Ebola Virus VP35 Protein Binds Double-Stranded RNA and Inhibits Alpha/Beta Interferon Production Induced by RIG-I Signaling. J. Virol. 80, 5168–5178. https://doi.org/10.1128/JVI.02199-05

Cárdenas, W.B., Loo, Y.-M., Gale, M., Hartman, A.L., Kimberlin, C.R., Martínez-Sobrido, L., Saphire, E.O., Basler, C.F., 2006. Ebola virus VP35 protein binds double-stranded RNA and inhibits alpha/beta interferon production induced by RIG-I signaling. J. Virol. 80, 5168–78. https://doi.org/10.1128/JVI.02199-05

Cardile, A.P., Downey, L.G., Wiseman, P.D., Warren, T.K., Bavari, S., 2016. Antiviral therapeutics for the treatment of Ebola virus infection. Curr. Opin. Pharmacol. 30, 138–143. https://doi.org/10.1016/j.coph.2016.08.016

Cavlar, T., Ablasser, A., Hornung, V., 2012. Induction of type i IFNs by intracellular DNA-sensing pathways. Immunol. Cell Biol.

https://doi.org/10.1038/icb.2012.11

Centers for Disease Control, 1990. Update: filovirus infections among persons with occupational exposure to nonhuman primates. MMWR Morb Mortal Wkly Rep 39, 266–273.

Chan, J.F.W., Chik, K.K.H., Yuan, S., Yip, C.C.Y., Zhu, Z., Tee, K.M., Tsang, J.O.L., Chan, C.C.S., Poon, V.K.M., Lu, G., Zhang, A.J., Lai, K.K., Chan, K.H., Kao, R.Y.T., Yuen, K.Y., 2017. Novel antiviral activity and mechanism of bromocriptine as a Zika virus NS2B-NS3 protease inhibitor. Antiviral Res. 141, 29–37. https://doi.org/10.1016/j.antiviral.2017.02.002

Chang, T.H., Kubota, T., Matsuoka, M., Jones, S., Bradfute, S.B., Bray, M., Ozato, K., 2009. Ebola Zaire virus blocks type I interferon production by exploiting the host SUMO modification machinery. PLoS Pathog. 5, e1000493. https://doi.org/10.1371/journal.ppat.1000493

Chaplin, D.D., 2010. Overview of the immune response. J. Allergy Clin. Immunol. 125. https://doi.org/10.1016/j.jaci.2009.12.980

Chaudhary, V., Yuen, K.-S., Chan, J.F.-W., Chan, C.-P., Wang, P.-H., Cai, J.-P., Zhang, S., Liang, M., Kok, K.-H., Chan, C.-P., Yuen, K.-Y., Jin, D.-Y., 2017. Selective Activation of Type II Interferon Signaling by Zika Virus NS5 Protein. J. Virol. 91, e00163-17. https://doi.org/10.1128/JVI.00163-17

Chen, C.W., Tsay, Y.G., Wu, H.L., Lee, C.H., Chen, D.S., Chen, P.J., 2002. The double-stranded RNA-activated kinase, PKR, can phosphorylate hepatitis D virus small delta antigen at functional serine and threonine residues. J. Biol. Chem. 277, 33058–33067. https://doi.org/10.1074/jbc.M200613200

Chen, Q., Sun, L., Chen, Z.J., 2016. Regulation and function of the cGAS-STING pathway of cytosolic DNA sensing. Nat. Immunol. https://doi.org/10.1038/ni.3558

Chen, X., Vinkemeier, U., Zhao, Y., Jeruzalmi, D., Darnell, J.E., Kuriyan, J., 1998. Crystal structure of a tyrosine phosphorylated STAT-1 dimer bound to DNA. Cell 93, 827–839. https://doi.org/10.1016/S0092-8674(00)81443-9

Chen, Z.J., Sun, L.J., 2009. Nonproteolytic Functions of Ubiquitin in Cell Signaling. Mol. Cell 33, 275–286. https://doi.org/10.1016/j.molcel.2009.01.014

Chieux, V., Chehadeh, W., Harvey, J., Haller, O., Wattré, P., Hober, D., 2001. Inhibition of coxsackievirus B4 replication in stably transfected cells expressing human MxA protein. Virology 283, 84–92. https://doi.org/10.1006/viro.2001.0877

Chiu, Y.H., MacMillan, J.B., Chen, Z.J., 2009. RNA Polymerase III Detects

Cytosolic DNA and Induces Type I Interferons through the RIG-I Pathway. Cell 138, 576–591. https://doi.org/10.1016/j.cell.2009.06.015

Clementz, M.A., Chen, Z., Banach, B.S., Wang, Y., Sun, L., Ratia, K., Baez-Santos, Y.M., Wang, J., Takayama, J., Ghosh, A.K., Li, K., Mesecar, A.D., Baker, S.C., 2010. Deubiquitinating and Interferon Antagonism Activities of Coronavirus Papain-Like Proteases. J. Virol. 84, 4619–4629. https://doi.org/10.1128/JVI.02406-09

Coccia, E.M., Battistini, A., 2015. Early IFN type I response: Larning from microbial evasion strategies. Semin. Immunol. 27, 85–101. https://doi.org/10.1016/j.smim.2015.03.005

Cox, N.J., McCormick, J.B., Johnson, K.M., Kiley, M.P., 1983. Evidence for two subtypes of Ebola virus based on oligonucleotide mapping of RNA. J. Infect. Dis. 147, 272–275. https://doi.org/10.1093/infdis/147.2.272

Cumberworth, S.L., Clark, J.J., Kohl, A., Donald, C.L., 2017. Inhibition of type I interferon induction and signalling by mosquito-borne flaviviruses. Cell. Microbiol. https://doi.org/10.1111/cmi.12737

Cushnie, T.P.T., Lamb, A.J., 2005. Antimicrobial activity of flavonoids. Int. J. Antimicrob. Agents 26, 343–356. https://doi.org/10.1016/j.ijantimicag.2005.09.002

da Silva, S., Martins, D.O.S., Jardim, A.C.G., 2018. A review of the ongoing research on Zika virus treatment. Viruses. https://doi.org/10.3390/v10050255

Daino, G.L., Frau, A., Sanna, C., Rigano, D., Distinto, S., Madau, V., Esposito, F., Fanunza, E., Bianco, G., Taglialatela-Scafati, O., Zinzula, L., Maccioni, E., Corona, A., Tramontano, E., 2018. Identification of Myricetin as an Ebola Virus VP35-Double-Stranded RNA Interaction Inhibitor through a Novel Fluorescence-Based Assay. Biochemistry. https://doi.org/10.1021/acs.biochem.8b00892

Dalet, A., Gatti, E., Pierre, P., 2015. Integration of PKR-dependent translation inhibition with innate immunity is required for a coordinated anti-viral response. FEBS Lett. https://doi.org/10.1016/j.febslet.2015.05.006

Dalrymple, N.A., Cimica, V., Mackow, E.R., 2015. Dengue virus NS proteins inhibit RIG-I/MAVS signaling by blocking TBK1/IRF3 phosphorylation: Dengue virus serotype 1 NS4A is a unique interferon-regulating virulence determinant. MBio 6, 1–12. https://doi.org/10.1128/mBio.00553-15

Darapaneni, V., 2014. Virion Protein 24 of Ebola Virus as a Potential Drug Target. Am. J. Curr. Microbiol. 3, 14–22.

Davey, R.T.J., Dodd, L., Proschan, M.A., Neaton, J., Neuhaus Nordwall, J., Koopmeiners, J.S., Beigel, J., Tierney, J., Lane, H.C., Fauci, A.S., Massaquoi, M.B.F., Sahr, F., Malvy, D., 2016. A Randomized, Controlled Trial of ZMapp for Ebola Virus Infection. N. Engl. J. Med. 375, 1448–1456. https://doi.org/10.1056/NEJMoa1604330

Davidson, E., Bryan, C., Fong, R.H., Barnes, T., Pfaff, J.M., Mabila, M., Rucker, J.B., Doranz, B.J., 2015. Mechanism of Binding to Ebola Virus Glycoprotein by the ZMapp, ZMAb, and MB-003 Cocktail Antibodies. J. Virol. 89, 10982–10992. https://doi.org/10.1128/JVI.01490-15

Deguine, J., Barton, G.M., 2014. MyD88: a central player in innate immune signaling. F1000Prime Rep. 6, 97. https://doi.org/10.12703/P6-97

Delvecchio, R., Higa, L.M., Pezzuto, P., Valadão, A.L., Garcez, P.P., Monteiro, F.L., Loiola, E.C., Dias, A.A., Silva, F.J.M., Aliota, M.T., Caine, E.A., Osorio, J.E., Bellio, M., O'Connor, D.H., Rehen, S., De Aguiar, R.S., Savarino, A., Campanati, L., Tanuri, A., 2016. Chloroquine, an endocytosis blocking agent, inhibits zika virus infection in different cell models. Viruses 8, 322. https://doi.org/10.3390/v8120322

Dempsey, A., Bowie, A.G., 2015. Innate immune recognition of DNA: A recent history. Virology. https://doi.org/10.1016/j.virol.2015.03.013

den Boon, J.A., Ahlquist, P., 2010. Organelle-Like Membrane Compartmentalization of Positive-Strand RNA Virus Replication Factories. Annu. Rev. Microbiol. 64, 241–256. https://doi.org/10.1146/annurev.micro.112408.134012

Der, S.D., Zhou, A., Williams, B.R.G., Silverman, R.H., 1998. Identification of genes differentially regulated by interferon α, β, or γ using oligonucleotide arrays, in: Proc Natl Acad Sci U S A. pp. 15623–15628.

Dick, G.W.A., 1952. Zika Virus (I). Isolations and serological specificity. Trans. R. Soc. Trop. Med. Hyg. 46, 509–520. https://doi.org/10.1016/0035-9203(52)90042-4

Diebold, S.S., Kaisho, T., Hemmi, H., Akira, S., Reis E Sousa, C., 2004. Innate Antiviral Responses by Means of TLR7-Mediated Recognition of Single-Stranded RNA. Science (80-.). 303, 1529–1531. https://doi.org/10.1126/science.1093616

Ding, Q., Cao, X., Lu, J., Huang, B., Liu, Y.J., Kato, N., Shu, H.B., Zhong, J., 2013. Hepatitis C virus NS4B blocks the interaction of STING and TBK1 to evade host innate immunity. J. Hepatol. 59, 52–58. https://doi.org/10.1016/j.jhep.2013.03.019

Dos Santos, A.E., Kuster, R.M., Yamamoto, K.A., Salles, T.S., Campos, R., De Meneses, M.D.F., Soares, M.R., Ferreira, D., 2014. Quercetin and quercetin 3-O-glycosides from Bauhinia longifolia (Bong.) Steud. show anti-Mayaro virus activity. Parasites and Vectors 7, 130. https://doi.org/10.1186/1756-3305-7-130

Duffy, M.R., Chen, T.-H., Hancock, W.T., Powers, A.M., Kool, J.L., Lanciotti, R.S., Pretrick, M., Marfel, M., Holzbauer, S., Dubray, C., Guillaumot, L., Griggs, A., Bel, M., Lambert, A.J., Laven, J., Kosoy, O., Panella, A., Biggerstaff, B.J., Fischer, M., Hayes, E.B., 2009. Zika virus outbreak on Yap Island, Federated States of Micronesia. N Engl J Med 360, 2536–2543. https://doi.org/10.1056/NEJMoa0805715

Dunning, J., Kennedy, S.B., Antierens, A., Whitehead, J., Ciglenecki, I., Carson, G., Kanapathipillai, R., Castle, L., Howell-Jones, R., Pardinaz-Solis, R., Grove, J., Scott, J., Lang, T., Olliaro, P., Horby, P.W., Boyd, M., Das, D., Dawson, H., Fardolo, A.F., Gozalbes, J.G., Horace, M.T.C., Jackson, M., Kerrie, J., Leligdowicz, A., Longuere, K.S., Mambo, A., McSwiggan, S., Merson, L., Moore, M., Mulbah, F.M., Odam, M., Rojek, A., Scott, P., Welsley, E., Wemmah, B., 2016. Experimental treatment of ebola virus disease with brincidofovir. PLoS One 11. https://doi.org/10.1371/journal.pone.0162199

Ebihara, H., Takada, A., Kobasa, D., Jones, S., Neumann, G., Theriault, S., 2006. Molecular Determinants of Ebola Virus Virulence in Mice. PLoS Pathog. 2, 1–7. https://doi.org/10.1371/journal.ppat.0020073

Edwards, M.R., Johnson, B., Mire, C.E., Xu, W., Shabman, R.S., Speller, L.N., Leung, D.W., Geisbert, T.W., Amarasinghe, G.K., Basler, C.F., 2014. The Marburg Virus VP24 Protein Interacts with Keap1 to Activate the Cytoprotective Antioxidant Response Pathway. Cell Rep. 6, 1017–1025. https://doi.org/10.1016/j.celrep.2014.01.043

Empig, C.J., Goldsmith, M.A., 2002. Association of the Caveola Vesicular System with Cellular Entry by Filoviruses. J. Virol. 76, 5266–5270. https://doi.org/10.1128/JVI.76.10.5266–5270.2002

Esposito, F., Sanna, C., Del Vecchio, C., Cannas, V., Venditti, A., Corona, A., Bianco, A., Serrilli, A.M., Guarcini, L., Parolin, C., Ballero, M., Tramontano, E., 2013. Hypericum hircinum L. Components as new single-molecule inhibitors of both HIV-1 reverse transcriptase-associated DNA polymerase and ribonuclease H activities. Pathog. Dis. 68, 116–124. https://doi.org/10.1111/2049-632X.12051

Esposito, F., Tramontano, E., 2014. Past and future. Current drugs targeting

HIV-1 integrase and reverse transcriptase-associated ribonuclease H activity: Single and dual active site inhibitors. Antivir. Chem. Chemother. https://doi.org/10.3851/IMP2690

Evans, J.D., Seeger, C., 2007. Differential Effects of Mutations in NS4B on West Nile Virus Replication and Inhibition of Interferon Signaling. J. Virol. 81, 11809–11816. https://doi.org/10.1128/JVI.00791-07

Fanunza, E., Frau, A., Corona, A., Tramontano, E., 2018a. Antiviral Agents Against Ebola Virus Infection: Repositioning Old Drugs and Finding Novel Small Molecules, in: Annual Reports in Medicinal Chemistry.

Fanunza, E., Frau, A., Corona, A., Tramontano, E., 2018b. Restoring Type-I Interferon Response to Fight Ebola virus: VP35 and VP24 Viral Proteins are Attractive Drug Targets. Infect. Disord. Drug Target submitted.

Fanunza, E., Frau, A., Sgarbanti, M., Orsatti, R., Corona, A., Tramontano, E., 2018c. Development and Validation of a Novel Dual Luciferase Reporter Gene Assay to Quantify Ebola Virus VP24 Inhibition of IFN Signaling. Viruses 10, 98. https://doi.org/10.3390/v10020098

Feldmann, H., Geisbert, T.W., 2011. Ebola haemorrhagic fever. Lancet 377, 849–862. https://doi.org/10.1016/S0140-6736(10)60667-8.Ebola

Feng, Z., Cerveny, M., Yan, Z., He, B., 2007. The VP35 Protein of Ebola Virus Inhibits the Antiviral Effect Mediated by Double-Stranded RNA-Dependent Protein Kinase PKR. J. Virol. 81, 182–192. https://doi.org/10.1128/JVI.01006-06

Findlay, G.M., Maccallum, F.O.O., Findlay G. M., F.O.M., 1937. An interference phonomenon in relation to yellow fever and other viruses. J. Pathol. Bacteriol. 44, 405–424. https://doi.org/10.1002/path.1700440216

Fink, K., Grandvaux, N., 2013. STAT2 and IRF9. JAK-STAT 2, e27521. https://doi.org/10.4161/jkst.27521

Fitzgerald, K.A., McWhirter, S.M., Faia, K.L., Rowe, D.C., Latz, E., Golenbock, D.T., Coyle, A.J., Liao, S.-M., Maniatis, T., 2003. IKKε and TBK1 are essential components of the IRF3 signaling pathway. Nat. Immunol. 4, 491–496. https://doi.org/10.1038/ni921

Florescu, D.F., Kalil, A.C., Hewlett, A.L., Schuh, A.J., Stroher, U., Uyeki, T.M., Smith, P.W., 2015. Administration of Brincidofovir and Convalescent Plasma in a Patient with Ebola Virus Disease. Clin. Infect. Dis. 61, 969–973. https://doi.org/10.1093/cid/civ395

Friesner, R.A., Murphy, R.B., Repasky, M.P., Frye, L.L., Greenwood, J.R.,

Halgren, T.A., Sanschagrin, P.C., Mainz, D.T., 2006. Extra precision glide: Docking and scoring incorporating a model of hydrophobic enclosure for protein-ligand complexes. J. Med. Chem. 49, 6177–6196. https://doi.org/10.1021/jm051256o

Fros, J.J., Liu, W.J., Prow, N.A., Geertsema, C., Ligtenberg, M., Vanlandingham, D.L., Schnettler, E., Vlak, J.M., Suhrbier, A., Khromykh, A.A., Pijlman, G.P., 2010. Chikungunya Virus Nonstructural Protein 2 Inhibits Type I/II Interferon-Stimulated JAK-STAT Signaling. J. Virol. 84, 10877–10887. https://doi.org/10.1128/JVI.00949-10

Fu, X.Y., Kessler, D.S., Veals, S.A., Levy, D.E., Darnell, J.E., 1990. ISGF3, the transcriptional activator induced by interferon alpha, consists of multiple interacting polypeptide chains. Proc. Natl. Acad. Sci. 87, 8555–8559. https://doi.org/10.1073/pnas.87.21.8555

Furr, S.R., Marriott, I., 2012. Viral CNS infections: Role of glial pattern recognition receptors in neuroinflammation. Front. Microbiol. 3, 201. https://doi.org/10.3389/fmicb.2012.00201

Gack, M.U., Shin, Y.C., Joo, C., Urano, T., Liang, C., Sun, L., Takeuchi, O., Akira, S., Chen, Z., Inoue, S., Jung, J.U., 2007. TRIM25 RING-finger E3 ubiquitin ligase is essential for RIG-I-mediated antiviral activity 446, 916–920. https://doi.org/10.1038/nature05732

Garcia-Dorival, I., Wu, W., Dowall, S., Armstrong, S., Touzelet, O., Wastling, J., Barr, J.N., Matthews, D., Carroll, M., Hewson, R., Hiscox, J.A., 2014. Elucidation of the Ebola Virus VP24 Cellular Interactome and Disruption of Virus Biology through Targeted Inhibition of Host-Cell Protein Function. J. Proteome Res. 13, 5120–5135.

García-Sastre, A., 2017. Ten Strategies of Interferon Evasion by Viruses. Cell Host Microbe. https://doi.org/10.1016/j.chom.2017.07.012

García, M.A., Meurs, E.F., Esteban, M., 2007. The dsRNA protein kinase PKR: Virus and cell control. Biochimie. https://doi.org/10.1016/j.biochi.2007.03.001

Gastaminza, P., Whitten-Bauer, C., Chisari, F. V., 2010. Unbiased probing of the entire hepatitis C virus life cycle identifies clinical compounds that target multiple aspects of the infection. Proc. Natl. Acad. Sci. 107, 291–296. https://doi.org/10.1073/pnas.0912966107

Geiger, T.R., Martin, J.M., 2006. The Epstein-Barr Virus-Encoded LMP-1 Oncoprotein Negatively Affects Tyk2 Phosphorylation and Interferon Signaling in Human B Cells. J. Virol. 80, 11638–11650.

https://doi.org/10.1128/JVI.01570-06

Geisbert, T.W., Hensley, L.E., Larsen, T., Young, H.A., Reed, D.S., Geisbert, J.B., Scott, D.P., Kagan, E., Jahrling, P.B., Davis, K.J., 2003a. Pathogenesis of Ebola Hemorrhagic Fever in Cynomolgus Macaques: Evidence that Dendritic Cells are Early and Sustained Targets of Infection. Am. J. Pathol. 163, 2347–2370. https://doi.org/10.1016/S0002-9440(10)63591-2

Geisbert, T.W., Young, H.A., Jahrling, P.B., Davis, K.J., Larsen, T., Kagan, E., Hensley, L.E., 2003b. Pathogenesis of Ebola Hemorrhagic Fever in Primate Models: Evidence that Hemorrhage Is Not a Direct Effect of Virus-Induced Cytolysis of Endothelial Cells. Am. J. Pathol. 163, 2371–2382. https://doi.org/10.1016/S0002-9440(10)63592-4

Gordien, E., Rosmorduc, O., Peltekian, C., Garreau, F., Bréchot, C., Kremsdorf, D., 2001. Inhibition of hepatitis B virus replication by the interferon-inducible MxA protein. J. Virol. 75, 2684–91. https://doi.org/10.1128/JVI.75.6.2684-2691.2001

Gorman, M.J., Caine, E.A., Zaitsev, K., Begley, M.C., Weger-Lucarelli, J., Uccellini, M.B., Tripathi, S., Morrison, J., Yount, B.L., Dinnon, K.H., Rückert, C., Young, M.C., Zhu, Z., Robertson, S.J., McNally, K.L., Ye, J., Cao, B., Mysorekar, I.U., Ebel, G.D., Baric, R.S., Best, S.M., Artyomov, M.N., Garcia-Sastre, A., Diamond, M.S., 2018. An Immunocompetent Mouse Model of Zika Virus Infection. Cell Host Microbe 23, 672–685. https://doi.org/10.1016/j.chom.2018.04.003

Goubau, D., Deddouche, S., Reis e Sousa, C., 2013. Cytosolic Sensing of Viruses. Immunity 38, 855–869. https://doi.org/10.1016/j.immuni.2013.05.007

Gourinat, A.C., O'Connor, O., Calvez, E., Goarant, C., Dupont-Rouzeyrol, M., 2015. Detection of zika virus in urine. Emerg. Infect. Dis. 21, 84–86. https://doi.org/10.3201/eid2101.140894

Grant, A., Ponia, S.S., Tripathi, S., Balasubramaniam, V., Miorin, L., Sourisseau, M., Schwarz, M.C., Sánchez-Seco, M.P., Evans, M.J., Best, S.M., García-Sastre, A., 2016. Zika Virus Targets Human STAT2 to Inhibit Type i Interferon Signaling. Cell Host Microbe 19, 882–890. https://doi.org/10.1016/j.chom.2016.05.009

Groseth, A., Feldmann, H., Strong, J.E., 2007. The ecology of Ebola virus. Trends Microbiol. https://doi.org/10.1016/j.tim.2007.08.001

Guerra, S., Cáceres, A., Knobeloch, K.P., Horak, I., Esteban, M., 2008. Vaccinia virus E3 protein prevents the antiviral action of ISG15. PLoS Pathog. 4, e1000096. https://doi.org/10.1371/journal.ppat.1000096

Guo, J.-T., Hayashi, J., Seeger, C., 2005. West Nile virus inhibits the signal transduction pathway of alpha interferon. J. Virol. 79, 1343–50. https://doi.org/10.1128/JVI.79.3.1343-1350.2005

Guo, Q., Zhao, L., You, Q., Yang, Y., Gu, H., Song, G., Lu, N., Xin, J., 2007. Anti-hepatitis B virus activity of wogonin in vitro and in vivo. Antiviral Res. 74, 16–24. https://doi.org/10.1016/j.antiviral.2007.01.002

Halfmann, P., Neumann, G., Kawaoka, Y., 2011. The Ebolavirus VP24 Protein Blocks Phosphorylation of p38 Mitogen-Activated Protein Kinase 204, 953–956. https://doi.org/10.1093/infdis/jir325

Halgren, T.A., 1996. Merck molecular force field. I. Basis, form, scope, parameterization, and performance of MMFF94. J. Comput. Chem. 17, 490–519. https://doi.org/10.1002/(SICI)1096-987X(199604)17:5/6<490::AID-JCC1>3.0.CO;2-P

Haller, O., Kochs, G., Weber, F., 2006. The interferon response circuit: Induction and suppression by pathogenic viruses. Virology 344, 119–130. https://doi.org/10.1016/j.virol.2005.09.024

Hamel, R., Dejarnac, O., Wichit, S., Ekchariyawat, P., Neyret, A., Luplertlop, N., Perera-Lecoin, M., Surasombatpattana, P., Talignani, L., Thomas, F., Cao-Lormeau, V.-M., Choumet, V., Briant, L., Desprès, P., Amara, A., Yssel, H., Missé, D., 2015. Biology of Zika Virus Infection in Human Skin Cells. J. Virol. 89, 8880–8896. https://doi.org/10.1128/JVI.00354-15

Hamel, R., Liégeois, F., Wichit, S., Pompon, J., Diop, F., Talignani, L., Thomas, F., Desprès, P., Yssel, H., Missé, D., 2016. Zika virus: epidemiology, clinical features and host-virus interactions. Microbes Infect. 18, 441–449. https://doi.org/10.1016/j.micinf.2016.03.009

Han, Z., Boshra, H., Sunyer, J.O., Zwiers, S.H., Paragas, J., Harty, R.N., 2003. Biochemical and Functional Characterization of the Ebola Virus VP24 Protein: Implications for a Role in Virus Assembly and Budding. J. Virol. 77, 1793. https://doi.org/10.1128/JVI.77.3.1793

Harcourt, B.H., Sanchez, A., Offermann, M.K., 1999. Ebola virus selectively inhibits responses to interferons, but not to interleukin-1beta, in endothelial cells. J. Virol. 73, 3491–3496.

Harcourt, B.H., Sanchez, A., Offermann, M.K., 1998. Ebola virus inhibits induction of genes by double-stranded RNA in endothelial cells. Virology 252, 179–188. https://doi.org/10.1006/viro.1998.9446

Hartman, A.L., Bird, B.H., Towner, J.S., Antoniadou, Z.-A., Zaki, S.R., Nichol, S.T., 2008a. Inhibition of IRF-3 Activation by VP35 Is Critical for the High

Level of Virulence of Ebola Virus. J. Virol. 82, 2699–2704. https://doi.org/10.1128/JVI.02344-07

Hartman, A.L., Dover, J.E., Towner, J.S., Nichol, S.T., 2006. Reverse Genetic Generation of Recombinant Zaire Ebola Viruses Containing Disrupted IRF-3 Inhibitory Domains Results in Attenuated Virus Growth In Vitro and Higher Levels of IRF-3 Activation without Inhibiting Viral Transcription or Replication 80, 6430–6440. https://doi.org/10.1128/JVI.00044-06

Hartman, A.L., Ling, L., Nichol, S.T., Hibberd, M.L., 2008b. Whole-Genome Expression Profiling Reveals That Inhibition of Host Innate Immune Response Pathways by Ebola Virus Can Be Reversed by a Single Amino Acid Change in the VP35 Protein. J. Virol. 82, 5348–5358. https://doi.org/10.1128/JVI.00215-08

Hartman, A.L., Towner, J.S., Nichol, S.T., 2004. A C-terminal basic amino acid motif of Zaire ebolavirus VP35 is essential for type I interferon antagonism and displays high identity with the RNA-binding domain of another interferon antagonist , the NS1 protein of influenza A virus 328, 177–184. https://doi.org/10.1016/j.virol.2004.07.006

He, F., Melén, K., Maljanen, S., Lundberg, R., Jiang, M., Österlund, P., Kakkola, L., Julkunen, I., 2017. Ebolavirus protein VP24 interferes with innate immune responses by inhibiting interferon-λ1 gene expression. Virology 509, 23–34. https://doi.org/10.1016/j.virol.2017.06.002

Heang, V., Yasuda, C.Y., Sovann, L., Haddow, A.D., da Rosa, A.P.T., Tesh, R.B., Kasper, M.R., 2012. Zika virus infection, Cambodia, 2010. Emerg. Infect. Dis. https://doi.org/10.3201/eid1802.111224

Hijikata, M., Ohta, Y., Mishiro, S., 2000. Identification of a single nucleotide polymorphism in the MxA gene promoter (G/T at nt -88) correlated with the response of hepatitis C patients to interferon. Intervirology 43, 124–127. https://doi.org/10.1159/000025035

Hiller, S., Bucklow, S., Endres, J., Ginzburg, C., Kee, J., Papapetros, S., Rifkin, A., Roche, J., Rowe, N., Schnapp, A., Stimson, B., Williams, R., 2015. Evidence of Zika Virus Infection in Brain and Placental Tissues from Two Congenitally Infected Newborns and Two Fetal Losses - Brazil, 2015. Source Art Bull. 94, 490–514.

Honda, K., Yanai, H., Mizutani, T., Negishi, H., Shimada, N., Suzuki, N., Ohba, Y., Takaoka, A., Yeh, W.-C., Taniguchi, T., 2004. Role of a transductional-transcriptional processor complex involving MyD88 and IRF-7 in Toll-like receptor signaling. Proc. Natl. Acad. Sci. U. S. A. 101, 15416–21. https://doi.org/10.1073/pnas.0406933101

Hoskins, M., 1935. A Protective Action of Neurotropic Against Viscerotropic Yellow Fever Virus in Macarus Rhesus. Am. J. Trop. Med. Hyg. s1-15, 675–680. https://doi.org/DOI: https://doi.org/10.4269/ajtmh.1935.s1-15.675

Hou, F., Sun, L., Zheng, H., Skaug, B., Jiang, Q.X., Chen, Z.J., 2011. MAVS forms functional prion-like aggregates to activate and propagate antiviral innate immune response. Cell. https://doi.org/10.1016/j.cell.2011.06.041

Huang, Y., Xu, L., Sun, Y., Nabel, G.J., 2002. The assembly of Ebola virus nucleocapsid requires virion-associated proteins 35 and 24 and posttranslational modification of nucleoprotein. Mol. Cell 10, 307–316. https://doi.org/10.1016/S1097-2765(02)00588-9

Hwang, S., Kim, K.S., Flano, E., Wu, T.T., Tong, L.M., Park, A.N., Song, M.J., Sanchez, D.J., O'Connell, R.M., Cheng, G., Sun, R., 2009. Conserved Herpesviral Kinase Promotes Viral Persistence by Inhibiting the IRF-3-Mediated Type I Interferon Response. Cell Host Microbe 5, 166–178. https://doi.org/10.1016/j.chom.2008.12.013

International Committee on Taxonomy of Viruses, 2015. International committee on taxonomy of viruses. Int. Comm. Taxon. Viruses. https://doi.org/http://www.ictvonline.org/index.asp

International Committee on Taxonomy of Viruses, 2012. Virus Taxonomy: Classification and Nomenclature of Viruses, Ninth Report of the International Committee on Taxonomy of Viruses. https://doi.org/10.1016/B978-0-12-384684-6.00057-4

Invivogen, 2005. Type I IFN Production and Signaling [WWW Document]. URL https://www.invivogen.com/review-type1-ifn-production

Isaacs, A., Lindenmann, J., Valentine, R.C., 1957. Virus Interference. II. Some Properties of Interferon. Proc. R. Soc. B Biol. Sci. 147, 268–273. https://doi.org/10.1098/rspb.1957.0049

Ishikawa, H., Barber, G.N., 2008. STING is an endoplasmic reticulum adaptor that facilitates innate immune signalling. Nature 455, 674–678. https://doi.org/10.1038/nature07317

Ishikawa, H., Ma, Z., Barber, G.N., 2009. STING regulates intracellular DNA-mediated, type i interferon-dependent innate immunity. Nature 461, 788–792. https://doi.org/10.1038/nature08476

Iversen, P.L., Warren, T.K., Wells, J.B., Garza, N.L., Mourich, D. V., Welch, L.S., Panchal, R.G., Sina, B., 2012. Discovery and Early Development of AVI-7537 and AVI-7288 for the Treatment of Ebola Virus and Marburg Virus Infections. Viruses 4, 2806–2830. https://doi.org/10.3390/v4112806

Iversen, P.W., Beck, B., Chen, Y.F., Dere, W., Devanarayan, V., Eastwood, B.J., Farmen, M.W., Iturria, S.J., Montrose, C., Moore, R.A., Weidner, J.R., Sittampalam, G.S., 2012. HTS Assay Validation, in: Assay Guidance Manual. Eli Lilly & Company and the National Center for Advancing Translational Sciences, 2004-., Bethesda (MD), pp. 875–905.

Jia, D., Rahbar, R., Chan, R.W.Y., Lee, S.M.Y., Chan, M.C.W., Xuhao, B., Baker, D.P., Sun, B., Peiris, J.S.M., Nicholls, J.M., Fish, E.N., 2010. Influenza Virus Non-Structural Protein 1 (NS1) Disrupts Interferon Signaling. PLoS Pathog. 5 (11), e13927. https://doi.org/10.1371/journal.pone.0013927

Johari, J., Kianmehr, A., Mustafa, M.R., Abubakar, S., Zandi, K., 2012. Antiviral activity of baicalein and quercetin against the Japanese encephalitis virus. Int. J. Mol. Sci. 13, 16020–16045. https://doi.org/10.3390/ijms131216785

Johnson, C.L., Gale, M., 2006. CARD games between virus and host get a new player. Trends Immunol. https://doi.org/10.1016/j.it.2005.11.004

Johnson, K.M., Breman, J.G., Burke, J., Declerq, R., Ghysebrechts, G., Pattyn, S.R., Piot, P., Ronsmans, M., Ruppol, J.F., Thonon, D., Van Der Groen, G., Van Nieuwenhove, S., Witvrouwen, M., Colbourne, G., Courtois, D., Dujeu, G., Germain, M., Raffier, G., Sureau, P., Vita, K., Koth, A., Mandiangu, Massamba, M., Matundu, M., Mbuyi, M., Miatudila, M., Tamfum, M., Muyingi, M.L., Nguete, K., Omombo, Tshibamba, Isaacson, M., Berquist, H., Close, W., Conn, D., Foster, S.O., Heymann, D.L., Kennedy, J., Lange, J. V, McCormick, J.B., Webb, P.A., White, M.K., Wulff, H., Adrien, S., Collas, R., 1978. Ebola haemorrhagic fever in Zaire, 1976. Bull. World Health Organ. 56, 271–93. https://doi.org/1978;56(2):271-293.

Jones, M., Cunningham, M.E., Wing, P., DeSilva, S., Challa, R., Sheri, A., Padmanabhan, S., Iyer, R.P., Korba, B.E., Afdhal, N., Foster, G.R., 2017. SB 9200, a novel agonist of innate immunity, shows potent antiviral activity against resistant HCV variants. J. Med. Virol. 89, 1620–1628. https://doi.org/10.1002/jmv.24809

Julander, J.G., Siddharthan, V., Evans, J., Taylor, R., Tolbert, K., Apuli, C., Stewart, J., Collins, P., Gebre, M., Neilson, S., Van Wettere, A., Lee, Y.M., Sheridan, W.P., Morrey, J.D., Babu, Y.S., 2017. Efficacy of the broad-spectrum antiviral compound BCX4430 against Zika virus in cell culture and in a mouse model. Antiviral Res. 137, 14–22. https://doi.org/10.1016/j.antiviral.2016.11.003

Kakumani, P.K., Ponia, S.S., S, R.K., Sood, V., Chinnappan, M., Banerjea, A.C., Medigeshi, G.R., Malhotra, P., Mukherjee, S.K., Bhatnagar, R.K., 2013. Role of RNA Interference (RNAi) in Dengue Virus Replication and Identification

of NS4B as an RNAi Suppressor. J. Virol. 87, 8870–8883.
https://doi.org/10.1128/JVI.02774-12

Kaminski, G.A., Friesner, R.A., Tirado-Rives, J., Jorgensen, W.L., 2001.
Evaluation and reparametrization of the OPLS-AA force field for proteins
via comparison with accurate quantum chemical calculations on peptides.
J. Phys. Chem. B 105, 6474–6487. https://doi.org/10.1021/jp003919d

Kang, C.B., Keller, T.H., Luo, D., 2017. Zika Virus Protease: An Antiviral Drug
Target. Trends Microbiol. https://doi.org/10.1016/j.tim.2017.07.001

Katoh, K., Standley, D.M., 2013. MAFFT multiple sequence alignment software
version 7: Improvements in performance and usability. Mol. Biol. Evol. 30,
772–780. https://doi.org/10.1093/molbev/mst010

Kawai, T., Akira, S., 2006. Innate immune recognition of viral infection. Nat.
Immunol. 7, 131–137. https://doi.org/10.1038/ni1303

Kawai, T., Sato, S., Ishii, K.J., Coban, C., Hemmi, H., Yamamoto, M., Terai, K.,
Matsuda, M., Inoue, J.I., Uematsu, S., Takeuchi, O., Akira, S., 2004.
Interferon-α induction through Toll-like receptors involves a direct
interaction of IRF7 with MyD88 and TRAF6. Nat. Immunol. 5, 1061–1068.
https://doi.org/10.1038/ni1118

Kawai, T., Takahashi, K., Sato, S., Coban, C., Kumar, H., Kato, H., Ishii, K.J.,
Takeuchi, O., Akira, S., 2005. IPS-1, an adaptor triggering RIG-I- and Mda5-
mediated type I interferon induction. Nat. Immunol. 6, 981–988.
https://doi.org/10.1038/ni1243

Kearse, M., Moir, R., Wilson, A., Stones-Havas, S., Cheung, M., Sturrock, S.,
Buxton, S., Cooper, A., Markowitz, S., Duran, C., Thierer, T., Ashton, B.,
Meintjes, P., Drummond, A., 2012. Geneious Basic: An integrated and
extendable desktop software platform for the organization and analysis of
sequence data. Bioinformatics 28, 1647–1649.
https://doi.org/10.1093/bioinformatics/bts199

Kessler, D.S., Levy, D.E., Darnell, J.E., 1988. Two interferon-induced nuclear
factors bind a single promoter element in interferon-stimulated genes. Proc.
Natl. Acad. Sci. U. S. A. 85, 8521–5. https://doi.org/10.1073/pnas.85.22.8521

Khachatoorian, R., Arumugaswami, V., Raychaudhuri, S., Yeh, G.K., Maloney,
E.M., Wang, J., Dasgupta, A., French, S.W., 2012. Divergent antiviral effects
of bioflavonoids on the hepatitis C virus life cycle. Virology 433, 346–355.
https://doi.org/10.1016/j.virol.2012.08.029

Khiar, S., Lucas-Hourani, M., Nisole, S., Smith, N., Helynck, O., Bourgine, M.,
Ruffié, C., Herbeuval, J.P., Munier-Lehmann, H., Tangy, F., Vidalain, P.O.,

2017. Identification of a small molecule that primes the type i interferon response to cytosolic DNA. Sci. Rep. 7. https://doi.org/10.1038/s41598-017-02776-z

Kim, Y., Narayanan, S., Chang, K.O., 2010. Inhibition of influenza virus replication by plant-derived isoquercetin. Antiviral Res. 88, 227–235. https://doi.org/10.1016/j.antiviral.2010.08.016

Kimberlin, C.R., Bornholdt, Z.A., Li, S., Woods, V.L., MacRae, I.J., Saphire, E.O., 2010. Ebolavirus VP35 uses a bimodal strategy to bind dsRNA for innate immune suppression. Proc. Natl. Acad. Sci. 107, 314–319. https://doi.org/10.1073/pnas.0910547107

Kollman, P.A., Massova, I., Reyes, C., Kuhn, B., Huo, S., Chong, L., Lee, M., Lee, T., Duan, Y., Wang, W., Donini, O., Cieplak, P., Srinivasan, J., Case, D.A., Cheatham, T.E., 2000. Calculating structures and free energies of complex molecules: Combining molecular mechanics and continuum models. Acc. Chem. Res. 33, 889–897. https://doi.org/10.1021/ar000033j

Kühl, A., Pöhlmann, S., 2012. How Ebola Virus Counters the Interferon System. Zoonoses Public Health 59, 116–131. https://doi.org/10.1111/j.1863-2378.2012.01454.x

Kumar, A., Hou, S., Airo, A.M., Limonta, D., Mancinelli, V., Branton, W., Power, C., Hobman, T.C., 2016. Zika virus inhibits type-I interferon production and downstream signaling. EMBO Rep. 17, 1766–1775. https://doi.org/10.15252/embr.201642627

Kumar, S., Pandey, A.K., 2013. Chemistry and biological activities of flavonoids: An overview. Sci. World J. https://doi.org/10.1155/2013/162750

Lani, R., Hassandarvish, P., Chiam, C.W., Moghaddam, E., Jang, J., Chu, H., Rausalu, K., Merits, A., Higgs, S., Vanlandingham, D., Bakar, S.A., Zandi, K., Chu, J.J.H., Rausalu, K., Merits, A., Higgs, S., Vanlandingham, D., Abu Bakar, S., Zandi, K., 2015. Antiviral activity of silymarin against chikungunya virus. Sci. Rep. 5, 11421. https://doi.org/10.1038/srep11421

Lazear, H.M., Daniels, B.P., Pinto, A.K., Huang, A.C., Vick, S.C., Doyle, S.E., Gale, M., Klein, R.S., Diamond, M.S., 2015. Interferon-λ restricts West Nile virus neuroinvasion by tightening the blood-brain barrier. Sci. Transl. Med. 7, 284ra57. https://doi.org/10.1126/scitranslmed.aaa4304

Le Guenno, B., Formenty, P., Formentry, P., Wyers, M., Gounon, P., Walker, F., Boesch, C., 1995. Isolation and partial characterisation of a new strain of Ebola virus. Lancet (London, England) 345, 1271–4. https://doi.org/10.5555/URI:PII:S0140673695909257

Lee, H., Ren, J., Nocadello, S., Rice, A.J., Ojeda, I., Light, S., Minasov, G., Vargas, J., Nagarathnam, D., Anderson, W.F., Johnson, M.E., 2017. Identification of novel small molecule inhibitors against NS2B/NS3 serine protease from Zika virus. Antiviral Res. 139, 49–58. https://doi.org/10.1016/j.antiviral.2016.12.016

Lee, M., Son, M., Ryu, E., Kang, H., Shin, Y.S., Kim, J.G., Kang, B.W., Cho, H., 2015. Quercetin-induced apoptosis prevents EBV infection. Oncotarget 6, 12603–12624. https://doi.org/10.18632/oncotarget.3687

Lee, S., Lee, H.H., Shin, Y.S., Kang, H., Cho, H., 2017. The anti-HSV-1 effect of quercetin is dependent on the suppression of TLR-3 in Raw 264.7 cells. Arch. Pharm. Res. 40, 623–630. https://doi.org/10.1007/s12272-017-0898-x

Lenschow, D.J., Giannakopoulos, N. V., Gunn, L.J., Johnston, C., O'Guin, A.K., Schmidt, R.E., Levine, B., Virgin, H.W., 2005. Identification of Interferon-Stimulated Gene 15 as an Antiviral Molecule during Sindbis Virus Infection In Vivo. J. Virol. 79, 13974–13983. https://doi.org/10.1128/JVI.79.22.13974-13983.2005

Leung, D.W., Borek, D., Farahbakhsh, M., Ramanan, P., Nix, J.C., Wang, T., Prins, K.C., Otwinowski, Z., Honzatko, R.B., Helgeson, L.A., Basler, C.F., Amarasinghe, G.K., 2010a. Crystallization and preliminary X-ray analysis of Ebola VP35 interferon inhibitory domain mutant proteins. Acta Crystallogr. Sect. F Struct. Biol. Cryst. Commun. 66, 689–692. https://doi.org/10.1107/S1744309110013266

Leung, D.W., Ginder, N.D., Fulton, D.B., Nix, J., Basler, C.F., Honzatko, R.B., Amarasinghe, G.K., 2009. Structure of the Ebola VP35 interferon inhibitory domain. Proc. Natl. Acad. Sci. 106, 411–416. https://doi.org/10.1073/pnas.0807854106

Leung, D.W., Prins, K.C., Basler, C.F., Amarasinghe, G.K., 2010b. *Ebolavirus* VP35 is a multifunctional virulence factor. Virulence 1, 526–531. https://doi.org/10.4161/viru.1.6.12984

Leung, D.W., Prins, K.C., Borek, D.M., Farahbakhsh, M., Tufariello, J.M., Ramanan, P., Nix, J.C., Helgeson, L.A., Otwinowski, Z., Honzatko, R.B., Basler, C.F., Amarasinghe, G.K., 2010c. Structural basis for dsRNA recognition and interferon antagonism by Ebola VP35. Nat. Struct. Mol. Biol. 17, 165–172. https://doi.org/10.1038/nsmb.1765

Leung, J.Y., Pijlman, G.P., Kondratieva, N., Hyde, J., Mackenzie, J.M., Khromykh, A.A., 2008. Role of Nonstructural Protein NS2A in Flavivirus Assembly. J. Virol. 82, 4731–4741. https://doi.org/10.1128/JVI.00002-08

Li, C., Zhu, X., Ji, X., Quanquin, N., Deng, Y.Q., Tian, M., Aliyari, R., Zuo, X., Yuan, L., Afridi, S.K., Li, X.F., Jung, J.U., Nielsen-Saines, K., Qin, F.X.F., Qin, C.F., Xu, Z., Cheng, G., 2017. Chloroquine, a FDA-approved Drug, Prevents Zika Virus Infection and its Associated Congenital Microcephaly in Mice. EBioMedicine 24, 189–194. https://doi.org/10.1016/j.ebiom.2017.09.034

Li, T., Chen, J., Cristea, I.M., 2013. Human cytomegalovirus tegument protein pUL83 inhibits IFI16-mediated DNA sensing for immune evasion. Cell Host Microbe 14, 591–599. https://doi.org/10.1016/j.chom.2013.10.007

Li, X.D., Wu, J., Gao, D., Wang, H., Sun, L., Chen, Z.J., 2013. Pivotal roles of cGAS-cGAMP signaling in antiviral defense and immune adjuvant effects. Science (80-.). 341, 1390–1394. https://doi.org/10.1126/science.1244040

Lin, R.-J., Chang, B.-L., Yu, H.-P., Liao, C.-L., Lin, Y.-L., 2006. Blocking of Interferon-Induced Jak-Stat Signaling by Japanese Encephalitis Virus NS5 through a Protein Tyrosine Phosphatase-Mediated Mechanism. J. Virol. 80, 5908–5918. https://doi.org/10.1128/JVI.02714-05

Liu, A.L., Wang, H. Di, Lee, S.M., Wang, Y.T., Du, G.H., 2008. Structure-activity relationship of flavonoids as influenza virus neuraminidase inhibitors and their in vitro anti-viral activities. Bioorganic Med. Chem. 16, 7141–7147. https://doi.org/10.1016/j.bmc.2008.06.049

Liu, H.M., Loo, Y.M., Horner, S.M., Zornetzer, G.A., Katze, M.G., Gale, M., 2012. The mitochondrial targeting chaperone 14-3-3ε regulates a RIG-I translocon that mediates membrane association and innate antiviral immunity. Cell Host Microbe 11, 528–537. https://doi.org/10.1016/j.chom.2012.04.006

Liu, J., HuangFu, W.C., Kumar, K.G.S., Qian, J., Casey, J.P., Hamanaka, R.B., Grigoriadou, C., Aldabe, R., Diehl, J.A., Fuchs, S.Y., 2009. Virus-Induced Unfolded Protein Response Attenuates Antiviral Defenses via Phosphorylation-Dependent Degradation of the Type I Interferon Receptor. Cell Host Microbe 5, 72–83. https://doi.org/10.1016/j.chom.2008.11.008

Liu, W.J., Chen, H.B., Wang, X.J., Huang, H., Khromykh, A. a, 2004. Analysis of adaptive mutations in Kunjin virus replicon RNA reveals a novel role for the flavivirus nonstructural protein NS2A in inhibition of beta interferon promoter-driven transcription. J. Virol. 78, 12225–12235. https://doi.org/10.1128/JVI.78.22.12225-12235.2004

Liu, W.J., Wang, X.J., Clark, D.C., Lobigs, M., Hall, R. a, Khromykh, A. a, 2006. A Single Amino Acid Substitution in the West Nile Virus Nonstructural Protein NS2A Disables Its Ability To Inhibit Alpha / Beta Interferon Induction and Attenuates Virus Virulence in Mice A Single Amino Acid

Substitution in the West Nile Virus Nonstructur. J. Virol. 80, 2396–2404. https://doi.org/10.1128/JVI.80.5.2396

Liu, W.J., Wang, X.J., Mokhonov, V. V., Shi, P.-Y., Randall, R., Khromykh, A.A., 2005. Inhibition of Interferon Signaling by the New York 99 Strain and Kunjin Subtype of West Nile Virus Involves Blockage of STAT1 and STAT2 Activation by Nonstructural Proteins. J. Virol. 79, 1934–1942. https://doi.org/10.1128/JVI.79.3.1934-1942.2005

Loeb, K.R., Haas, A.L., 1992. The interferon-inducible 15-kDa ubiquitin homolog conjugates to intracellular proteins. J. Biol. Chem. 267, 7806–7813.

Loo, Y.-M., Owen, D.M., Li, K., Erickson, A.K., Johnson, C.L., Fish, P.M., Carney, D.S., Wang, T., Ishida, H., Yoneyama, M., Fujita, T., Saito, T., Lee, W.M., Hagedorn, C.H., Lau, D.T.-Y., Weinman, S.A., Lemon, S.M., Gale, M., 2006. Viral and therapeutic control of IFN-beta promoter stimulator 1 during hepatitis C virus infection. Proc. Natl. Acad. Sci. U. S. A. 103, 6001–6. https://doi.org/10.1073/pnas.0601523103

Luthra, P., Ramanan, P., Mire, C.E., Weisend, C., Tsuda, Y., Yen, B., Liu, G., Leung, D.W., Geisbert, T.W., Ebihara, H., Amarasinghe, G.K., Basler, C.F., 2013. Mutual Antagonism between the Ebola Virus VP35 Protein and the RIG-I Activator PACT Determines Infection Outcome. Cell Host Microbe 14, 74–84. https://doi.org/10.1016/j.chom.2013.06.010

Ma, D.Y., Suthar, M.S., 2015. Mechanisms of innate immune evasion in re-emerging RNA viruses. Curr. Opin. Virol. 12, 26–37. https://doi.org/10.1016/j.coviro.2015.02.005

MacKenzie, J.M., Khromykh, A.A., Jones, M.K., Westaway, E.G., 1998. Subcellular localization and some biochemical properties of the flavivirus Kunjin nonstructural proteins NS2A and NS4A. Virology 245, 203–215. https://doi.org/10.1006/viro.1998.9156

Madrid, P.B., Chopra, S., Manger, I.D., Gilfillan, L., Keepers, T.R., Shurtleff, A.C., Green, C.E., Iyer, L. V., Dilks, H.H., Davey, R.A., Kolokoltsov, A.A., Carrion, R., Patterson, J.L., Bavari, S., Panchal, R.G., Warren, T.K., Wells, J.B., Moos, W.H., Burke, R.L.L., Tanga, M.J., 2013. A Systematic Screen of FDA-Approved Drugs for Inhibitors of Biological Threat Agents. PLoS One 8, e60579. https://doi.org/10.1371/journal.pone.0060579

Magrassi, F., 1935. Studii sull'infezione e sull'immunità da virus erpetico. Zeitschrift für Hyg. und Infekt. 117, 573–620.

Malakhova, O.A., Zhang, D.E., 2008. ISG15 inhibits Nedd4 ubiquitin E3 activity and enhances the innate antiviral response. J. Biol. Chem. 283, 8783–8787.

https://doi.org/10.1074/jbc.C800030200

Malathi, K., Dong, B., Gale, M., Silverman, R.H., 2007. Small self-RNA generated by RNase L amplifies antiviral innate immunity. Nature 448, 816–819. https://doi.org/10.1038/nature06042

Mateo, M., Carbonnelle, C., Martinez, M.J., Reynard, O., Page, A., Volchkova, V.A., Volchkov, V.E., 2011a. Knockdown of Ebola virus VP24 impairs viral nucleocapsid assembly and prevents virus replication. J. Infect. Dis. 204, S892–S896. https://doi.org/10.1093/infdis/jir311

Mateo, M., Carbonnelle, C., Reynard, O., Kolesnikova, L., Nemirov, K., Page, A., Volchkova, V.A., Volchkov, V.E., 2011b. VP24 Is a molecular determinant of Ebola virus virulence in guinea pigs. J. Infect. Dis. 204, 1011–1020. https://doi.org/10.1093/infdis/jir338

Mateo, M., Reid, S.P., Leung, L.W., Basler, C.F., Volchkov, V.E., 2010. Ebolavirus VP24 binding to karyopherins is required for inhibition of interferon signaling. J. Virol. 84, 1169–75. https://doi.org/10.1128/JVI.01372-09

McAllister, C.S., Samuel, C.E., 2009. The RNA-activated protein kinase enhances the induction of interferon-β and apoptosis mediated by cytoplasmic RNA sensors. J. Biol. Chem. 284, 1644–1651. https://doi.org/10.1074/jbc.M807888200

McBride, K.M., Banninger, G., McDonald, C., Reich, N.C., 2002. Regulated nuclear import of the STAT1 transcription factor by direct binding of importin-α. EMBO J. 21, 1754–1763. https://doi.org/10.1093/emboj/21.7.1754

McMullan, L.K., Flint, M., Dyall, J., Albariño, C., Olinger, G.G., Foster, S., Sethna, P., Hensley, L.E., Nichol, S.T., Lanier, E.R., Spiropoulou, C.F., 2016. The lipid moiety of brincidofovir is required for in vitro antiviral activity against Ebola virus. Antiviral Res. 125, 71–78. https://doi.org/https://doi.org/10.1016/j.antiviral.2015.10.010

Medin, C.L., Rothman, A.L., 2017. Zika virus: The agent and its biology, with relevance to pathology. Arch. Pathol. Lab. Med. 141, 33–42. https://doi.org/10.5858/arpa.2016-0409-RA

Mesci, P., Macia, A., Moore, S.M., Shiryaev, S.A., Pinto, A., Huang, C.T., Tejwani, L., Fernandes, I.R., Suarez, N.A., Kolar, M.J., Montefusco, S., Rosenberg, S.C., Herai, R.H., Cugola, F.R., Russo, F.B., Sheets, N., Saghatelian, A., Shresta, S., Momper, J.D., Siqueira-Neto, J.L., Corbett, K.D., Beltrão-Braga, P.C.B., Terskikh, A. V., Muotri, A.R., 2018. Blocking Zika virus vertical transmission. Sci. Rep. 8. https://doi.org/10.1038/s41598-018-

19526-4

Mesman, A.W., Zijlstra-Willems, E.M., Kaptein, T.M., De Swart, R.L., Davis, M.E., Ludlow, M., Duprex, W.P., Gack, M.U., Gringhuis, S.I., Geijtenbeek, T.B.H., 2014. Measles virus suppresses RIG-I-like receptor activation in dendritic cells via DC-SIGN-mediated inhibition of PP1 phosphatases. Cell Host Microbe 16, 31–42. https://doi.org/10.1016/j.chom.2014.06.008

Messaoudi, I., Amarasinghe, G.K., Basler, C.F., 2015. Filovirus pathogenesis and immune evasion: Insights from Ebola virus and Marburg virus. Nat. Rev. Microbiol. https://doi.org/10.1038/nrmicro3524

Meylan, E., Curran, J., Hofmann, K., Moradpour, D., Binder, M., Bartenschlager, R., Tschopp, J., 2005. Cardif is an adaptor protein in the RIG-I antiviral pathway and is targeted by hepatitis C virus. Nature 437, 1167–1172. https://doi.org/10.1038/nature04193

Mibayashi, M., Martinez-Sobrido, L., Loo, Y.-M., Cardenas, W.B., Gale, M., Garcia-Sastre, A., 2007. Inhibition of Retinoic Acid-Inducible Gene I-Mediated Induction of Beta Interferon by the NS1 Protein of Influenza A Virus. J. Virol. 81, 514–524. https://doi.org/10.1128/JVI.01265-06

Ming, G. li, Tang, H., Song, H., 2016. Advances in Zika Virus Research: Stem Cell Models, Challenges, and Opportunities. Cell Stem Cell. https://doi.org/10.1016/j.stem.2016.11.014

Mlakar, J., Korva, M., Tul, N., Popović, M., Poljšak-Prijatelj, M., Mraz, J., Kolenc, M., Resman Rus, K., Vesnaver Vipotnik, T., Fabjan Vodušek, V., Vizjak, A., Pižem, J., Petrovec, M., Avšič Županc, T., 2016. Zika Virus Associated with Microcephaly. N. Engl. J. Med. 374, 951–958. https://doi.org/10.1056/NEJMoa1600651

Mohamadi, F., Richards, N.G.J., Guida, W.C., Liskamp, R., Lipton, M., Caufield, C., Chang, G., Hendrickson, T., Still, W.C., 1990. Macromodel—an integrated software system for modeling organic and bioorganic molecules using molecular mechanics. J. Comput. Chem. 11, 440–467. https://doi.org/10.1002/jcc.540110405

Monteiro, G.E.R., Jansen van Vuren, P., Wichgers Schreur, P.J., Odendaal, L., Clift, S.J., Kortekaas, J., Paweska, J.T., 2018. Mutation of adjacent cysteine residues in the NSs protein of Rift Valley fever virus results in loss of virulence in mice. Virus Res. 249, 31–44. https://doi.org/10.1016/j.virusres.2018.03.005

Mora-Rillo, M., Arsuaga, M., Ramirez-Olivencia, G., de la Calle, F., Borobia, A.M., Sanchez-Seco, P., Lago, M., Figueira, J.C., Fernandez-Puntero, B.,

Viejo, A., Negredo, A., Nunez, C., Flores, E., Carcas, A.J., Jimenez-Yuste, V., Lasala, F., Garcia-de-Lorenzo, A., Arnalich, F., Arribas, J.R., 2015. Acute respiratory distress syndrome after convalescent plasma use: treatment of a patient with Ebola virus disease contracted in Madrid, Spain. Lancet. Respir. Med. 3, 554–562. https://doi.org/10.1016/S2213-2600(15)00180-0

Morrison, J., Laurent-Rolle, M., Maestre, A.M., Rajsbaum, R., Pisanelli, G., Simon, V., Mulder, L.C.F., Fernandez-Sesma, A., García-Sastre, A., 2013. Dengue Virus Co-opts UBR4 to Degrade STAT2 and Antagonize Type I Interferon Signaling. PLoS Pathog. 9. https://doi.org/10.1371/journal.ppat.1003265

Mühlberger, E., 2007. Filovirus replication and transcription. Future Virol. https://doi.org/10.2217/17460794.2.2.205

Mühlberger, E., Weik, M., Volchkov, V.E., Klenk, H.D., Becker, S., 1999. Comparison of the Transcription and Replication Strategies of Marburg Virus and Ebola Virus by Using Artificial Replication Systems. J. Virol. 73, 2333–2342.

Muñoz-Jordán, J.L., Fredericksen, B.L., 2010. How flaviviruses activate and suppress the interferon response. Viruses 2, 676–691. https://doi.org/10.3390/v2020676

Muñoz-Jordán, J.L., Laurent-rolle, M., Martínez-sobrido, L., Ashok, M., Ian, W., Mun, J.L., 2005. Inhibition of Alpha / Beta Interferon Signaling by the NS4B Protein of Flaviviruses Inhibition of Alpha / Beta Interferon Signaling by the NS4B Protein of Flaviviruses. J. Virol. 79, 8004–8013. https://doi.org/10.1128/JVI.79.13.8004

Munoz-Jordan, J.L., Sanchez-Burgos, G.G., Laurent-Rolle, M., Garcia-Sastre, A., 2003. Inhibition of interferon signaling by dengue virus. Proc. Natl. Acad. Sci. 100, 14333–14338. https://doi.org/10.1073/pnas.2335168100

Musso, D., Roche, C., Nhan, T.X., Robin, E., Teissier, A., Cao-Lormeau, V.M., 2015a. Detection of Zika virus in saliva. J. Clin. Virol. 68, 53–55. https://doi.org/10.1016/j.jcv.2015.04.021

Musso, D., Roche, C., Robin, E., Nhan, T., Teissier, A., Cao-Lormeau, V.M., 2015b. Potential sexual transmission of zika virus. Emerg. Infect. Dis. 21, 359–361. https://doi.org/10.3201/eid2102.141363

Nagai, K., Wong, A.H.-T., Li, S., Tam, N.W.N., Cuddihy, A.R., Sonenberg, N., Mathews, M.B., Hiscott, J., Wainberg, M.A., Koromilas, A.E., 1997. Induction of CD4 expression and human immunodeficiency virus type 1 replication by mutants of the interferon-inducible protein kinase PKR. J.

Virol. 71.

Nitta, S., Sakamoto, N., Nakagawa, M., Kakinuma, S., Mishima, K., Kusano-Kitazume, A., Kiyohashi, K., Murakawa, M., Nishimura-Sakurai, Y., Azuma, S., Tasaka-Fujita, M., Asahina, Y., Yoneyama, M., Fujita, T., Watanabe, M., 2013. Hepatitis C virus NS4B protein targets STING and abrogates RIG-I-mediated type I interferon-dependent innate immunity. Hepatology 57, 46–58. https://doi.org/10.1002/hep.26017

Noda, T., Ebihara, H., Muramoto, Y., Fujii, K., Takada, A., Sagara, H., Jin, H.K., Kida, H., Feldmann, H., Kawaoka, Y., 2006. Assembly and budding of Ebolavirus. PLoS Pathog. 2, 0864–0872. https://doi.org/10.1371/journal.ppat.0020099

Noda, T., Halfmann, P., Sagara, H., Kawaoka, Y., 2007. Regions in Ebola Virus VP24 That Are Important for Nucleocapsid Formation. J. Infect. Dis. 196, S247–S250. https://doi.org/10.1086/520596

Noguchi, T., Satoh, S., Noshi, T., Hatada, E., Fukuda, R., Kawai, A., Ikeda, S., Hijikata, M., Shimotohno, K., 2001. Effects of mutation in hepatitis C virus nonstructural protein 5A on interferon resistance mediated by inhibition of PKR kinase activity in mammalian cells. Microbiol. Immunol. 45, 829–40. https://doi.org/10.1111/j.1348-0421.2001.tb01322.x

Oehler, E., Watrin, L., Larre, P., Leparc-Goffart, I., Last??re, S., Valour, F., Baudouin, L., Mallet, H.P., Musso, D., Ghawche, F., 2014. Zika virus infection complicated by Guillain-Barré Syndrome – case report"case report, French Polynesia, December 2013. Eurosurveillance 19, 20720. https://doi.org/10.2807/1560-7917.ES2014.19.9.20720

Oganesyan, G., Saha, S., Guo, B., He, J., 2005. Critical role of TRAF3 in the Toll-like receptor-dependent and-independent antiviral response. Nature 439, 208–11. https://doi.org/10.1038/nature04374

Okumura, A., Lu, G., Pitha-Rowe, I., Pitha, P.M., 2006. Innate antiviral response targets HIV-1 release by the induction of ubiquitin-like protein ISG15. Proc. Natl. Acad. Sci. 103, 1440–1445. https://doi.org/10.1073/pnas.0510518103

Oliveira Melo, A.S., Malinger, G., Ximenes, R., Szejnfeld, P.O., Alves Sampaio, S., Bispo De Filippis, A.M., 2016. Zika virus intrauterine infection causes fetal brain abnormality and microcephaly: Tip of the iceberg? Ultrasound Obstet. Gynecol. https://doi.org/10.1002/uog.15831

Osiak, A., Utermohlen, O., Niendorf, S., Horak, I., Knobeloch, K.-P., 2005. ISG15, an Interferon-Stimulated Ubiquitin-Like Protein, Is Not Essential for STAT1 Signaling and Responses against Vesicular Stomatitis and

Lymphocytic Choriomeningitis Virus. Mol. Cell. Biol. 25, 6338–6345. https://doi.org/10.1128/MCB.25.15.6338-6345.2005

Oudshoorn, D., Versteeg, G.A., Kikkert, M., 2012. Regulation of the innate immune system by ubiquitin and ubiquitin-like modifiers. Cytokine Growth Factor Rev. 23, 273–282. https://doi.org/10.1016/j.cytogfr.2012.08.003

Panne, D., Maniatis, T., Harrison, S.C., 2007. An Atomic Model of the Interferon-β Enhanceosome. Cell 129, 1111–1123. https://doi.org/10.1016/j.cell.2007.05.019

Pasetto, S., Pardi, V., Murata, R.M., 2014. Anti-HIV-1 activity of flavonoid myricetin on HIV-1 infection in a dual-chamber in vitro model. PLoS One 9. https://doi.org/10.1371/journal.pone.0115323

Paz, S., Semenza, J.C., U.S. Department of Health and Human Services, Schuler-Faccini, L., Tetro, J.A., Nhan, T.-X., Musso, D., Gulland, A., Ioos, S., Mallet, H.-P., Goffart, I.L., Gauthier, V., Cardoso, T., Herida, M., Ministerio de Salud y Protección Social, U.S. Department of Health and Human Services, Schuler-Faccini, L., Paz, S., Semenza, J.C., Tetro, J.A., Cadu, R., Harish, T., Gulland, A., Nhan, T.-X., Musso, D., CDC, Ioos, S., Mallet, H.-P., Goffart, I.L., Gauthier, V., Cardoso, T., Herida, M., Ministerio de Salud y Protección Social, OMS, 2016. Current Zika virus epidemiology and recent epidemics. Med. Mal. Infect. 44, 302–307. https://doi.org/10.1016/S0140-6736(16)00256-7

Pestka, S., Krause, C.D., Walter, M.R., 2004. Interferons, interferon-like cytokines, and their receptors. Immunol. Rev. https://doi.org/10.1111/j.0105-2896.2004.00204.x

Pinto, A.K., Williams, G.D., Szretter, K.J., White, J.P., Proença-Módena, J.L., Liu, G., Olejnik, J., Brien, J.D., Ebihara, H., Mühlberger, E., Amarasinghe, G., Diamond, M.S., Boon, A.C.M., 2015. Human and Murine IFIT1 Proteins Do Not Restrict Infection of Negative-Sense RNA Viruses of the Orthomyxoviridae, Bunyaviridae, and Filoviridae Families. J. Virol. 89, 9465–9476. https://doi.org/10.1128/JVI.00996-15

Pizzolla, A., Smith, J.M., Brooks, A.G., Reading, P.C., 2017. Pattern recognition receptor immunomodulation of innate immunity as a strategy to limit the impact of influenza virus. J. Leukoc. Biol. 101, 851–861. https://doi.org/10.1189/jlb.4MR0716-290R

Platanias, L.C., 2005. Mechanisms of type-I- and type-II-interferon-mediated signalling. Nat. Rev. Immunol. https://doi.org/10.1038/nri1604

Plesko, S., Volk, H., Luksic, M., Podlipnik, C., 2015. In Silico Study of Plant

Polyphenols ' Interactions with VP24 – Ebola Virus Matrix Protein In Silico Study of Plant Polyphenols ' Interactions with VP24 – Ebola Virus Membrane-associated Protein. Acta Chim. Slov 62. https://doi.org/10.17344/acsi.2015.1505

Pleško, S., Volk, H., Lukšič, M., Podlipnik, Č., 2015. In silico study of plant polyphenols' interactions with VP24-ebola virus membrane-associated protein. Acta Chim. Slov. 62, 555–564. https://doi.org/10.17344/acsi.2015.1505

Pourrut, X., Kumulungui, B., Wittmann, T., Moussavou, G., Délicat, A., Yaba, P., Nkoghe, D., Gonzalez, J.P., Leroy, E.M., 2005. The natural history of Ebola virus in Africa. Microbes Infect. https://doi.org/10.1016/j.micinf.2005.04.006

Prins, K.C., Ca, W.B., Basler, C.F., 2009. Ebola Virus Protein VP35 Impairs the Function of Interferon Regulatory Factor-Activating Kinases IKK ε and TBK-1. J Virol 83, 3069–3077. https://doi.org/10.1128/JVI.01875-08

Prins, K.C., Delpeut, S., Leung, D.W., Reynard, O., Volchkova, V.A., Reid, S.P., Ramanan, P., Cárdenas, W.B., Amarasinghe, G.K., Volchkov, V.E., Basler, C.F., 2010. Mutations Abrogating VP35 Interaction with Double-Stranded RNA Render Ebola Virus Avirulent in Guinea Pigs. J. Virol. 84, 3004–3015. https://doi.org/10.1128/JVI.02459-09

Pythoud, C., Rodrigo, W.W.S.I., Pasqual, G., Rothenberger, S., Martinez-Sobrido, L., de la Torre, J.C., Kunz, S., 2012. Arenavirus Nucleoprotein Targets Interferon Regulatory Factor-Activating Kinase IKK . J. Virol. 86, 7728–7738. https://doi.org/10.1128/JVI.00187-12

Qiu, X., Audet, J., Wong, G., Pillet, S., Bello, A., Cabral, T., Strong, J.E., Plummer, F., Corbett, C.R., Alimonti, J.B., Kobinger, G.P., 2012. Successful treatment of ebola virus-infected cynomolgus macaques with monoclonal antibodies. Sci. Transl. Med. 4, 138ra81. https://doi.org/10.1126/scitranslmed.3003876

Qiu, X., Kroeker, A., He, S., Kozak, R., Audet, J., Mbikay, M., Chrétien, M., 2016. Prophylactic efficacy of quercetin 3-β-O-D-glucoside against Ebola virus infection. Antimicrob. Agents Chemother. 60, 5182–5188. https://doi.org/10.1128/AAC.00307-16

Qu, B., Qi, X., Wu, X., Liang, M., Li, C., Cardona, C.J., Xu, W., Tang, F., Li, Z., Wu, B., Powell, K., Wegner, M., Li, D., Xing, Z., 2012. Suppression of the interferon and NF-kappaB responses by severe fever with thrombocytopenia syndrome virus. J. Virol. 86, 8388–8401. https://doi.org/JVI.00612-12 [pii]\r10.1128/JVI.00612-12

Quicke, K.M., Bowen, J.R., Johnson, E.L., McDonald, C.E., Ma, H., O'Neal, J.T., Rajakumar, A., Wrammert, J., Rimawi, B.H., Pulendran, B., Schinazi, R.F., Chakraborty, R., Suthar, M.S., 2016. Zika Virus Infects Human Placental Macrophages. Cell Host Microbe 20, 83–90. https://doi.org/10.1016/j.chom.2016.05.015

Raj, U., Varadwaj, P.K., 2016. Flavonoids as Multi-target Inhibitors for Proteins Associated with Ebola Virus: In Silico Discovery Using Virtual Screening and Molecular Docking Studies. Interdiscip. Sci. Comput. Life Sci. 8, 132–141. https://doi.org/10.1007/s12539-015-0109-8

Rajak, H., Jain, D.K., Singh, A., Sharma, A.K., Dixit, A., 2015. Ebola virus disease: Past, present and future. Asian Pac. J. Trop. Biomed. 5, 337–343. https://doi.org/10.1016/S2221-1691(15)30365-8

Rajsbaum, R., García-Sastre, A., 2013. Viral evasion mechanisms of early antiviral responses involving regulation of ubiquitin pathways. Trends Microbiol. 21, 421–429. https://doi.org/10.1016/j.tim.2013.06.006

Rajsbaum, R., Versteeg, G.A., Schmid, S., Maestre, A.M., Belicha-Villanueva, A., Martínez-Romero, C., Patel, J.R., Morrison, J., Pisanelli, G., Miorin, L., Laurent-Rolle, M., Moulton, H.M., Stein, D.A., Fernandez-Sesma, A., tenOever, B.R., García-Sastre, A., 2014. Unanchored K48-Linked Polyubiquitin Synthesized by the E3-Ubiquitin Ligase TRIM6 Stimulates the Interferon-IKKε Kinase-Mediated Antiviral Response. Immunity 40, 880–895. https://doi.org/10.1016/j.immuni.2014.04.018

Ramana, C. V., Chatterjee-Kishore, M., Nguyen, H., Stark, G.R., 2000. Complex roles of Stat1 in regulating gene expression. Oncogene. https://doi.org/10.1038/sj.onc.1203525

Ramanan, P., Shabman, R.S., Brown, C.S., Amarasinghe, G.K., Basler, C.F., Leung, D.W., Amarasinghe, G.K., 2011. Filoviral immune evasion mechanisms. Viruses 3, 1634–1649. https://doi.org/10.3390/v3091634

Randall, R.E., Goodbourn, S., Randall, R.E., 2015. Interferons and viruses: an interplay between induction , signalling , antiviral responses and virus countermeasures 1–47. https://doi.org/10.1099/vir.0.83391-0

Rebouillat, D., Hovanessian, A.G., 1999. The human 2',5'-oligoadenylate synthetase family: interferon-induced proteins with unique enzymatic properties. J Interf. Cytokine Res 19, 295–308. https://doi.org/10.1089/107999099313992

Reich, N., Evans, B., Levy, D., Fahey, D., Knight, E., Darnell, J.E., 1987. Interferon-induced transcription of a gene encoding a 15-kDa protein

depends on an upstream enhancer element. Proc. Natl. Acad. Sci. U. S. A. 84, 6394–8. https://doi.org/10.1073/pnas.84.18.6394

Reid, S.P.., Leung, L.W.., Hartman, A.L.., Martinez, O.., Shaw, M.L.., Carbonnelle, C., Volchkov, V.E.., Nichol, S.T.., Basler, C.F.. D., 2006. Ebola virus VP24 binds karyopherin α1 and blocks STAT1 nuclear accumulation. J. Virol. 80, 5156–5167. https://doi.org/10.1128/JVI.02349-05

Reid, S.P., Ca, W.B., Basler, C.F., 2005. Homo-oligomerization facilitates the interferon-antagonist activity of the ebolavirus VP35 protein 341, 179–189. https://doi.org/10.1016/j.virol.2005.06.044

Reid, S.P., Valmas, C., Martinez, O., Mauricio Sanchez, F., Basler, C.F., 2007. Ebola Virus VP24 Proteins Inhibit the Interaction of NPI-1 Subfamily Karyopherin α Proteins with Activated STAT1. J. Virol. 81, 13469–13477. https://doi.org/10.1128/JVI.01097-07

Renwick, D., 2016. The Zika Virus [WWW Document]. URL https://www.cfr.org/backgrounder/zika-virus

Reuben, A., 2005. Prepared minds and the introduction of imaginon for hepatitic contagions. Hepatology 41, 1437–1442. https://doi.org/10.1002/hep.20751

Sadler, A.J., Williams, B.R.G., 2009. Interferon-inducible antiviral effectors. Nat. Rev. Immunol. 8, 559–568. https://doi.org/10.1038/nri2314.Interferon-inducible

Samuel, M.A., Whitby, K., Keller, B.C., Marri, A., Barchet, W., Williams, B.R.G., Silverman, R.H., Gale, M., Diamond, M.S., 2006. PKR and RNase L Contribute to Protection against Lethal West Nile Virus Infection by Controlling Early Viral Spread in the Periphery and Replication in Neurons. J. Virol. 80, 7009–7019. https://doi.org/10.1128/JVI.00489-06

Sanna, C., Rigano, D., Corona, A., Piano, D., Formisano, C., Farci, D., Franzini, G., Ballero, M., Chianese, G., Tramontano, E., Taglialatela-Scafati, O., Esposito, F., 2018. Dual HIV-1 reverse transcriptase and integrase inhibitors from Limonium morisianum Arrigoni, an endemic species of Sardinia (Italy). Nat. Prod. Res. 1–6. https://doi.org/10.1080/14786419.2018.1434649

Sarkar, S.N., Peters, K.L., Elco, C.P., Sakamoto, S., Pal, S., Sen, G.C., 2004. Novel roles of TLR3 tyrosine phosphorylation and PI3 kinase in double-stranded RNA signaling. Nat. Struct. Mol. Biol. 11, 1060–1067. https://doi.org/10.1038/nsmb847

Savidis, G., Perreira, J.M., Portmann, J.M., Meraner, P., Guo, Z., Green, S., Brass, A.L., 2016. The IFITMs Inhibit Zika Virus Replication. Cell Rep. 15, 2323–

2330. https://doi.org/10.1016/j.celrep.2016.05.074

Scarabelli, T.M., Mariotto, S., Abdel-Azeim, S., Shoji, K., Darra, E., Stephanou, A., Chen-Scarabelli, C., Marechal, J.D., Knight, R., Ciampa, A., Saravolatz, L., de Prati, A.C., Yuan, Z., Cavalieri, E., Menegazzi, M., Latchman, D., Pizza, C., Perahia, D., Suzuki, H., 2009. Targeting STAT1 by myricetin and delphinidin provides efficient protection of the heart from ischemia/reperfusion-induced injury. FEBS Lett. 583, 531–541. https://doi.org/10.1016/j.febslet.2008.12.037

Schibler, M., Vetter, P., Cherpillod, P., Petty, T.J., Cordey, S., Vieille, G., Yerly, S., Siegrist, C.-A., Samii, K., Dayer, J.-A., Docquier, M., Zdobnov, E.M., Simpson, A.J.H., Rees, P.S.C., Sarria, F.B., Gasche, Y., Chappuis, F., Iten, A., Pittet, D., Pugin, J., Kaiser, L., 2015. Clinical features and viral kinetics in a rapidly cured patient with Ebola virus disease: a case report. Lancet. Infect. Dis. 15, 1034–1040. https://doi.org/10.1016/S1473-3099(15)00229-7

Schneider, W.M., Chevillotte, M.D., Rice, C.M., 2014. Interferon-Stimulated Genes: A Complex Web of Host Defenses. Annu. Rev. Immunol. 32, 513–545. https://doi.org/10.1146/annurev-immunol-032713-120231

Schumann, M., Gantke, T., Muhlberger, E., 2009. Ebola Virus VP35 Antagonizes PKR Activity through Its C-Terminal Interferon Inhibitory Domain. J. Virol. 83, 8993–8997. https://doi.org/10.1128/JVI.00523-09

Schwarz, T.M., Edwards, M.R., Diederichs, A., Alinger, J.B., Leung, D.W., Amarasinghe, G.K., Basler, C.F., 2017. VP24-Karyopherin Alpha Binding Affinities Differ between Ebolavirus Species, Influencing Interferon Inhibition and VP24 Stability. J. Virol. 91, e01715-16. https://doi.org/10.1128/JVI.01715-16

Seth, R.B., Sun, L., Ea, C.K., Chen, Z.J., 2005. Identification and characterization of MAVS, a mitochondrial antiviral signaling protein that activates NF-κB and IRF3. Cell 122, 669–682. https://doi.org/10.1016/j.cell.2005.08.012

Setlur, A.S., Naik, S.Y., Skariyachan, S., 2017. Herbal Lead as Ideal Bioactive Compounds Against Probable Drug Targets of Ebola Virus in Comparison with Known Chemical Analogue: A Computational Drug Discovery Perspective. Interdiscip. Sci. Comput. Life Sci. 9, 254–277. https://doi.org/10.1007/s12539-016-0149-8

Shah, R., Panda, P.K., Patel, P., Mumbai, N., Farm, A., Road, G.D., 2015. Pharmacophore Based Virtual Screening and Molecular Docking Studies of Inherited Compounds 4, 1268–1282.

Sharma, S., TenOever, B.R., Grandvaux, N., Zhou, G.P., Lin, R., Hiscott, J., 2003.

Triggering the interferon antiviral response through an IKK-related pathway. Science (80-.). 300, 1148–1151. https://doi.org/10.1126/science.1081315

Sheahan, T.P., Sims, A.C., Graham, R.L., Menachery, V.D., Gralinski, L.E., Case, J.B., Leist, S.R., Pyrc, K., Feng, J.Y., Trantcheva, I., Bannister, R., Park, Y., Babusis, D., Clarke, M.O., MacKman, R.L., Spahn, J.E., Palmiotti, C.A., Siegel, D., Ray, A.S., Cihlar, T., Jordan, R., Denison, M.R., Baric, R.S., 2017. Broad-spectrum antiviral GS-5734 inhibits both epidemic and zoonotic coronaviruses. Sci. Transl. Med. 9, eaal3653. https://doi.org/10.1126/scitranslmed.aal3653

Silverman, R.H., 2007. Viral Encounters with 2′,5′-Oligoadenylate Synthetase and RNase L during the Interferon Antiviral Response. J. Virol. 81, 12720–12729. https://doi.org/10.1128/JVI.01471-07

Simmons, G., Rennekamp, A.J., Chai, N., Vandenberghe, L.H., Riley, J.L., Bates, P., 2003. Folate Receptor Alpha and Caveolae Are Not Required for Ebola Virus Glycoprotein-Mediated Viral Infection. J. Virol. 77, 13433–13438. https://doi.org/10.1128/JVI.77.24.13433–13438.2003

Skaug, B., Chen, Z.J., 2010. Emerging Role of ISG15 in Antiviral Immunity. Cell. https://doi.org/10.1016/j.cell.2010.09.033

Song, X., Lu, L., Passioura, T., Suga, H., 2017. Macrocyclic peptide inhibitors for the protein–protein interaction of Zaire Ebola virus protein 24 and karyopherin alpha 5. Org. Biomol. Chem. 15, 5155–5160. https://doi.org/10.1039/C7OB00012J

Sritularak, B., Tantrakarnsakul, K., Lipipun, V., Likhitwitayawuid, K., 2013. Flavonoids with anti-HSV activity from the root bark of Artocarpus lakoocha. Nat. Prod. Commun. 8, 1079–1080.

Stancato, L.F., David, M., Carter-Su, C., Larner, A.C., Pratt, W.B., 1996. Preassociation of STAT1 with STAT2 and STAT3 in separate signalling complexes prior to cytokine stimulation. J. Biol. Chem. 271, 4134–4137. https://doi.org/10.1074/jbc.271.8.4134

Stark, G.R., Kerr, I.M., Williams, B.R.G., Silverman, R.H., Schreiber, R.D., 1998. How Cells Respond To Interferon. Annu. Rev. Biochem. 67, 227–264. https://doi.org/10.1146/annurev.biochem.67.1.227

Strnadova, P., Ren, H., Valentine, R., Mazzon, M., Sweeney, T.R., Brierley, I., Smith, G.L., 2015. Inhibition of Translation Initiation by Protein 169: A Vaccinia Virus Strategy to Suppress Innate and Adaptive Immunity and Alter Virus Virulence. PLoS Pathog. 11, 1–33.

https://doi.org/10.1371/journal.ppat.1005151

Subba-Reddy, C. V., Goodfellow, I., Kao, C.C., 2011. VPg-Primed RNA Synthesis of Norovirus RNA-Dependent RNA Polymerases by Using a Novel Cell-Based Assay. J. Virol. 85, 13027–13037. https://doi.org/10.1128/JVI.06191-11

Sun, L., Xing, Y., Chen, X., Zheng, Y., Yang, Y., Nichols, D.B., Clementz, M.A., Banach, B.S., Li, K., Baker, S.C., Chen, Z., 2012. Coronavirus papain-like proteases negatively regulate antiviral innate immune response through disruption of STING-mediated signaling. PLoS One 7, e30802. https://doi.org/10.1371/journal.pone.0030802

Sun, W., Li, Y., Chen, L., Chen, H., You, F., Zhou, X., Zhou, Y., Zhai, Z., Chen, D., Jiang, Z., 2009. ERIS, an endoplasmic reticulum IFN stimulator, activates innate immune signaling through dimerization. Proc Natl Acad Sci U S A 106, 8653–8658. https://doi.org/0900850106 [pii]\r10.1073/pnas.0900850106

Suthar, M.S., Brassil, M.M., Blahnik, G., Gale, M., 2012. Infectious Clones of Novel Lineage 1 and Lineage 2 West Nile Virus Strains WNV-TX02 and WNV-Madagascar. J. Virol. 86, 7704–7709. https://doi.org/10.1128/JVI.00401-12

Takada, A., Kawaoka, Y., 2001. The pathogenesis of Ebola hemorrhagic fever. Trends Microbiol. https://doi.org/10.1016/S0966-842X(01)02201-6

Takaoka, A., Wang, Z., Choi, M.K., Yanai, H., Negishi, H., Ban, T., Lu, Y., Miyagishi, M., Kodama, T., Honda, K., Ohba, Y., Taniguchi, T., 2007. DAI (DLM-1/ZBP1) is a cytosolic DNA sensor and an activator of innate immune response. Nature 448, 501–505. https://doi.org/10.1038/nature06013

Tamura, K., Stecher, G., Peterson, D., Filipski, A., Kumar, S., 2013. MEGA6: Molecular evolutionary genetics analysis version 6.0. Mol. Biol. Evol. 30, 2725–2729. https://doi.org/10.1093/molbev/mst197

Tanaka, K., Kasahara, Y., Miyamoto, Y., Takumi, O., Kasai, T., Onodera, K., Kuwahara, M., Oka, M., Yoneda, Y., Obika, S., 2018. Development of oligonucleotide-based antagonists of Ebola virus protein 24 inhibiting its interaction with karyopherin alpha 1. Org. Biomol. Chem. 16, 4456–4463. https://doi.org/10.1039/C8OB00706C

Tang, X., Gao, J.S., Guan, Y.J., McLane, K.E., Yuan, Z.L., Ramratnam, B., Chin, Y.E., 2007. Acetylation-Dependent Signal Transduction for Type I Interferon Receptor. Cell 131, 93–105. https://doi.org/10.1016/j.cell.2007.07.034

Tappe, D., Rissland, J., Gabriel, M., Emmerich, P., Günther, S., Held, G., Smola, S., Schmidt-Chanasit, J., 2014. First case of laboratory-confirmed zika virus infection imported into Europe, November 2013. Eurosurveillance 19, 20685. https://doi.org/10.2807/1560-7917.ES2014.19.4.20685

Team, S., Branch, S.P., Division, V., Control, D., Eradication, S., 1978. Ebola haemorrhagic fever in Sudan, 1976. Bull. World Health Organ. 56, 247–270. https://doi.org/(WHO 1978a)

Tognarelli, J., Ulloa, S., Villagra, E., Lagos, J., Aguayo, C., Fasce, R., Parra, B., Mora, J., Becerra, N., Lagos, N., Vera, L., Olivares, B., Vilches, M., Fernández, J., 2016. A report on the outbreak of Zika virus on Easter Island, South Pacific, 2014. Arch. Virol. 161, 665–668. https://doi.org/10.1007/s00705-015-2695-5

Towner, J.S., Sealy, T.K., Khristova, M.L., Albariño, C.G., Conlan, S., Reeder, S.A., Quan, P.L., Lipkin, W.I., Downing, R., Tappero, J.W., Okware, S., Lutwama, J., Bakamutumaho, B., Kayiwa, J., Comer, J.A., Rollin, P.E., Ksiazek, T.G., Nichol, S.T., 2008. Newly discovered Ebola virus associated with hemorrhagic fever outbreak in Uganda. PLoS Pathog. 4, e1000212. https://doi.org/10.1371/journal.ppat.1000212

Tu, Y.-C., Yu, C.-Y., Liang, J.-J., Lin, E., Liao, C.-L., Lin, Y.-L., 2012. Blocking double-stranded RNA-activated protein kinase PKR by Japanese encephalitis virus nonstructural protein 2A. J. Virol. 86, 10347–58. https://doi.org/10.1128/JVI.00525-12

Turvey, S.E., Broide, D.H., 2010. Innate immunity. J. Allergy Clin. Immunol. 125, S24-32. https://doi.org/10.1016/j.jaci.2009.07.016

Uetani, K., Hiroi, M., Meguro, T., Ogawa, H., Kamisako, T., Ohmori, Y., Erzurum, S.C., 2008. Influenza A virus abrogates IFN-gamma response in respiratory epithelial cells by disruption of the Jak/Stat pathway. Eur J Immunol 38, 1559–1573. https://doi.org/10.1002/eji.200737045

Umesh, C. V, Jamsheer, A.M., Prasad, M.A., 2018. The Role of Flavonoids in Drug Discovery- Review on potential applications. Res. J. Life Sci. Bioinformatics, Pharm. Chem. Sci. 4, 70–77.

Unterholzner, L., Sumner, R.P., Baran, M., Ren, H., Mansur, D.S., Bourke, N.M., Randow, F., Smith, G.L., Bowie, A.G., 2011. Vaccinia virus protein c6 is a virulence factor that binds tbk-1 adaptor proteins and inhibits activation of irf3 and irf7. PLoS Pathog. 7, e1002247. https://doi.org/10.1371/journal.ppat.1002247

van Boxel-Dezaire, A., Rani, M.R.S., Stark, G.R., 2006. Complex Modulation of

Cell Type-Specific Signaling in Response to Type I Interferons. Immunity 25, 361–372.

Van De Klundert, M.A.A., Zaaijer, H.L., Kootstra, N.A., 2016. Identification of FDA-approved drugs that target hepatitis B virus transcription. J. Viral Hepat. 23, 191–201. https://doi.org/10.1111/jvh.12479

Van Der Hoek, K.H., Eyre, N.S., Shue, B., Khantisitthiporn, O., Glab-Ampi, K., Carr, J.M., Gartner, M.J., Jolly, L.A., Thomas, P.Q., Adikusuma, F., Jankovic-Karasoulos, T., Roberts, C.T., Helbig, K.J., Beard, M.R., 2017. Viperin is an important host restriction factor in control of Zika virus infection. Sci. Rep. 7. https://doi.org/10.1038/s41598-017-04138-1

Versteeg, G.A., García-Sastre, A., 2010. Viral tricks to grid-lock the type I interferon system. Curr. Opin. Microbiol. https://doi.org/10.1016/j.mib.2010.05.009

VOA, 2016. Brazil: Most Confirmed Microcephaly Cases Probably Tied to Zika [WWW Document]. URL https://www.voanews.com/

Wan, W., Kolesnikova, L., Clarke, M., Koehler, A., Noda, T., Becker, S., Briggs, J.A.G., 2017. Structure and assembly of the Ebola virus nucleocapsid. Nat. Int. J. Sci. 551, 394–397.

Wang, L., Li, S., Dorf, M.E., 2012. NEMO Binds Ubiquitinated TANK-Binding Kinase 1 (TBK1) to Regulate Innate Immune Responses to RNA Viruses. PLoS One 7, e43756. https://doi.org/10.1371/journal.pone.0043756

Wang, Q.-Y., Dong, H., Zou, B., Karuna, R., Wan, K.F., Zou, J., Susila, A., Yip, A., Shan, C., Yeo, K.L., Xu, H., Ding, M., Chan, W.L., Gu, F., Seah, P.G., Liu, W., Lakshminarayana, S.B., Kang, C., Lescar, J., Blasco, F., Smith, P.W., Shi, P.-Y., 2015. Discovery of Dengue Virus NS4B Inhibitors. J. Virol. 89, 8233–8244. https://doi.org/10.1128/JVI.00855-15

Ward, S.V., Samuel, C.E., 2002. Regulation of the interferon-inducible PKR kinase gene: The KCS element is a constitutive promoter element that functions in concert with the interferon-stimulated response element. Virology 296, 136–146. https://doi.org/10.1006/viro.2002.1356

Warren, T.K., Jordan, R., Lo, M.K., Ray, A.S., Mackman, R.L., Soloveva, V., Siegel, D., Perron, M., Bannister, R., Hui, H.C., Larson, N., Strickley, R., Wells, J., Stuthman, K.S., Van Tongeren, S.A., Garza, N.L., Donnelly, G., Shurtleff, A.C., Retterer, C.J., Gharaibeh, D., Zamani, R., Kenny, T., Eaton, B.P., Grimes, E., Welch, L.S., Gomba, L., Wilhelmsen, C.L., Nichols, D.K., Nuss, J.E., Nagle, E.R., Kugelman, J.R., Palacios, G., Doerffler, E., Neville, S., Carra, E., Clarke, M.O., Zhang, L., Lew, W., Ross, B., Wang, Q., Chun,

K., Wolfe, L., Babusis, D., Park, Y., Stray, K.M., Trancheva, I., Feng, J.Y., Barauskas, O., Xu, Y., Wong, P., Braun, M.R., Flint, M., McMullan, L.K., Chen, S.-S., Fearns, R., Swaminathan, S., Mayers, D.L., Spiropoulou, C.F., Lee, W.A., Nichol, S.T., Cihlar, T., Bavari, S., 2016. Therapeutic efficacy of the small molecule GS-5734 against Ebola virus in rhesus monkeys. Nature 531, 381.

Warren, T.K., Wells, J., Panchal, R.G., Stuthman, K.S., Garza, N.L., Van Tongeren, S.A., Dong, L., Retterer, C.J., Eaton, B.P., Pegoraro, G., Honnold, S., Bantia, S., Kotian, P., Chen, X., Taubenheim, B.R., Welch, L.S., Minning, D.M., Babu, Y.S., Sheridan, W.P., Bavari, S., 2014. Protection against filovirus diseases by a novel broad-spectrum nucleoside analogue BCX4430. Nature 508, 402.

Warren, T.K., Whitehouse, C.A., Wells, J., Welch, L., Heald, A.E., Charleston, J.S., Sazani, P., Reid, P., Iversen, P.L., 2015. A Single Phosphorodiamidate Morpholino Oligomer Targeting VP24 Protects Rhesus Monkeys against Lethal Ebola Virus Infection 6, 1–4. https://doi.org/10.1128/mBio.02344-14.Editor

Watanabe, S., Noda, T., Halfmann, P., Jasenosky, L., Kawaoka, Y., 2007. Ebola Virus (EBOV) VP24 Inhibits Transcription and Replication of the EBOV Genome. J. Infect. Dis. 196, S284–S290. https://doi.org/10.1086/520582

Watanabe, S., Watanabe, T., Noda, T., Feldmann, H., Jasenosky, L.D., Takada, A., Kawaoka, Y., 2004. Production of novel Ebola virus-like particles from cDNAs: an alternative to Ebola virus generation by reverse genetics. J. Virol. 78, 999–1005. https://doi.org/10.1128/JVI.78.2.999

Weber, M., Sediri, H., Felgenhauer, U., Binzen, I., Bänfer, S., Jacob, R., Brunotte, L., García-Sastre, A., Schmid-Burgk, J.L., Schmidt, T., Hornung, V., Kochs, G., Schwemmle, M., Klenk, H.D., Weber, F., 2015. Influenza virus adaptation PB2-627K modulates nucleocapsid inhibition by the pathogen sensor RIG-I. Cell Host Microbe 17, 309–319. https://doi.org/10.1016/j.chom.2015.01.005

Westaway, E.G., Khromykh, A.A., Kenney, M.T., MacKenzie, J.M., Jones, M.K., 1997. Proteins C and NS4B of the flavivirus kunjin translocate independently into the nucleus. Virology 234, 31–41. https://doi.org/10.1006/viro.1997.8629

White, J.M., Schornberg, K.L., 2012. A new player in the puzzle of filovirus entry. Nat. Rev. Microbiol. https://doi.org/10.1038/nrmicro2764

Wong, G., Kobinger, G.P., Qiu, X., Kobinger, G.P., 2017. Characterization of host immune responses in Ebola virus infections 8409.

https://doi.org/10.1586/1744666X.2014.908705

World Health Organization, 2016a. Ebola Virus Disease. Situat. Rep.

World Health Organization, 2016b. WHO Director-General summarizes the outcome of the Emergency Committee regarding clusters of microcephaly and Guillain-Barré syndrome [WWW Document]. https://doi.org/http://www.who.int/mediacentre/news/statements/2016/emergency-committee-zika-microcephaly/en/

Wu, J.J., Li, W., Shao, Y., Avey, D., Fu, B., Gillen, J., Hand, T., Ma, S., Liu, X., Miley, W., Konrad, A., Neipel, F., Stürzl, M., Whitby, D., Li, H., Zhu, F., 2015. Inhibition of cGAS DNA Sensing by a Herpesvirus Virion Protein. Cell Host Microbe 18, 333–344. https://doi.org/10.1016/j.chom.2015.07.015

Wu, Y., Liu, Q., Zhou, J., Xie, W., Chen, C., Wang, Z., Yang, H., Cui, J., 2017. Zika virus evades interferon-mediated antiviral response through the co-operation of multiple nonstructural proteins in vitro. Cell Discov. 3, 1–14. https://doi.org/10.1038/celldisc.2017.6

Xia, H., Luo, H., Shan, C., Muruato, A.E., Nunes, B.T.D., Medeiros, D.B.A., Zou, J., Xie, X., Giraldo, M.I., Vasconcelos, P.F.C., Weaver, S.C., Wang, T., Rajsbaum, R., Shi, P.Y., 2018. An evolutionary NS1 mutation enhances Zika virus evasion of host interferon induction. Nat. Commun. 9, 414. https://doi.org/10.1038/s41467-017-02816-2

Xu, L.G., Wang, Y.Y., Han, K.J., Li, L.Y., Zhai, Z., Shu, H.B., 2005. VISA is an adapter protein required for virus-triggered IFN-β signaling. Mol. Cell 19, 727–740. https://doi.org/10.1016/j.molcel.2005.08.014

Xu, W., Edwards, M.R., Borek, D.M., Feagins, A.R., Mittal, A., Pappu, R. V, Leung, D.W., Basler, C.F., Amarasinghe, G.K., 2015. Ebola virus VP24 targets a unique NLS binding site on karyopherin alpha 5 to selectively compete with nuclear import of phosphorylated STAT1. 16, 187–200. https://doi.org/10.1016/j.chom.2014.07.008.Ebola

Yamamoto, A., Seya, T., Oshiumi, H., Shingai, M., Seto, Y., Matsumoto, M., Funami, K., Tanabe, M., 2003. Receptor 3 in Human Dendritic Cells Subcellular Localization of Toll-Like Subcellular Localization of Toll-Like Receptor 3 in Human Dendritic Cells 1. J Immunol Ref. J. Immunol. 171, 3154–3162. https://doi.org/10.4049/jimmunol.171.6.3154

Yan, H., Krishnan, K., Greenlund, A.C., Gupta, S., Lim, J.T., Schreiber, R.D., Schindler, C.W., Krolewski, J.J., 1996. Phosphorylated interferon-alpha receptor 1 subunit (IFNaR1) acts as a docking site for the latent form of the 113 kDa STAT2 protein. EMBO J. 15, 1064–1074.

Ye, J., Zhu, B., Fu, Z.F., Chen, H., Cao, S., 2013. Immune evasion strategies of flaviviruses. Vaccine 31, 461–471. https://doi.org/10.1016/j.vaccine.2012.11.015

Yoneyama, M., Kikuchi, M., Natsukawa, T., Shinobu, N., Imaizumi, T., Miyagishi, M., Taira, K., Akira, S., Fujita, T., 2004. The RNA helicase RIG-I has an essential function in double-stranded RNA-induced innate antiviral responses 5, 730.

Yonezawa, A., Cavrois, M., Greene, W.C., 2005. Studies of Ebola Virus Glycoprotein-Mediated Entry and Fusion by Using Pseudotyped Human Immunodeficiency Virus Type 1 Virions: Involvement of Cytoskeletal Proteins and Enhancement by Tumor Necrosis Factor Alpha 79, 918–926. https://doi.org/10.1128/JVI.79.2.918

Yoon, K.J., Song, G., Qian, X., Pan, J., Xu, D., Rho, H.S., Kim, N.S., Habela, C., Zheng, L., Jacob, F., Zhang, F., Lee, E.M., Huang, W.K., Ringeling, F.R., Vissers, C., Li, C., Yuan, L., Kang, K., Kim, S., Yeo, J., Cheng, Y., Liu, S., Wen, Z., Qin, C.F., Wu, Q., Christian, K.M., Tang, H., Jin, P., Xu, Z., Qian, J., Zhu, H., Song, H., Ming, G. li, 2017. Zika-Virus-Encoded NS2A Disrupts Mammalian Cortical Neurogenesis by Degrading Adherens Junction Proteins. Cell Stem Cell 21, 349–358.e6. https://doi.org/10.1016/j.stem.2017.07.014

Yu, D.-S., Weng, T.-H., Wu, X.-X., Wang, F.X.C., Lu, X.-Y., Wu, H.-B., Wu, N.-P., Li, L.-J., Yao, H.-P., 2017. The lifecycle of the Ebola virus in host cells. Oncotarget 8, 55750–55759. https://doi.org/10.18632/oncotarget.18498

Zandi, K., Teoh, B.T., Sam, S.S., Wong, P.F., Mustafa, M., Abubakar, S., 2011. Antiviral activity of four types of bioflavonoid against dengue virus type-2. Virol. J. 8. https://doi.org/10.1186/1743-422X-8-560

Zanluca, C., De Melo, V.C.A., Mosimann, A.L.P., Dos Santos, G.I.V., dos Santos, C.N.D., Luz, K., 2015. First report of autochthonous transmission of Zika virus in Brazil. Mem. Inst. Oswaldo Cruz 110, 569–572. https://doi.org/10.1590/0074-02760150192

Zanluca, C., Nunes, C., 2016. Zika virus e an overview. Microbes Infect. 18, 295–301. https://doi.org/10.1016/j.micinf.2016.03.003

Zhang, A.P.P., Bornholdt, Z.A., Liu, T., Abelson, D.M., Lee, D.E., Li, S., Woods, V.L., Saphire, E.O., 2012. The ebola virus interferon antagonist VP24 directly binds STAT1 and has a novel, pyramidal fold. PLoS Pathog. 8, e1002550. https://doi.org/10.1371/journal.ppat.1002550

Zhang, J., Chung, T., Oldenburg, K., 1999. A simple statistical Parameter for use

in Evaluation and Validation of High Throughput Screening Assay. J. Biomol. Screen. 4, 67–73.

Zhang, P., Samuel, C.E., 2008. Induction of protein kinase PKR-dependent activation of interferon regulatory factor 3 by vaccinia virus occurs through adapter IPS-1 signaling. J. Biol. Chem. 283, 34580–34587. https://doi.org/10.1074/jbc.M807029200

Zhao, L., Jha, B.K., Wu, A., Elliott, R., Ziebuhr, J., Gorbalenya, A.E., Silverman, R.H., Weiss, S.R., 2012. Antagonism of the interferon-induced OAS-RNase L pathway by murine coronavirus ns2 protein is required for virus replication and liver pathology. Cell Host Microbe 11, 607–616. https://doi.org/10.1016/j.chom.2012.04.011

Zhao, T., Yang, L., Sun, Q., Arguello, M., Ballard, D.W., Hiscott, J., Lin, R., 2007. The NEMO adaptor bridges the nuclear factor-kappaB and interferon regulatory factor signaling pathways. Nat. Immunol. 8, 592–600. https://doi.org/10.1038/ni1465

Zhao, Z., Martin, C., Fan, R., Bourne, P.E., Xie, L., 2016. Drug repurposing to target Ebola virus replication and virulence using structural systems pharmacology. BMC Bioinformatics 17, 1–12. https://doi.org/10.1186/s12859-016-0941-9

Zhong, B., Yang, Y., Li, S., Wang, Y.Y., Li, Y., Diao, F., Lei, C., He, X., Zhang, L., Tien, P., Shu, H.B., 2008. The Adaptor Protein MITA Links Virus-Sensing Receptors to IRF3 Transcription Factor Activation. Immunity 29, 538–550. https://doi.org/10.1016/j.immuni.2008.09.003

Zhou, A., Paranjape, J., Brown, T.L., Nie, H., Naik, S., Dong, B., Chang, A., Trapp, B., Fairchild, R., Colmenares, C., Silverman, R.H., 1997. Interferon action and apoptosis are defective in mice devoid of 2′,5′-oligoadenylate-dependent RNase L. EMBO J. 16, 6355–6363. https://doi.org/10.1093/emboj/16.21.6355

Zinzula, L., Esposito, F., Mühlberger, E., Trunschke, M., Conrad, D., Piano, D., Tramontano, E., 2009. Purification and functional characterization of the full length recombinant Ebola virus VP35 protein expressed in E. coli. Protein Expr. Purif. 66, 113–119. https://doi.org/10.1016/j.pep.2009.02.008

Zinzula, L., Esposito, F., Pala, D., Tramontano, E., 2012. DsRNA binding characterization of full length recombinant wild type and mutants Zaire ebolavirus VP35. Antiviral Res. 93, 354–363. https://doi.org/10.1016/j.antiviral.2012.01.005

Zinzula, L., Tramontano, E., 2013a. Strategies of highly pathogenic RNA viruses

to block dsRNA detection by RIG-I-like receptors: Hide, mask, hit. Antiviral Res. 100, 615–635. https://doi.org/10.1016/j.antiviral.2013.10.002

Zinzula, L., Tramontano, E., 2013b. Strategies of highly pathogenic RNA viruses to block dsRNA detection by RIG-I-like receptors: Hide, mask, hit. Antiviral Res. 100, 615–635. https://doi.org/10.1016/j.antiviral.2013.10.002

Zou, J., Xie, X., Lee, L.T., Chandrasekaran, R., Reynaud, A., Yap, L., Wang, Q.-Y., Dong, H., Kang, C., Yuan, Z., Lescar, J., Shi, P.-Y., 2014. Dimerization of Flavivirus NS4B Protein. J. Virol. 88, 3379–3391. https://doi.org/10.1128/JVI.02782-13